COMPUTER CONTROL OF A RECIPROCATING PLATE EXTRACTION COLUMN

by

INDRA KASUMA, B.ENG.

A Thesis

Submitted to the School of Graduate Studies
in partial fulfilment of the requirements
for the degree

Master of Engineering

McMaster University
November, 1981

COMPUTER CONTROL OF A RECIPROCATING PLATE EXTRACTION COLUMN

MASTER OF ENGINEERING (1981)
(Chemical Engineering)

McMASTER UNIVERSITY
Hamilton, Ontario

TITLE: Computer Control of A Reciprocating Plate Extraction Column.

AUTHOR: Indra Kusuma, B. Eng. (McGill University)

SUPERVISORS: Dr. P.A. Taylor and Dr. M.H.I. Baird

NUMBER OF PAGES: xv, 167

ABSTRACT

This work discusses the control of a pilot scale (15 cm Dia.) Karr reciprocating extraction column. The system used is Kerosene dispersed in water, in which mass transfer does not occur.

The control scheme developed were tested for servo tracking and regulator control of the holdup of the dispersed phase, the manipulated variance was frequency of the reciprocating plates. Holdup was determined from an empiriaal correlation using an on-line measurement of column differential pressure.

Dynamic tests indicated the process to be nonlinear and assymmetric in time constant, deadtime and gain. A deadtime was observed between manipulating plate frequency and hold-up of the dispersed phase.

Various controllers were tested; PI (in feedback or feed forward mode or the combination), Dahlin algorithm. These were compared to the performance of minimum variance controller and S.T.R. All controllers were implemented using a 16 bit microprocessor.

The Dahlin and Minimum variance controllers have been demonstrated to handle process with deadtime better than the PI controller, because they both have deadtime compensator.

It was shown that the S.T.R. is superior over all fixed parameters controllers in handling the non-linearity of the process.

ACKNOWLEDGEMENTS

I would like to express my gratitude to Dr. P.A. Taylor and Dr. M.H.I. Baird for their support and guidance in making this work possible.

It was especially through the difficult periods of the project that their understanding and encouragement was very much appreciated.

Funding for the project was provided by the Chemical engineering Department of McMaster University and is gratefully acknowledged.

I would also like to thank Mrs. Amy Stott for her excellent work in typing up the manuscript.

TABLE OF CONTENTS

Table of contents cont'd

LIST OF FIGURES

List of Figures cont'd

List of Figures cont'd.

List of Figures cont'd

List of Figures cont'd

List of Figures cont'd

LIST OF TABLES

NOMENCLATURE

$\Delta\rho \mid \rho_D - \rho_C \mid$	difference between phase density
ρ_C	density of continuous phase
ρ_D	density of dispersed phase
ρ_W	density of water
ρ_K	density of kerosene
d_m	Suter mean diamter
ϵ	holdup of dispersed phase (volume fraction)
A	amplitude (stroke)
U_c	superficial velocity of dispersed phase
U_s	superficial slip velocity
Hx or Hy	total phase holdup volumes in each stage
L and V	phase volumetric throughput rates (eqn. 2.5.1 - 2.5.3)
X_n and Y_n	solute concentration in the two phases leaving stage n
A_n	Total interfacial area for mass transfer in stage n
K_n	overall coefficient for mass transfer in stage n
X_n^*	equilibrium solut concentration in stage n
Δp	differential pressure between two points in the column
f	frequency
g	gravitational acceleration
a	cross-sectional area of the column
Co	orifice coefficient for holes
σ	fraction open area of plate

NOMENCLATURE (cont'd)

ω	angular frequency = $2\pi f$
U_c	viscosity of continuous phase
K_c	proportional gain
T_R	reset time
T	sampling time
λ	tuning constant of the Dahlin controller
∇	$1 - Z^{-1}$

ERRATA

Page]27 ,]28 and]29 are missing due to mistake in paging.

CHAPTER 1

1 INTRODUCTION

The control of physical systems by digital computer is becoming more and more common, especially with the continuous development of low cost and reliable minicomputers. One of the advantages of digital logic of control is the increased flexibility of the control programs. Therefore, not only conventional PI controller but also other various modern controllers can be used.

However, there have been very few reports on the computer control directly related to a liquid extraction process. Liquid extraction plays an important role in industry, being used in a wide range of operations from copper production to the manufacture of antibiotics. The liquid extraction process is generally highly non-linear and has a long dead time. Therefore it needs more than a conventional PI controller to regulate and optimize the plant operation. Hence, inevitably computer control will also be used in the liquid extraction process.

There are many kinds of countercurrent extraction column, but the Karr reciprocating plate column, has become more widely used for its ease of scaling up and high throughout (8). Many works have been carried out on the Karr column's performance, hydrodynamics and scale up ever since its development in 1959 [8]. But the control problem in this type of column has not yet been investigated.

This work presents a case study aimed at the selection of the most suitable controller to prevent flooding and to optimize the operation in a 15 cm-diameter Karr column. The studies were conducted in the absence of mass transfer.

In chapter two, the literature review on the Karr column's characteristics and previous control work done on solvent extraction is presented.

Chapter three describes the experimental apparatus used including the Karr column, the holdup measurement set-up and the controller network.

Chapter four presents the steady state and unsteady state holdup responses and the development of on-line holdup measurement.

Chapter five, describes the testing of various controllers from the conventional PI to the sophisticated Self-Tuning-Regulator. The test results along with the discussion on each controller are given in the chapter.

Chapter six gives the criteria and justifications for the choice of the most suitable controller for the Karr column.

Chapter seven gives the conclusions of this work and recommendations for future work.

CHAPTER 2

2 LITERATURE RESEARCH

This chapter reviews the important characteristics of Karr column and some previous work done in extraction process simulation and control, before the control problem is considered.

2.1 Karr Column Performance and Characteristics

The ideal extraction column is one which has a high capacity and a high efficiency. The efficiency of the extraction column can be enhanced by application of some form of mechanical energy other than that due to the difference in the specific gravity of the countercurrent streams.

Three major types of industrial extraction columns utilizing added mechanical energy are [1, 2]:

(i) Columns employing a series of rotating impellers of various designs, e.g. Rotating-disc contactor, Oldshue - Rushton column, Kühni column.

(ii) Pulse columns in which the entire contents of the column are given a reciprocating motion by means of a pulsing mechanism located near the bottom of the column.

(iii) Reciprocating plate columns in which the plates are employed as reciprocating agitators which impart energy to the counterflowing streams as they flow through the column.

Columns having rotating impellers are inherently difficult to scale up accurately [3]. Some data [4,5] on pulsed Sieve-plate extraction columns indicated that it should be possible to scale up such column with no increase in the height of the column. However, the main problem, as Woodfield and Sege [6] have shown, is that when the column diameter is increased, the countercurrently flowing liquid phases are not distributed evenly across column's cross section. The design of reciprocating plate columns has minimized this channelling effect in that the H.E.T.S. in this type of column is only weakly dependent on column diameter, so that the scale up of such a column is much more straightforward.

A survey [7] indicates growing interest in the reciprocating plate columns, in particular the Karr column due to its ease of scaleup [8]. Furthermore, the plates employed in the Karr column have large perforations which minimize resistance to flow of the countercurrent streams and therefore the capacity of the column is increase; this design also eliminates the tendency of dispersed droplets to flow toward the wall of the column instead of through the perforation.

Studies on mass transfer [9], scale up [9,10] and hydrodynamics [11,12] in the Karr column have been carried out ever since its introduction in 1959 [8]. Karr himself [8] experimentally studied the effect of reciprocating speed, throughout, amplitude, plate spacing and physical properties on the H.E.T.S. of the Karr column. With certain organic systems the Karr column, unlike other types of columns, gives an H.E.T.S that sometimes goes through a minimum value with respect to

agitation level. The H.E.T.S. was found to be substantially independent of throughput, especially when the column was operating near the flooding point. The capacity of the reciprocating plate column was shown to exceed those of other columns reported in the literature. Furthermore, the reciprocating plate column required the smallest volume of column to do a given extraction job. Several papers [9,13, 14] have been published on the overall mass transfer characteristics of this column as measured by the H.E.T.S.

2.2 Flooding in the Reciprocating Plate Column

For optimality, that is high throughput and transfer rate, the column should usually be operated as near to the flooding zone as possible. This is because the H.E.T.S. often decreases monotonically with agitation level until the flooding point is reached. Even in those cases where H.E.T.S. reaches a minimum, this value occurs quite close to the flooding point. The flooding characteristic of this type of column has been studied by Hafez et al. [15] and a flooding correlation was developed for a 15 cm Diam. column, using kerosene dispersed in water, as follows: A balance of forces between fluid friction and buoyancy led to an equation of the form:

$$\frac{g\,\Delta\rho\,d_m\,(1-\varepsilon)^3}{\rho_c\,U_s^2} = \frac{150\,\varepsilon}{Re} + 1.75 \qquad (2.2.1)$$

where U_s is the superficial slip velocity defined as

$$U_s = U_d\left(\frac{1-\varepsilon}{\varepsilon}\right) + U_c \qquad (2.2.2)$$

$$d_m = 1.16\ (Af)^{-1.2} \qquad (2.2.3)$$

Re = drop Reynolds number defined as $U_s\, d\, \rho_c/\mu_c$.

At intermediate drop Reynolds numbers, the right hand side of eqn. (2.2.1) was approximately proportional to $Re^{-0.5}$. This had previously been confirmed [12] by extensive measurement of holdup under conditions where the Sauter mean drop diameter d_m was calculated from the power input:

$$\frac{g\ \Delta\rho\ d_m\ (1-\epsilon)^3}{\rho_c\ U_s^2} = K(Re/\epsilon)^{-0.5} \qquad (2.2.4)$$

For rigid spheres the dimensionless value K was found to be 30 $\pm$ 10%; for air bubbles rising in water, K had a value of 15 $\pm$ 10%.

As the flooding condition is reached, the holdup ϵ increases very rapidly with U_s. Thornton [16] has derived a general expression for the variation of ϵ_F (holdup at flooding) as a function of flow ratio based on a consideration of slip velocity:

$$\epsilon_F = \frac{(L^2 + 8L)^{0.5} - 3L}{4(1-L)} \qquad (2.2.5)$$

where $L = U_d/U_c$

A rearrangement of eqn. (2.2.4) for the flooding condition gives:

$$U_{sF} = \frac{(1-\epsilon_F)^3}{K\ \epsilon_f^{0.5}}^{2/3} \cdot d \cdot \left[\frac{g^2\ \Delta\rho^2}{\rho_c\ \mu_c}\right]^{1/3} \qquad (2.2.6)$$

where ϵ_F is determined by eqn. (2.2.5).

2.3 Holdup in a Reciprocating Plate Column

Quite extensive data on holdup for different systems in the absence of mass transfer have been obtained by Baird and Lane [12]. As expected, holdup is a function of physical properties, agitation rate and phase velocity. Physical properties include density difference, viscosity and surface tnesion. As density difference increases, the driving force causing the lighter phase to rise to the top is also increased. It is expected that if all other conditions, such as viscosity, remain constant then the increased rise velosity should result in lower holdups.

The effect of (A*f) can be seen by increasing the speed of reciprocation. As greater energy is imparted to the system, a finer dispersion is produced and this leads to higher holdup.

Some typical data of ϵ for the Kerosene/water system [12] is shown in Fig. 2.3.1. The rapid increase of holdup, as flooding condition is approached, is particularly apparent when the continuous phase is flowing as well as the dispersed phase. As U_c is increased, at constant agitation rate and U_d, the holdup ϵ will increase. Physically, this is explained as an increased drag and retention of the dispersed phase. In mathematical terms, we can see from the general form of eqn. (2.2.6) (non-flooding conditions) that increased ϵ has the effect of reducing both sides of the equation despite the increase in U_c.

In the results presented above the average holdup between two positions was measured. Recently, measurements of <u>local</u> holdup of the dispersed phase in a reciprocating plate extractor have shown [17] that

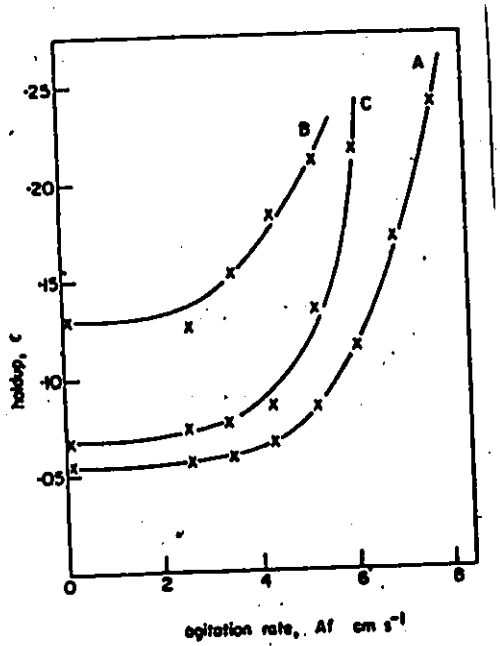

Fig. 2.3.1 Hold up Data for Kerosene/Water System in A 5 cm Dia. Column (Reprinted from Ref. 12)
Curve: A: U_D = .484 cm sec.$^{-1}$; U_C = 0
B: U_D = .895 cm sec.$^{-1}$; U_C = 0
C: U_D = .484 cm sec.$^{-1}$; U_C = .76 cm sec.$^{-1}$

large variations along the column may occur. Monotonically decreasing profiles as well as profiles with a maximum in the middle of the column have been observed at high throughputs approaching the flooding point.

2.4 Dynamic Characteristics of Solvent Extraction Contactors

In contrast to mixer-settler type extractors, differential column contactors are generally characterised by high throughputs and low holdup volumes, and thus by relatively rapid response characteristics. Optimum operational efficiencies are usually obtained over a relatively narrow range of operating conditions. Column contactors usually operate under non-equilibrium conditions, in which the rate of mass transfer is related directly to the area available for interfacial mass transfer and thus to the volumetric holdup of dispersed phase. Any large controller action can have a substantial effect on the hydrodynamic conditions within the column, either by reducing the holdup and hence the effective rate of mass transfer or by increasing holdup with attendant dangers of column failure by flooding or by phase inversion. Thus the resultant effects of controller action are not so easily predictable and the column will not generally have very much overdesign capacity, so the controller action must be limited to narrower ranges of operation than for mixer-settlers.

2.5 DYNAMIC MODEL OF EXTRACTOR

Dynamic mathematical modelling has the advantage that it can be applied to new processes. It can also help at the very earliest plant

design stage when the actual plant dynamics are unknown.

Many people have contributed to the development of modelling techniques for extraction column [18]. The general approach to the modelling of the non-equilibrium stagewise extractor dynamics has been reviewed by Wilkinson and Ingham [19]: the component continuity equation for the solute in each phase of any stage n may be expressed by:

$$\left[\begin{matrix}\text{rate of accumulation}\\ \text{of solute in phase i}\end{matrix}\right] = \left[\begin{matrix}\text{Inflow rate of}\\ \text{solute in phase i}\end{matrix}\right] - \left[\begin{matrix}\text{outflow rate of}\\ \text{solute in phase i}\end{matrix}\right] \pm \left[\begin{matrix}\text{rate of}\\ \text{solute mass transfer}\end{matrix}\right]$$

Thus, for phase x,

$$Hx \frac{dx_n}{dt} = L\,[X_{n-1} - X_n] - Q_n \qquad (2.5.1)$$

and for phase y,

$$Hy \frac{dy_n}{dt} = V\,[Y_{n+1} - Y_n] + Q_n \qquad (2.5.2)$$

where, $Q_n = K_n A_n [X_n - X_n^*]$ (2.5.3).

From eqn. (2.5.3), it is clear that the rate of mass transfer per unit driving force can be enhanced by maximizing A_n and hence the holdup as near flooding as possible.

2.6 CONTROL STUDIES ON SOLVENT EXTRACTION

The above theoretical model equations [19] for a non-equilibrium stagewise contactor with backmixing were used by McDonald and Wilkinson [20] to investigate possible control strategies to maintain constant raffinate composition, following changes in the inlet feed

concentration, by regulator of the feed flow rate. The theoretical predictions were compared with the results of experiments on a 23 stage, 150 mm diameter Oldshue-Rushton column using the system, nitric acid/water/TBP.

The open-loop response of the controlled variable, X_{raf}, following step changes in the feed concentration, X_F, and feed flow rate, L, were compared with the corresponding theoretical predicitions. Fig. (2.6.1) shows the response of X_{raf} to downward and upward steps of equal magnitude L. Fig. (2.6.2) shows the response to step changes in X_F.

The system was examined with proportional and proportional plus integral controller actions and the experimental results are shown in Fig. (2.6.3), where K_{pr} is the feedback proportional gain and $K_{ir} = K_{pr}/\tau_i$ is the feedback integral constant. The proportional control improves the raffinate response considerably, compared to the open-loop case, but some off-set remains. Integral action eliminates offset as expected.

Fig. (2.6.4) shows the results of a sequence of tests comparing an open-loop response with the corresponding feedback only and feedback/feedforward controller results. Where K_{pf} is the feed forward proportional gain. In this case, the K_{pf} is found by trial and error, which in fact can be estimated off-line if the dynamics of X_{raf} due to a change in X_F are known. For $K_{pf} = 2.6$, the response passes through an oscillatory period before settling down at a steady state value near to the zero off-set point. For $K_{pf} = 5.2$, the overshoot is higher and the

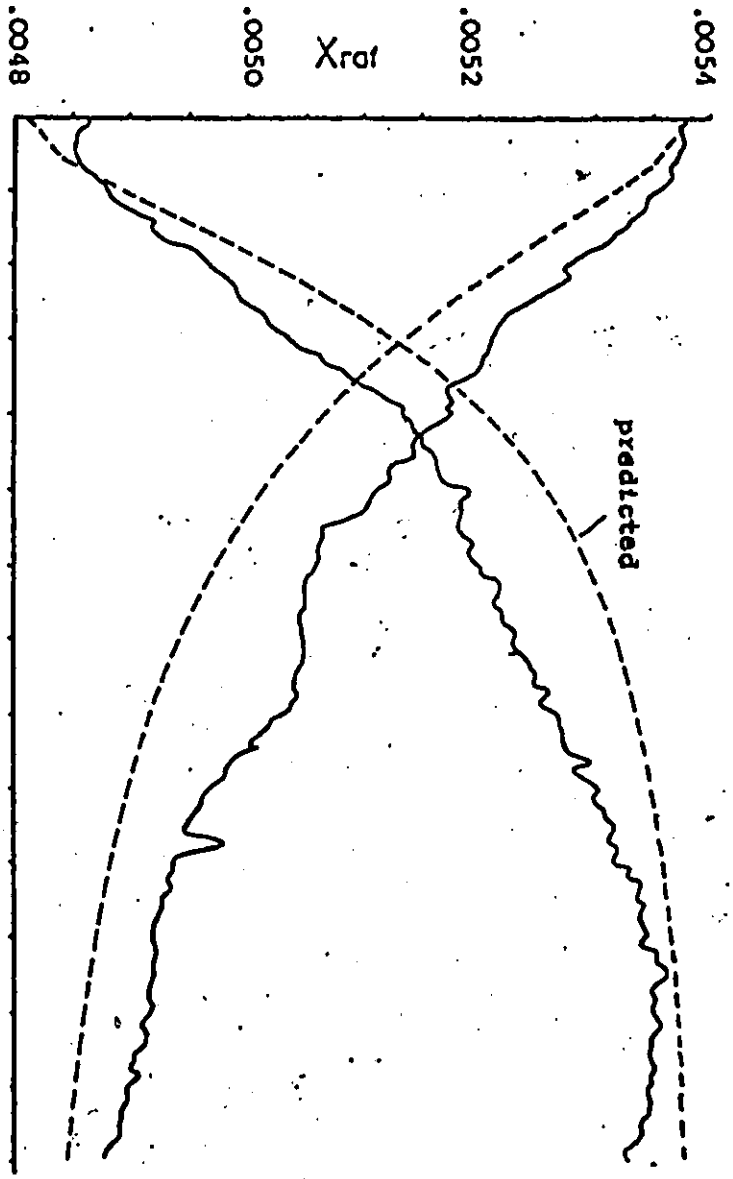

Fig. 2.6.1 Open Loop Response to Step Changes in the Feed Rate (Reprinted from Ref. 19)

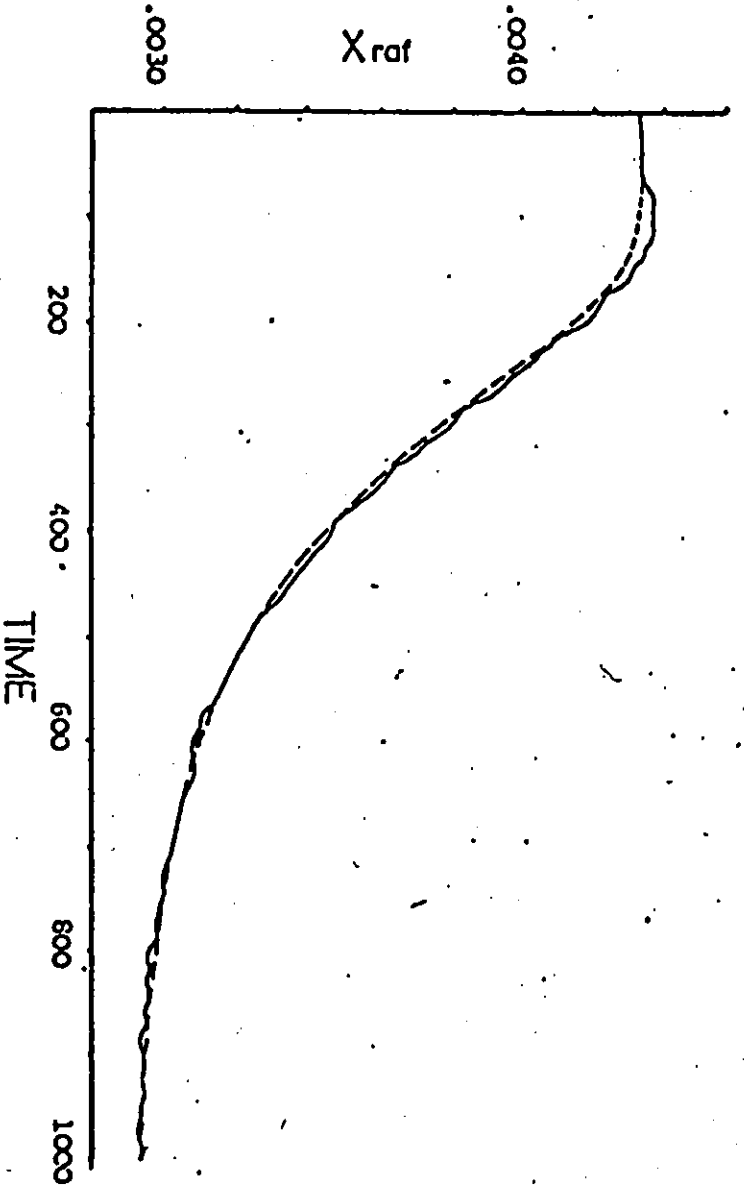

Fig. 2.6.2 Open Loop Response to Step Change in Feed Concentration (Reprinted from Ref. 19)

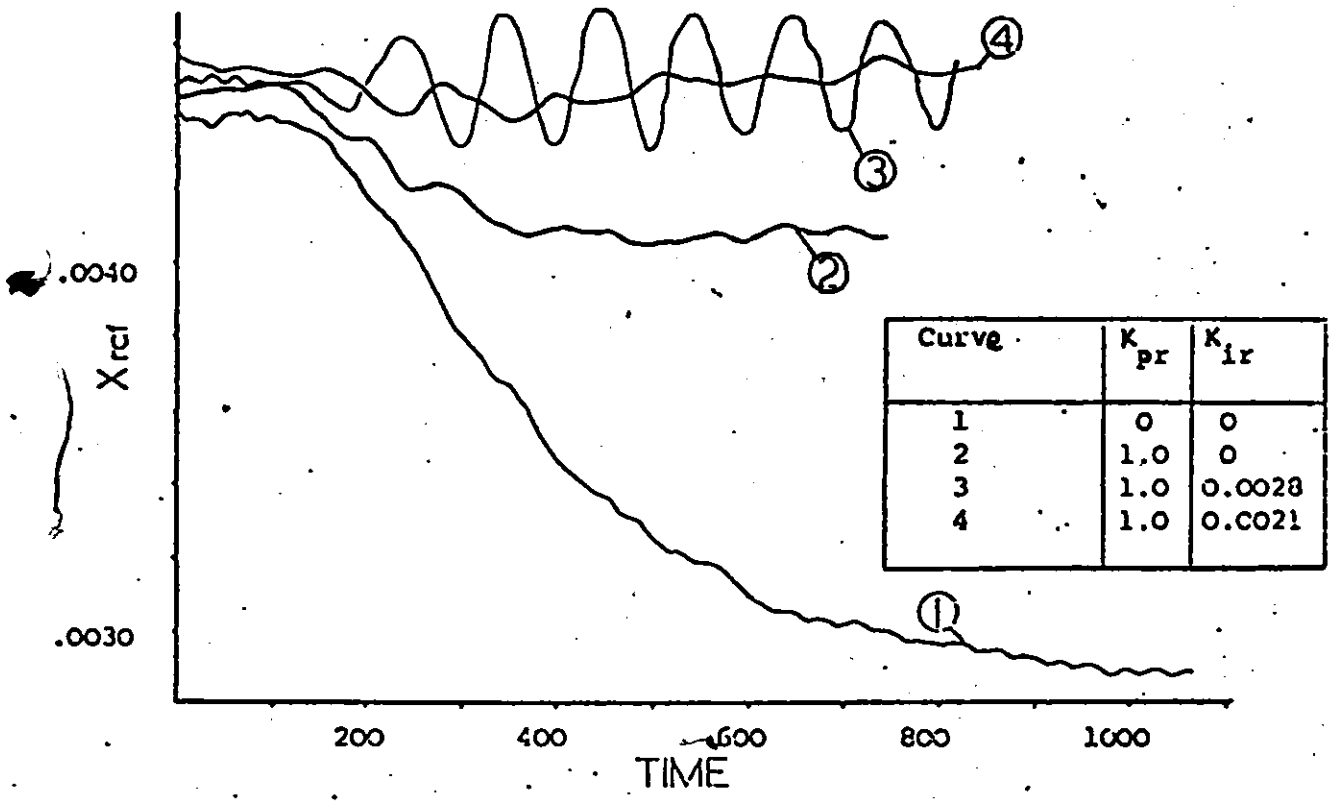

Fig. 2.6.3 Results of PI Feedback Control (Reprinted from Reference 19)

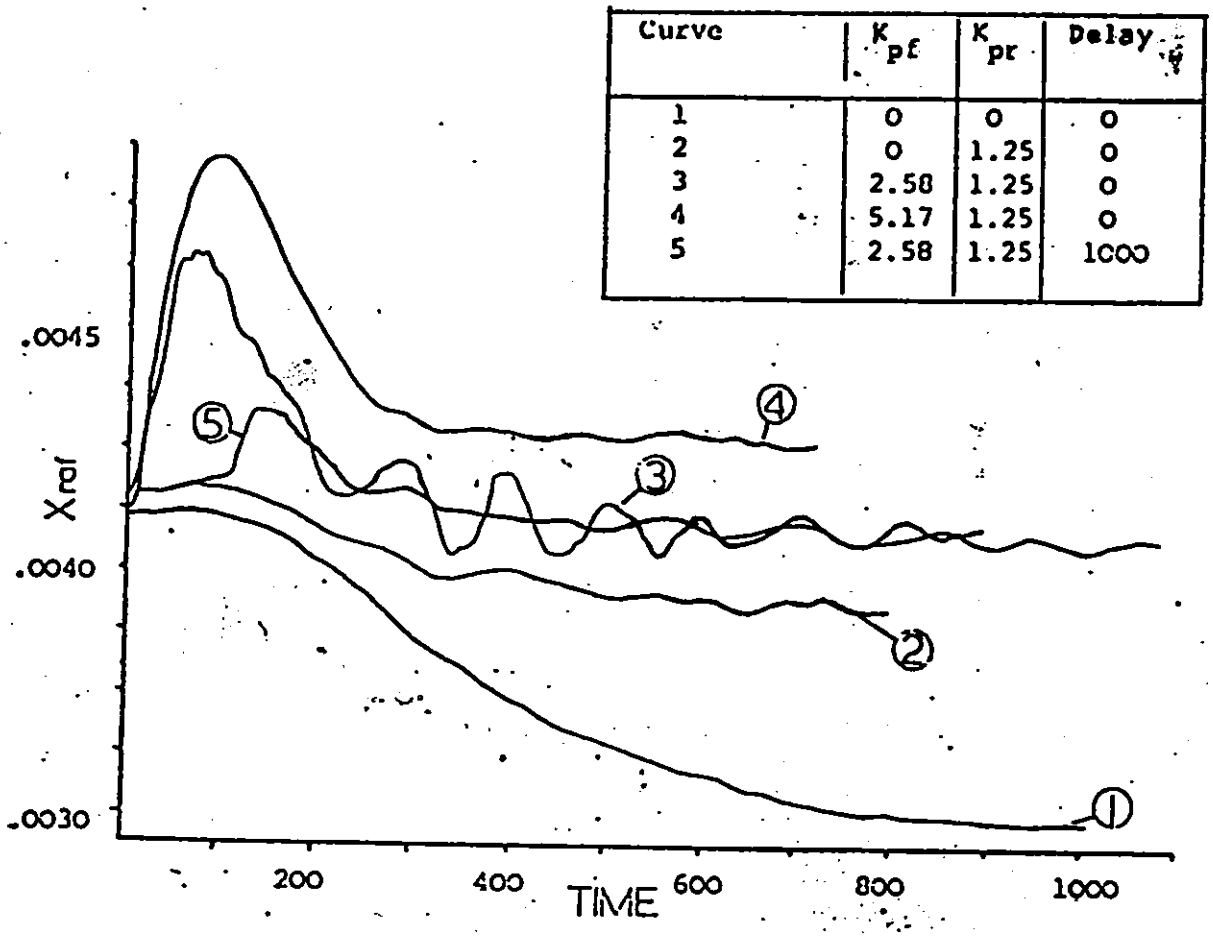

Fig. 2.6.4 Results of Open Loop, Feedback and Feedback/Feedforward Control (Reprinted from Ref. 19)

final steady state settles to a negative off-set value. The high overshoot for feedforward control is due to the fact that there is a dead time in the response of X_{raf} to a change of S_F; the downward step in X_F is detected even before it enters the column and corrective action is applied immediately through a corresponding upward step in L, which immediately increase X_{raf}. An experiment was carried out in which the feedforward element of the controller was delayed for 1000 seconds, an approximation to the dead time associated with the disturbance in X_F; the magnitude of overshoot and oscillation was greatly reduced and the offset was also eliminated as before.

In solvent extraction, it is unlikely that the plant model can give an exact representation of plant behavior especially where the plant has highly non-linear characteristics which may change with time. By the use of modern control identification techniques it is possible to utilize the computer as a self optimizing and as a model reference adaptive control system to automatically compensate for variations in the system dynamics. However, there have been very few actual reports of direct computer control specifically related to solvent extraction applications. The primary objective of this work is to fill this gap.

CHAPTER 3

3. EXPERIMENTAL APPARATUS

The experimental apparatuses can be considered under three headings; the basic apparatus, the measurement apparatus and the computer controller network. The basic apparatus has been set up in the Department for about five years. For this research work, the measurement apparatus was added initially, to study the dynamics of the column. Later, the controller network was added for control studies.

The Basic Apparatus

This consists of the reciprocating plate column, shown schematically in Fig. (3.1). The column was constructed of 3 flanged glass sections of 15.3 cm (6 inch) nominal internal diameter and had an overall height of 3.96 m. An assembly of reciprocating perforated plates was supported in the column on a central shaft attached by means of a yoke to a variable speed electric motor.

Water was fed by gravity through a rotameter to the top of the column and kerosene (the dispersed phase) was pumped from a surge tank (not shown on Figure) by a metering pump (Milton Roy) to a perforated-plate distributor, pitch at the base of the column. The operation was in the emulsion regime; dispersed phase remained dispersed throughout the plate stack and no coalescence into layers occurred at the plates.

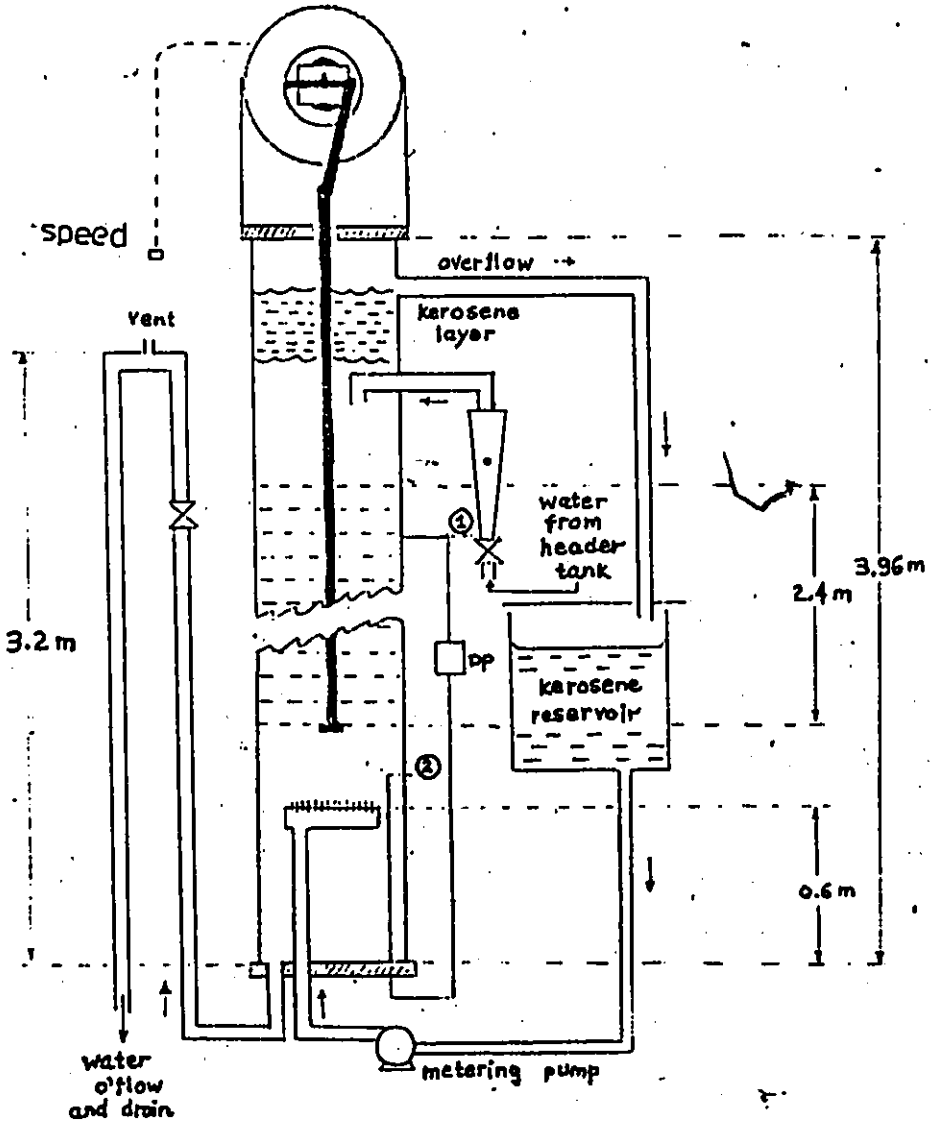

Fig. 3.1
Schematic diagram of experimental equipment

A liquid liquid interface was allowed to form about 25 cm above the top of plate stack and during two-phase operation the interface level was stabilized by allowing both phases to leave the column through overflow pipes, as shown.

The plate stack was approximately 2.4 m in height and was mounted on a stainless steel reciprocating drive shaft. The perforated plates had an outer diameter about 2 mm less than the internal diameter of the glass column. Each plate was provided with many 14.7 mm diameter perforations to give a fraction open area (σ) of 0.581. The plate spacing used was 5.08 cm.

Reciprocation was provided by a 373 W electric motor coupled to a variable speed reducer and an adjustable yoke. The amplitude (half stroke) can be varied by changing the yoke setting, but in the present work the amplitude was always 1.27 cm, and the frequency was varied between 0.5 to 5 HZ.

Because of the size of the equipment, it was not practicable to take special precautions on the purity of the liquids. Tap water at 5 to 10°C depending upon the time of year, and commercial kerosene (Imperial Oil Ltd., Sarnia) were used throughout. Some buildup of a wax-like material at the liquid-liquid interface occurred after prolonged operation of the column, but not to the extent that it interfered with the measurements. When the column was not in use, it was left full of water with a small flow of water maintained in order to prevent buildup of rust deposits.

Measurement Apparatus

Holdup was determined by on-line measurement of column differential pressure between points 1 and 2 as shown in Fig. (3.1). The differential pressure across the plate stack (P_2-P_1) was measured by means of a calibrated differential pressure transducer Dp (Pace Eng. Co., Model P7D). The transducer was connected to the column by 6 mm diameter stainless steel tubing which was kept completely full of water. The signal from the Dp transducer was sent to the Carrier-Demodulator CD (Pace Eng. Co., model CD10) which gave a maximum $\pm$ 10 volt DC output. To remove the 0.5 to 5.0 Hz component of the transducer signal, due to the plate oscillation, a Fourth-order Butterworth low pass filter with cut-off frequency of 0.25 Hz was built to filter the output of the demodulator. The details of the filter design are given in Appendix A.

Computer Controller Network

The controller network is shown as a block diagram in Fig. 3.2. The Δp signal from the filter was fed into a MACSYM 2 microcomputer (from Analog Devices, Inc., Norwood, Massachusetts) via an analog input. The microcomputer provides real time multitasking basic (MACBASIC) [22] and therefore various control schemes could easily be implemented. A frequency measurement of the plate reciprocation was also available to the controller as an analog signal.

Commands from the controller were sent to the stepping motor via a digital output. The stepping motor, which was coupled to the origianl manual controller of the variable speed motor, then changed the speed of

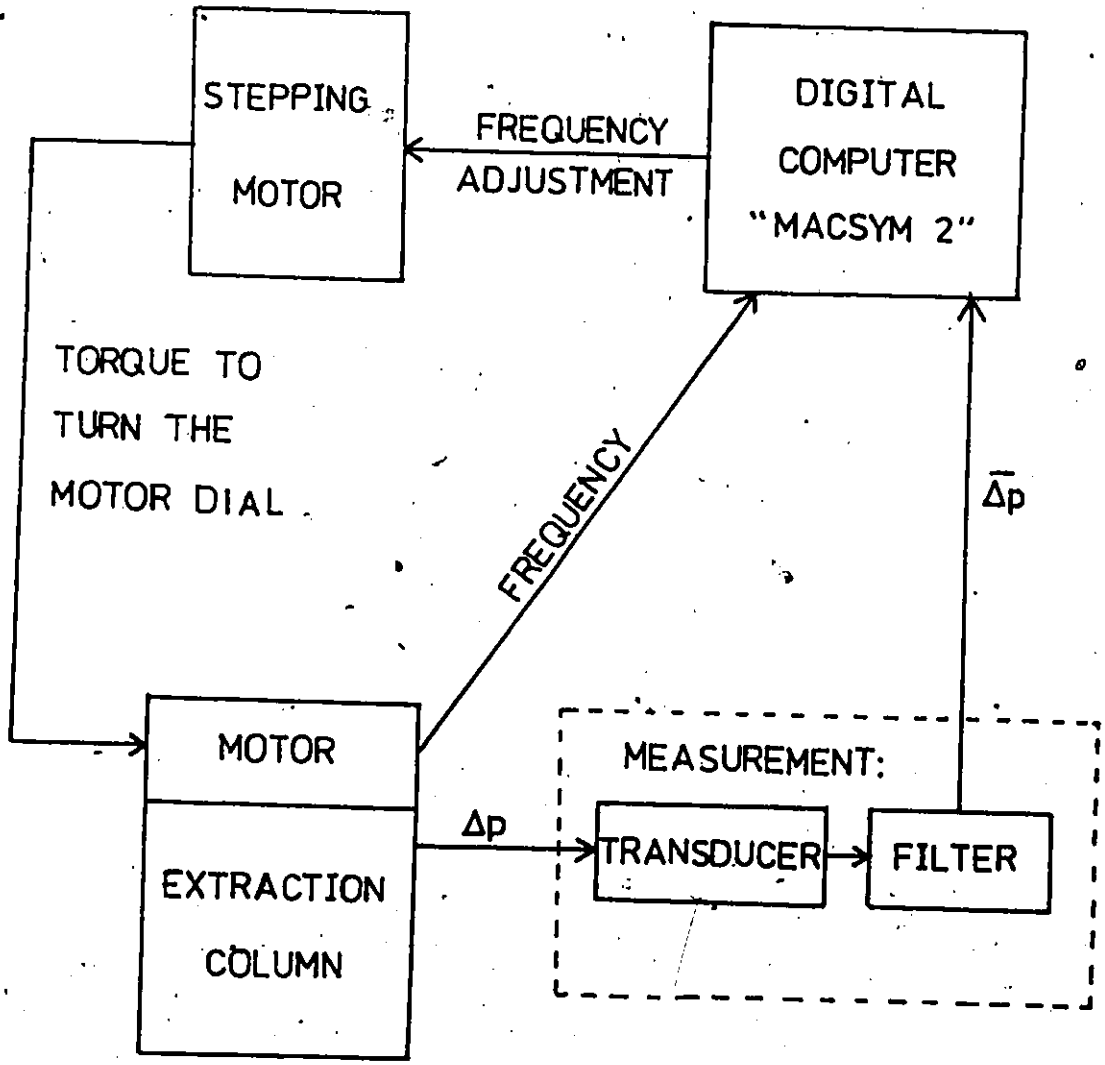

Fig. 3.2 The Controller Network

plate reciprocation of the column accordingly.

The stepping motor used was a stepping/synchronous motor from Superior Electric, type M112-FD12, with step size of 200 step/revolution and a speed of .2 sec/revolution.

CHAPTER 4

4. RESPONSE MEASUREMENT

The dispersed phase holdup ϵ in the column, for a given liquid-liquid system and plate stack, is affected by the following operating variables: superficial velocity of dispersed phase (U_d) and continuous phase (U_c) and agitation rate (A*f). This work was carried out in the absence of mass transfer, but since holdup directly affects flooding and mass transfer rate, the holdup was studied as the most important dependent variable.

In this chapter, the calibration curves for estimating U_d, f, U_c and Δp are presented first. This is followed by the subsections on the steady and unsteady state holdup response measurement, and lastly, on-line measurement of holdup via differential pressure transducer.

4.1 CALIBRATIONS

Several calibration lines were obtained by regression analysis and are shown, along with data points, in Fig. (4.1.1) to Fig. (4.1.5).

The calibrations of superficial velocities, U_d and U_c were done by observing the level increases in the column and a stop watch. The results are shown in Fig. (4.1.1) for U_d and Fig. (4.1.2) for U_c.

The calibration of differential pressure transducer was done via measuring the absolute static head in the column. The results are shown in Fig. (4.1.3).

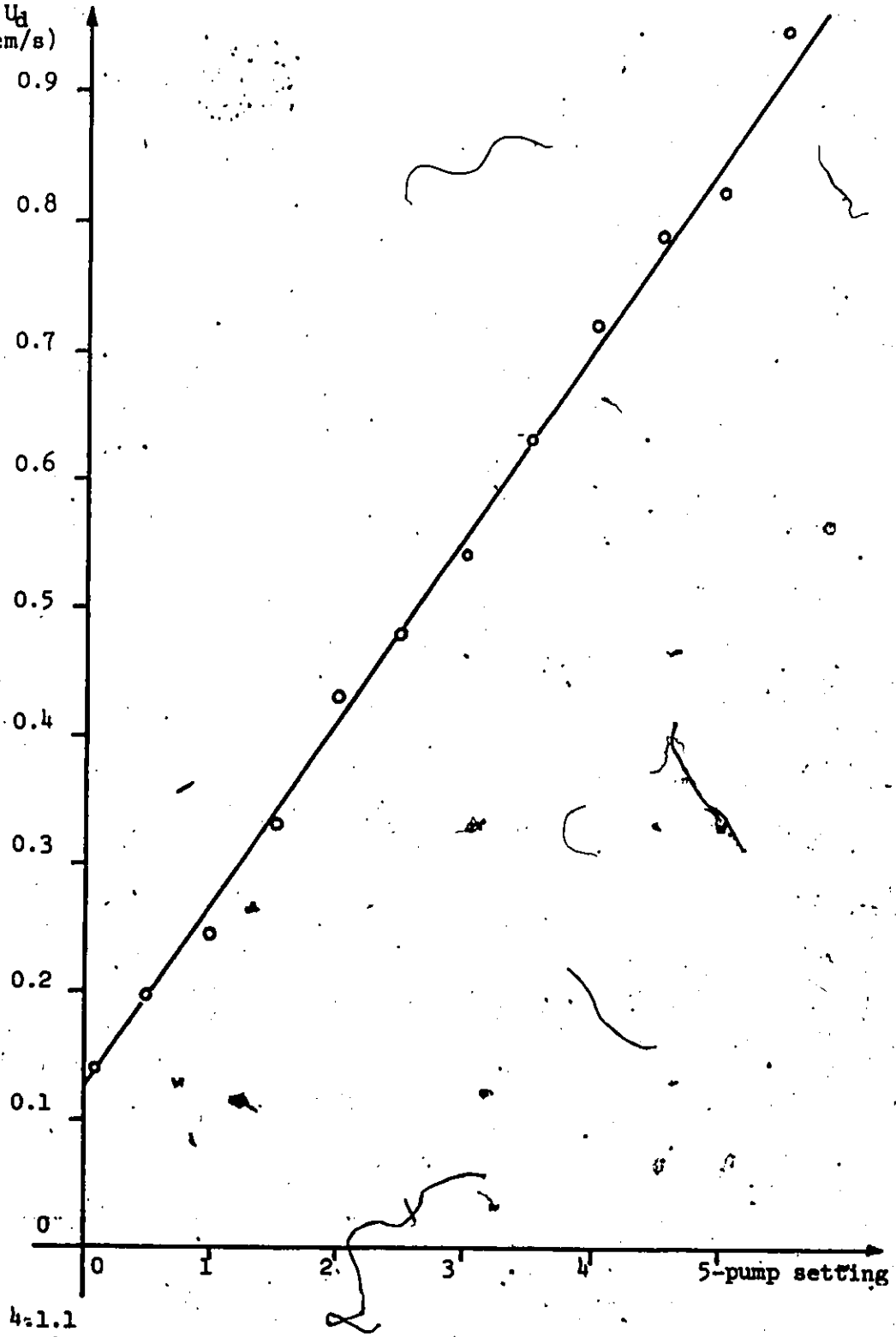

Fig. 4.1.1
Calibration curve: superficial velocity U_d vs pump setting

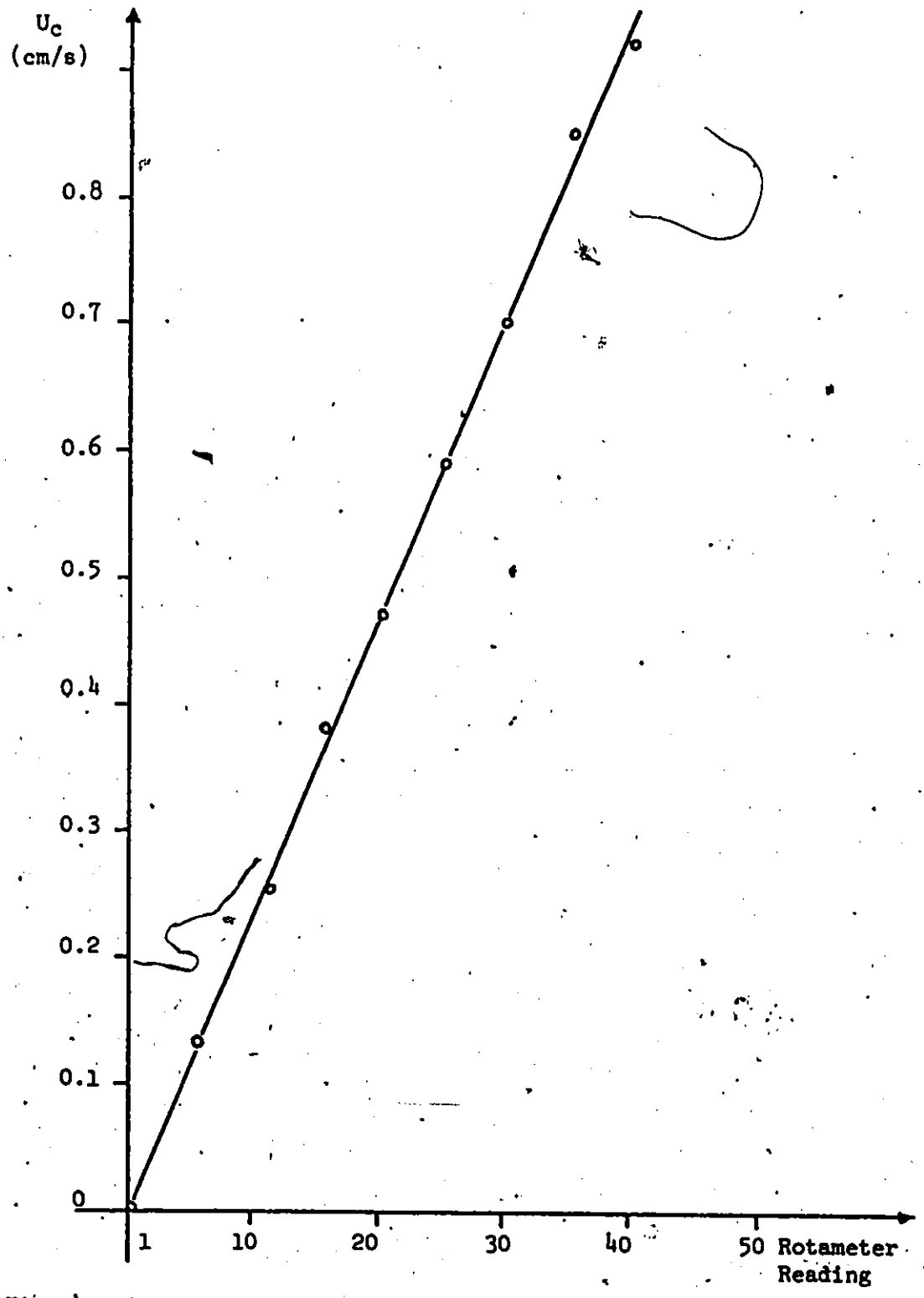

Fig. 4.1.2
Calibration curve: superficial velocity U_c vs Rotameter reading

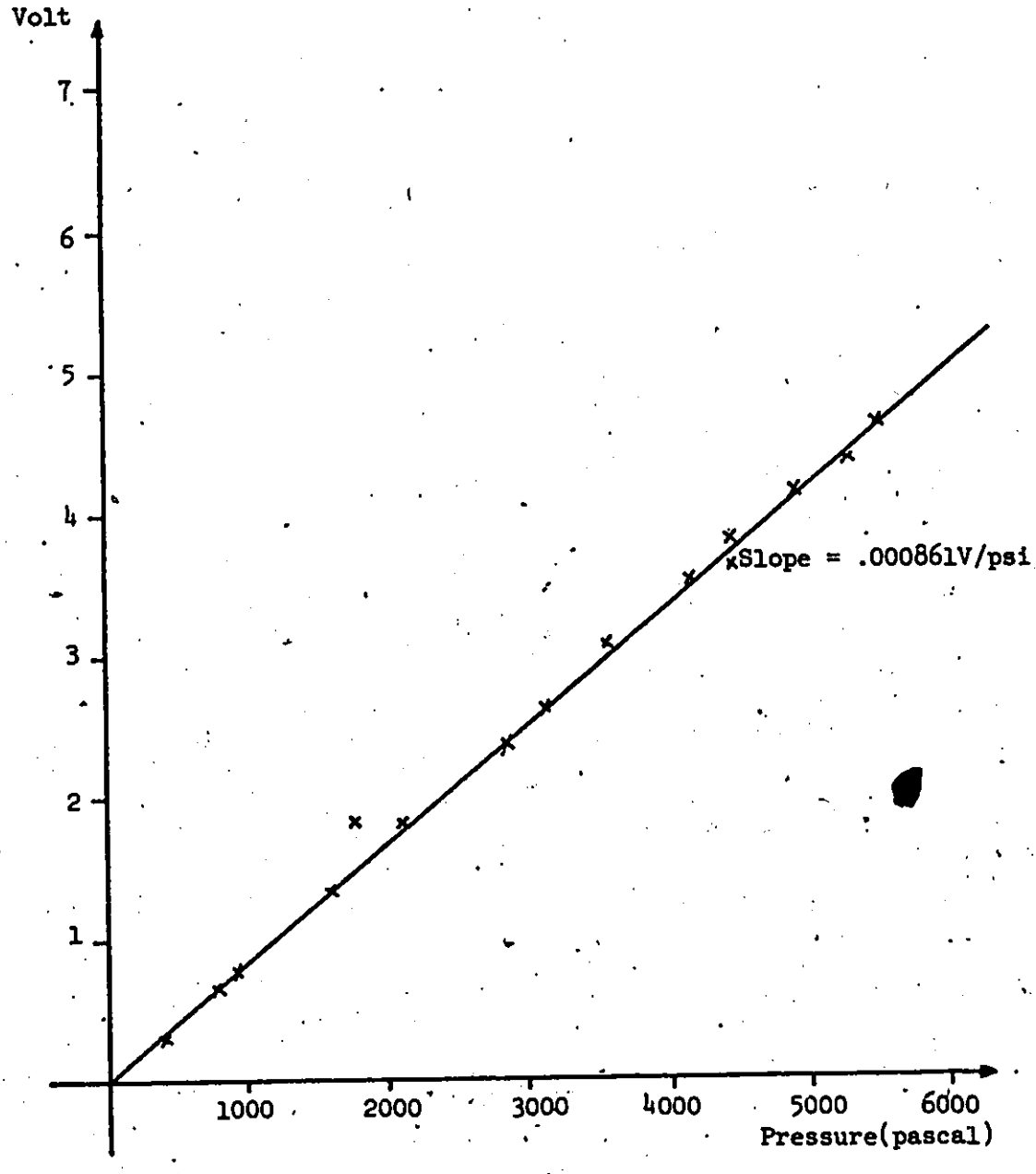

Fig. 4.1.3
Calibration curve: pressure transducer reading(volt) vs pressure in pascal

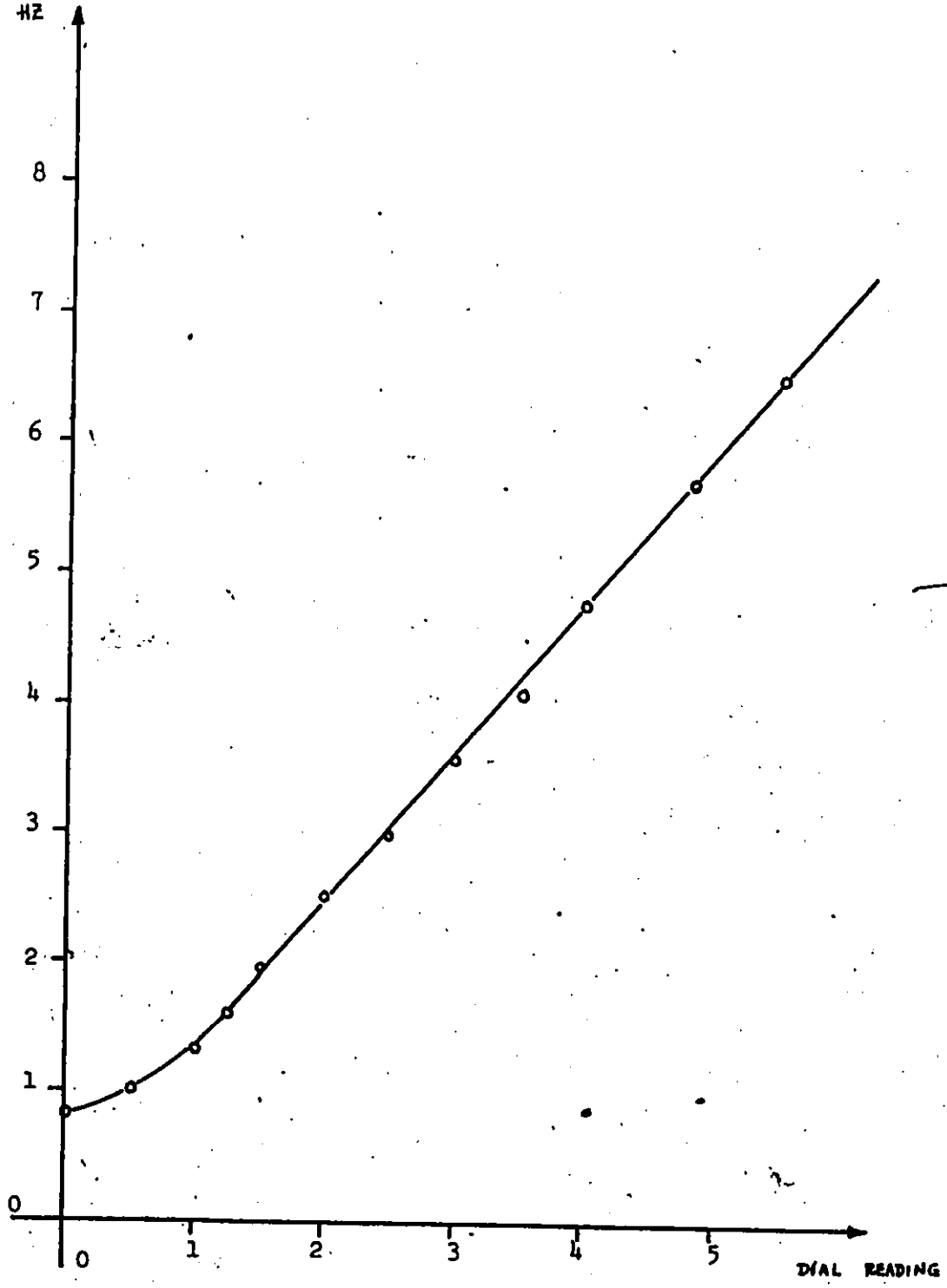

Fig. 4.1.4
Calibration curve: frequency f in Hz vs motor dial reading

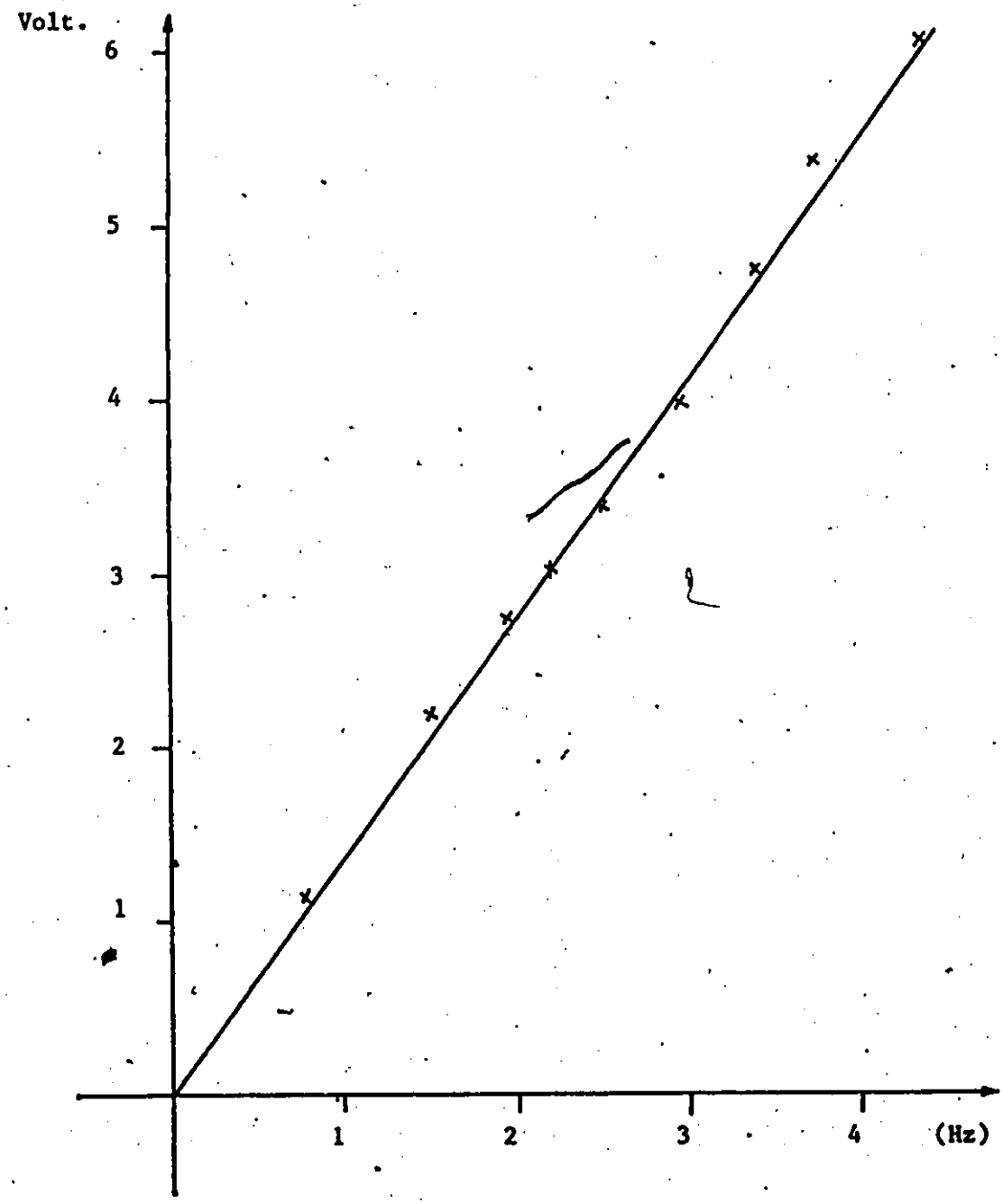

Fig. 4.1.5 Calibration Curve: Frequency in Hz Vs Voltage in Volt for on line frequency Measurement

The calibration of frequency dial and voltage measurement were done using an oscilloscope, where the absolute frequency can be calculated. The calibration of dial reading to HZ is shown in Fig. (4.1.4) and of voltage measured (by frequency measurement circuit) to HZ is shown in Fig. (4.1.5).

4.2 STEADY STATE AND UNSTEADY STATE HOLDUP RESPONSE

As ε is the volume fraction of Kerosene (dispersed phase) in the emulsion zone, a direct measurement could be done by drawing samples from various points in the column and separating the dispersed phase. However, the accuracy of this method is sensitive to the sampling rate and it cannot conveniently be done with a glass-walled column. Instead, with the present equipment setup, the steady state overall holdup was determined by shutting off the flows and allowing the dispersed phase droplets in the column to rise up to the interface. The resulting shift in interface level, gives the total volume of the dispersed droplets, and in relation to the volume of the column between the initial interface and the bottom of the agitated section, enabled the overall holdup to be calculated.

The relation between ε and interface level can be derived as follows (see Fig. 4.2.1):

$$\varepsilon = \frac{(H_{io} - H_{if}) * a}{(H_{io} - H_N) * a} = \frac{H_{io} - H_{if}}{H_{io} - H_N} \qquad (4.2.1)$$

In this work, H_N is constant and equal to 0.60 m.

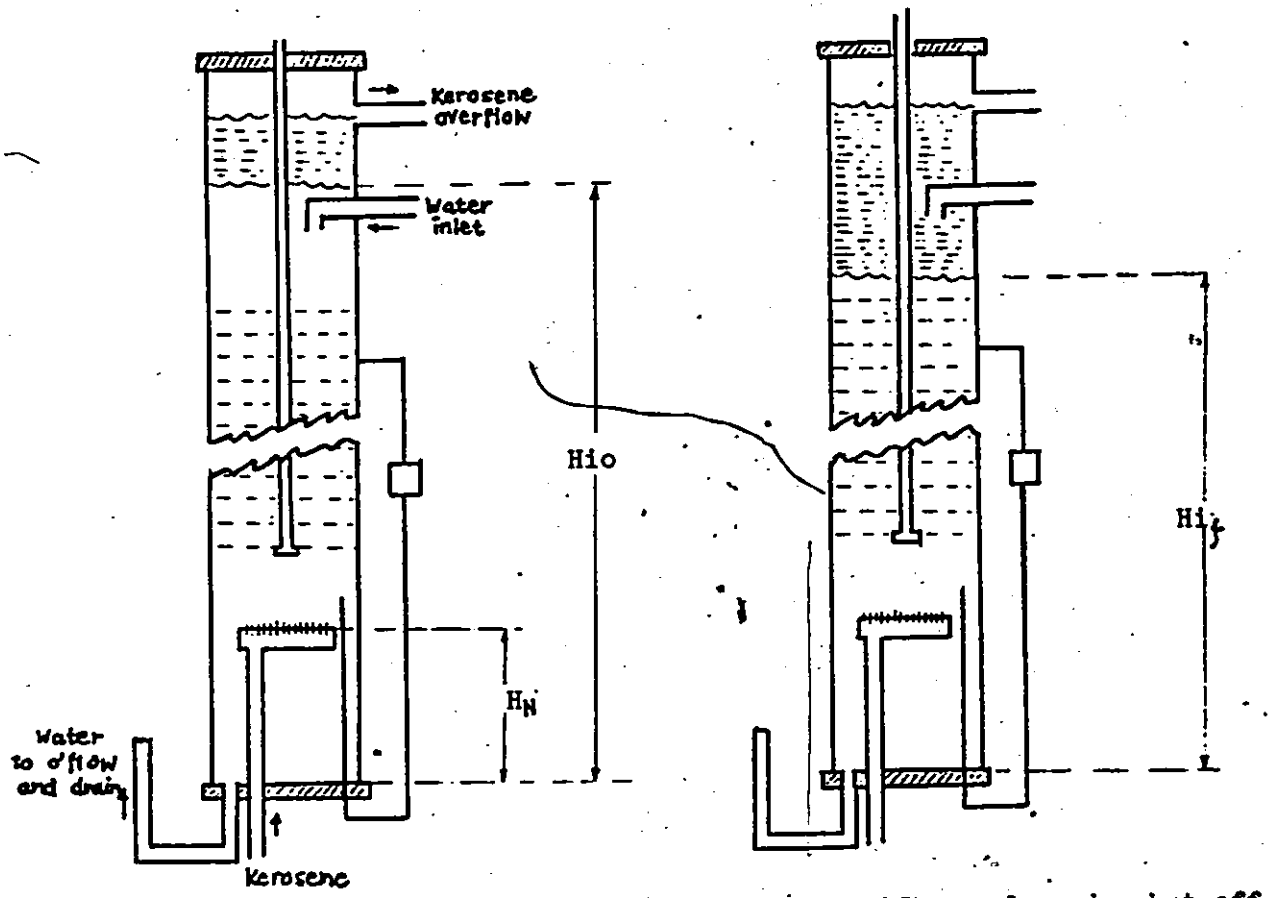

Fig. 4.2.1
Measurement of hold up by shutting off the flows.

A series of measurements of ϵ with various levels of U_d, U_c and f were collected; the accuracy of an individual measurement was estimated to be within $\pm$ 10%.

Some typical data of ϵ, as a function of the agitation velocity and superficial velocity, is shown in Fig. (4.2.2). With the given plate spacing, the highest value of ϵ that could be directly measured was in the region of 0.25.

These results agree well with data in Fig. 7 of ref. [12]. In ref. [12] it was shown that the following equation held approximately:

$$\frac{g\ \Delta\rho\ d_m(1-\epsilon)^3}{\rho_c\ U_s^2} = K\ (Re/\epsilon)^{-0.5} \qquad (2.2.4)$$

For drops behaving as rigid spheres, K was found to have a value of 30 $\pm$ 10%. A computer program was written to compute K from the present data using eqn. (2.2.4). The resulting K values for various ϵ were found, on the average, to be larger than 30, but when the data points are superimposed on Fig. 7 on ref. [12] as shown on Fig. (4.2.3), the variation is reasonable.

These results were in agreement with those presented on Fig. 5 on ref. [12] also. As one sees in Fig. 5 ref. [12], at a given agitation rate and U_d, ϵ increases with increasing U_c, since the change in superficial velocity changes the velocity of the droplets relative to the continuous phase (slip velocity). This in turn changes the effective Reynolds number and as a result increases the drag, leading to a decrease in droplets rise velocity, therefore ϵ will increase. However, as one sees in Fig. 4.2.2, at given U_d and a given <u>low</u>

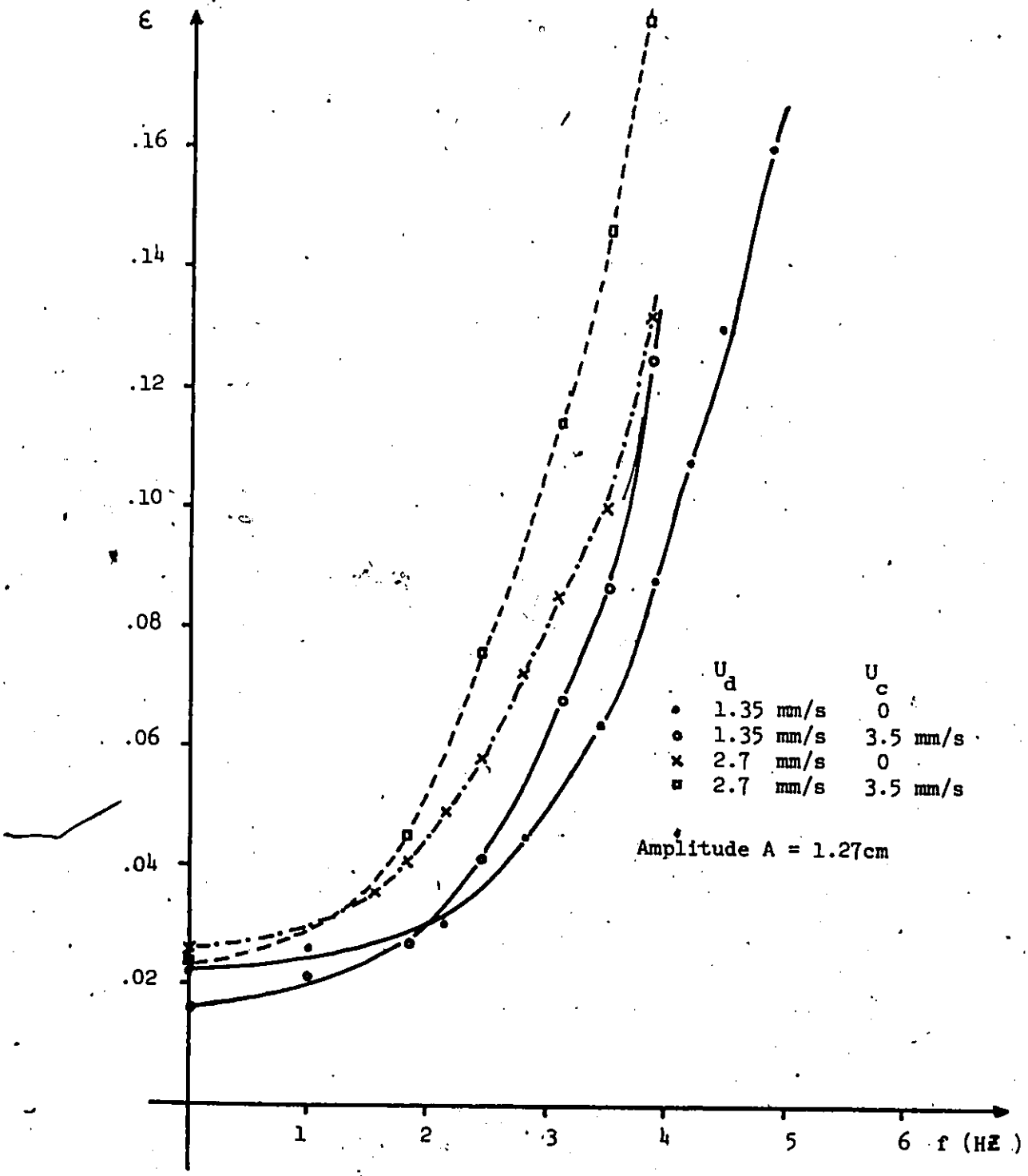

Fig. 4.2.2 Holdup data at various levels of U_d and U_c

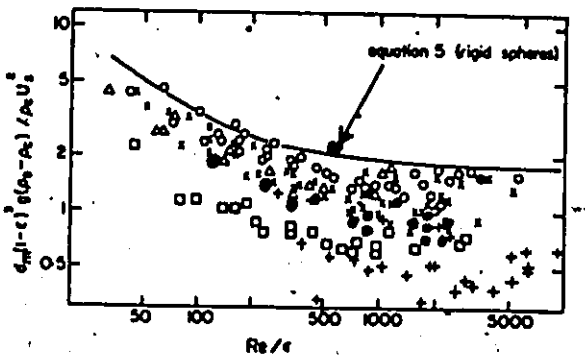

○ × □ △ Data from Ref. 12

• Data from this work

Fig: 4.2.3 Ergun friction factor plot from holdup data of Ref. 12 (Reprinted from Ref. 12) and from this work.

agitation rate, as U_c increased, sometimes ε decreased. This could be due to the fact that at zero or low agitation, the holdup is partly due to droplets clustering beneath the plates; an increase in Uc could have the effect of sweeping some of these clustering droplets off, thereby reducing the holdup.

In the origin, i.e. as U_d=0, the non zero ε values could be due to the trapped drops beneath the plates.

Since there is a linear relationship between ε and interface level (H_i), as described in eqn. (4.2.1), the unsteady state ε response can be determined by plotting instantaneous interface level vs time when making a step change on f or U_d, with the important proviso that Uc=0 and the continuous phase overflow valve is closed.

Both step up and step down of f and Ud were applied to the column nonconcurrently. Fig. (4.2.4) shows a typical unsteady state response of H_i when U_d was changed from 0 to 2.65 mm/s. The slope in the linear part of the response is approximately equal to U_d. Fig. (4.2.5) shows that when U_d was step decreased from 2.1 mm/s to 0, the slope in the linear part of the curve is also approximately equal to U_d. The times to reach steady state in both cases were approximately 70 seconds.

In the case where f was stepped up, as shown in Fig. (4.2.6), the times to reach steady state were much longer, about 150 seconds. The slope in this case is still close to U_d but having smaller value. But when f was stepped down, not only the slope is very different from U_d value, the column exhibit a different response as shown in Fig. (4.2.7). There is a longer dead time at the beginning and the interface level

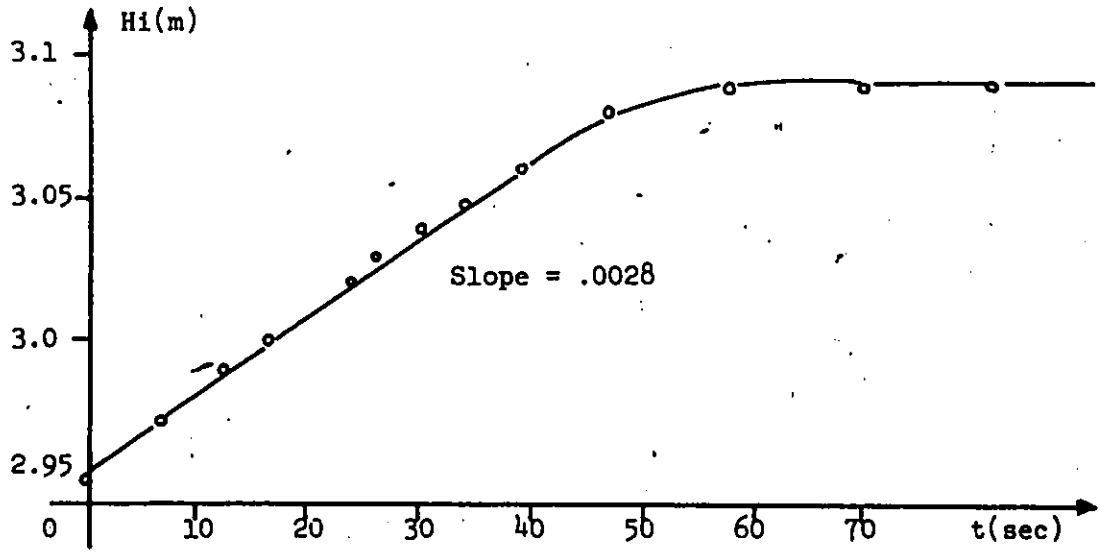

Fig. 4.2.4 Unsteady state response of Hi as U_d is changed from 0 to .00265 m/s (U_c = 0 and continuous phase overflow valve was closed)

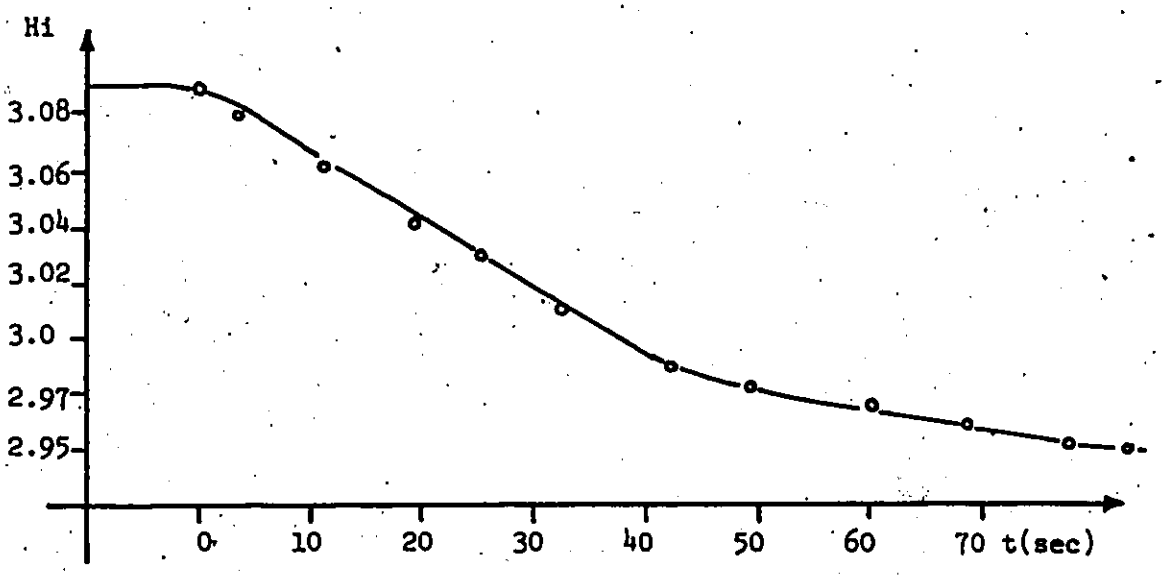

Fig. 4.2.5
Unsteady state response of Hi as U_d is changed from .0021 m/s to 0 (U_c = 0 and continuous phase overflow valve was closed)

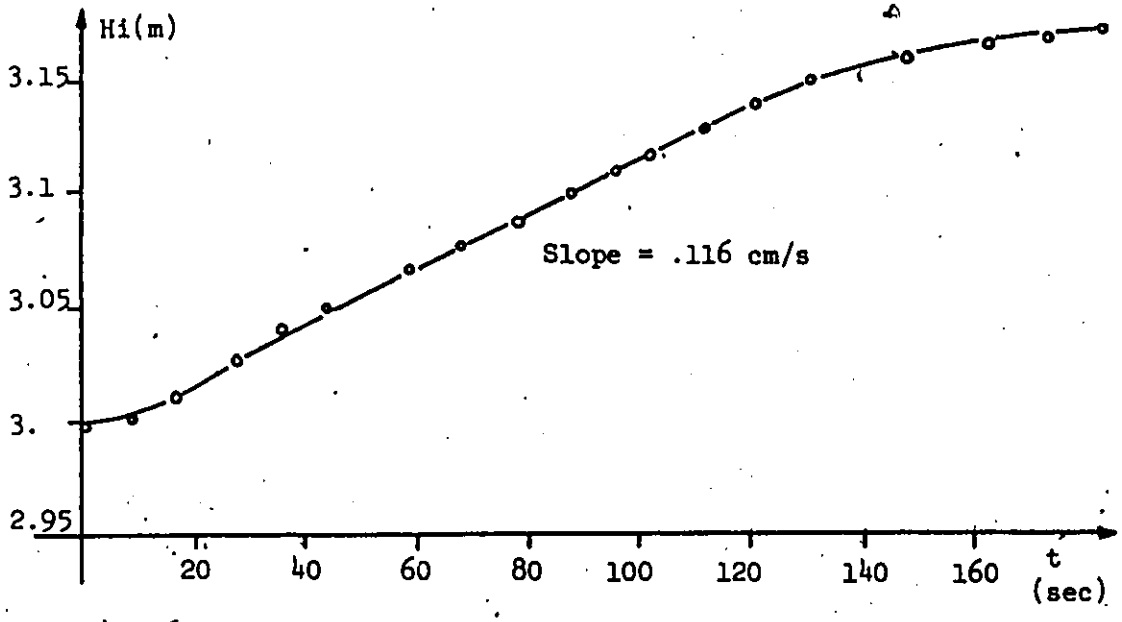

Fig. 4.2.6
Unsteady state response of interphase level Hi as f is changed from 0 to 4.2 Hz , U_d = 1.3 mm/s, U_c = 0 and continuous phase overflow valve was closed.

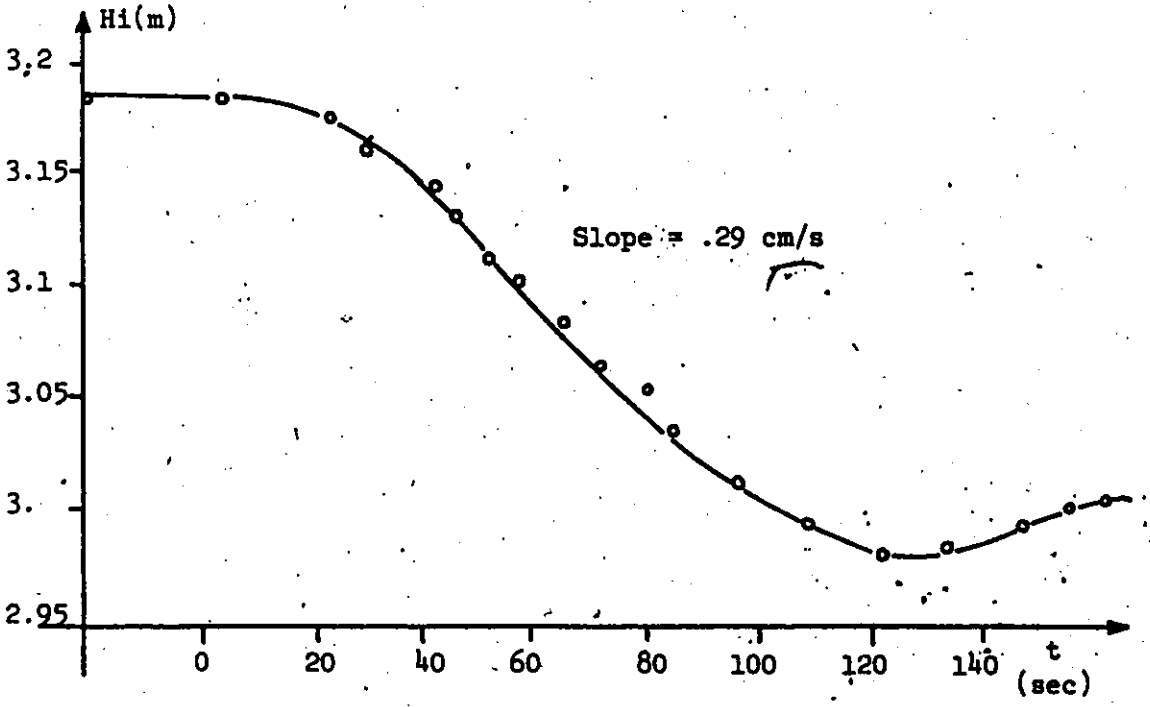

Fig. 4.2.7
Unsteady state response of interphase level as f is changed from 4.2 Hz to 0 Hz, U_d=1.3 mm/s, U_c=0 and continuous phase overflow valve was closed.

passes through a minimum before steady state is reached. This could be explained by the fact that when f is decreased, the larger drops "pick up" remaining small drops and for a short time at the end of the response period the holdup is abnormally low due to the very large, fast drops. Finally, the exit drop size decreases slightly to the steady state value.

In all cases, the time taken to reach steady state at a different operating point will be different as the process is non-linear.

4.3 ON-LINE MEASUREMENT OF HOLD-UP VIA DIFFERENTIAL PRESSURE TRANSDUCER

For control purposes, an on-line measurement or estimate of holdup is necessary. Baird et al [12] have developed a model for ϵ, which was presented earlier as eqn. (2.2.4) in section 2.2. In practice, there is difficulty in accurately calculating ϵ using the model, because it is difficult to classify a system as having a K of 15 or 30. Furthermore, Fig. (7) of reference (12) showed that the function plotted on the Y-axis is not very sensitive to changes in ϵ. Therefore, this model, though based on the fundamentals of two-phase flow, is not feasible for on-line estimation of ϵ.

It would be more feasible to measure the holdup directly, e.g. by relating it to the refractive index, the electrical conductivity of the emulsion zone, or the differential pressure between two fixed vertical levels.

In this study the last method was used because it was the simplest to implement in the time available, even though it is rather

limited by the requirement that constant densities of both phases be maintained in the emulsion zone. Since this study is concerned with hydrodynamic effects on operation and no mass transfer took place, there is no violation of this restriction.

The measurement of the differential pressure across the plate stack (P_2-P_1) was done by means of a calibrated differential pressure transducer Dp (Pace. Eng. Co., Model P7D) as shown in Fig. 4.3.1. The signal from the Dp transducer was sent to the Carrier-Demodulator (CD, pace Eng. Co., Model CD 10) which gave a maximum of $\pm$ 10 volt DC output.

Neglecting friction effects, a direct relation between overall holdup, ε (calculated from eqn. (4.2.1)) and Δp measured by the transducer Dp, can be derived as follows (refer to Figure 4.3.1):

$$P_2 - P_1 = \Delta P + \rho_w g H \quad \text{(via water-filled lines to transducer)} \quad (4.3.1)$$

But, also

$$P_2 - P_1 = (\varepsilon \rho_k + (1-\varepsilon)\rho_w) gH \quad \text{(via column in the absence of } \Delta p \text{ due to friction)} \quad (4.3.2)$$

Combining eqn (4.3.1) and (4.3.2), one will get:

$$\Delta P = -\rho_w g H + (\varepsilon \rho_K + (1-\varepsilon) \rho_w) g H \quad (4.3.3)$$

rearranging, one gets:

$$\Delta P = - \varepsilon g H (\rho_K - \rho_w) \quad (4.3.4)$$

Knowing that H = 1.8 m, ρ_w = 1000 kg/m^3 and ρ_K = 805 kg/m^3 rearranging eqn (4.3.4) and computing $1/(\rho_K - \rho_w) g H$ gives:

$$\varepsilon = .000\ 29\ \Delta p \quad (4.3.5)$$

where Δp is in pascal.

Under dynamic conditions, two problems emerged. With the

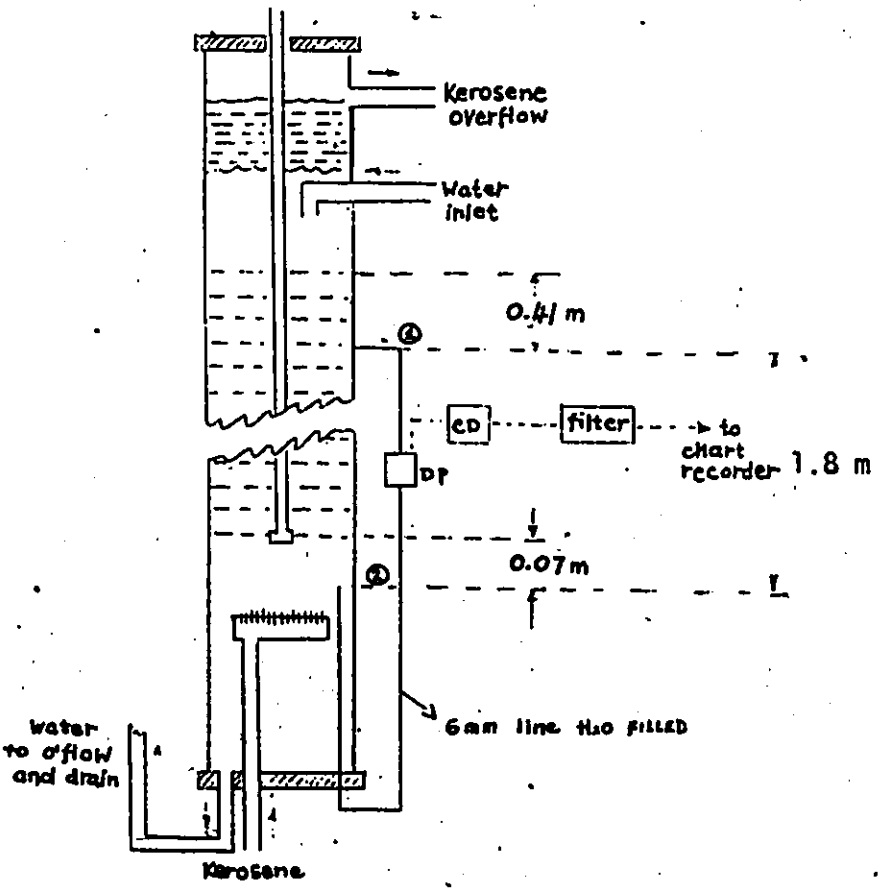

Fig. 4.3.1
Diagram set up of the differential pressure transducer

reciprocating plate oscillating, the measured Δp contained a sinusoidal noise having the frequency of the reciprocating plates. To get a time average measurement ($\overline{\Delta p}$) , i.e. to remove the noise generated by the plates, the Δp signal has to be filtered. Since the lowest drive frequency is about .75 HZ and the system time constant (1/5 of the time to reach steady state) is approximately 25 seconds, a fourth-order Butterworth low pass filter with cut off frequency of .25 HZ was designed to do the job. A fourth-order filter is used; because it has a sharp roll-off frequency. The details of the calculation is discussed in Appendix A.

The second problem was encountered when U_d, U_c, f, or any combination of the 3 variables were non-zero. Under this condition the relation in eqn. (4.3.5) does not hold, since the friction effects in Δp measurement need to be accounted for. The higher the Δp due to pressure drop, the less accurate was the representation of ϵ by Δp according to eqn (4.3.5).

This can be clearly seen in the experimental results shown in Fig. (4.3.2). The value of ϵ measured directly (sect. 4.2) was plotted against $-\Delta\bar{p}$ (after filtering) measured by the transducer.

In the same figure (Fig. 4.3.2), Δp calculated using eqn (4.3.5) was also plotted against ϵ. If this Δp was called "Δp static", one can see the Δp due to friction is the deviation from the "Δp static" line along the direction of the x-axis. It can be seen in Fig. 4.3.2 that under various conditions, friction constitutes only a small percentage of $\Delta\bar{p}$. Hence, $\Delta\bar{p}$ varies primarily with ϵ. It is also clear that Δp due

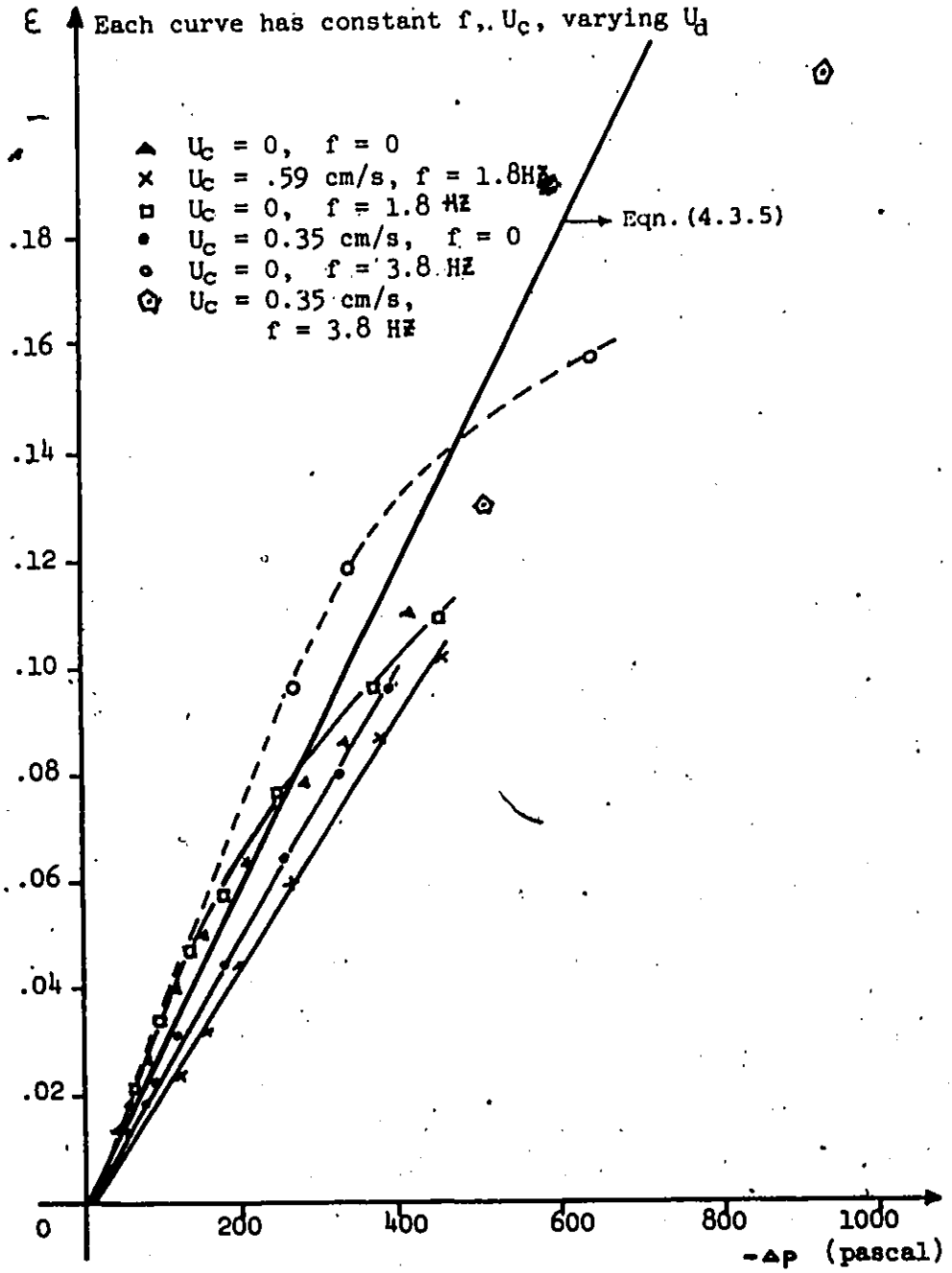

Fig. 4.3.2
A plot of ε vs (-Δp) at various levels of U_d, U_c, and f.

to friction is a function of U_d, U_c and (A^*f).

The theoretical prediction of the pressure drop due to frictional loss in a reciprocating plate column under various conditions can be described by following theoretical equations developed for single phase operation in Appendix B:

Case 1: plate oscillation in the absence of flow

$$\overline{\Delta p} = \frac{\frac{1}{4} \rho A^2 \omega^2}{C_o^2} \left(\frac{1 - \sigma}{\sigma}\right)^2 \tag{4.3.6}$$

The effect of oscillation in the absence of flow can be attributed to Bernouilli's law. This effect should be considered as additive to the values given under case 2 below.

Case 2: continuous phase flow, with plate oscillation

$$-\overline{\Delta p} = \frac{\frac{1}{2} n \rho_c U_c^2}{C_o^2} \left[\frac{1 - \sigma^2}{\sigma^2} + \frac{V^2}{2\sigma^2}\right] \tag{4.3.7}$$

$$\text{where } V = A \omega (1 - \sigma)/U_c \tag{4.3.8}$$

Case 3: continuous phase flow, no plate oscillation

$$-\Delta P = \frac{\frac{1}{2} n \rho_c U_c^2}{C_o^2} \frac{1 - \sigma^2}{\sigma^2} \tag{4.3.9}$$

To verify the prediction, a series of experiments were carried out under each case. In all cases, ε was measured from the interface level change (Sect. 4.2), the $\overline{\Delta P}$ measured was recorded on a chart recorder which was connected to the output of the low pass filter, and

static $\bar{\Delta}P$ was calculated using eqn. (4.3.5). the value of C_o was taken from ref. [21]. Accuracy in an individual c and $\bar{\Delta}P$ measurement is approximately $\pm$ 10%.

Case 1: Here the following settings were used; $U_d = 0$, $U_c = 0$, and f variable. In making the run, the column was first filled with water (continuous phase) before the oscillation was started..

The experimental results and the theoretical predictions are presented on Fig. (4.3.3) as a plot of (Af) vs $\overline{\Delta p}$. As can be seen, they are in good agreement, except that the theoretical prediction seems to be slightly lower, this could be due to the orifice coefficient used, C_o, which is not too accurate. As a precaution, the $\overline{\Delta p}$ signal was verified. A simple manometer was set up, as shown in Fig. (4.3.4). The experiments were repeated and the $\overline{\Delta p}$ data from the pressure transducer were compared with those obtained from the manometer. This comparison is also shown in Fig. (4.3.3) confirming that the two results were in agreement.

Case 2 : In this run, both U_c and f were varied, and U_d was kept at zero. The experimental results (adjusted to account for the Bernoulli effect in Case 1) and the theoretical prediction for U_d = 3.5 mm/s and 5.9 mm/s were plotted as $\overline{\Delta p}$ vs (A * f) on Fig. (4.3.5).

It can be seen that the experimental results agree with the theoretical prediction only at very low frequency, and deviate substantially as f increases, also they exhibit a minimum in Δp. This could be due to that there were a couple of assumptions made in deriving

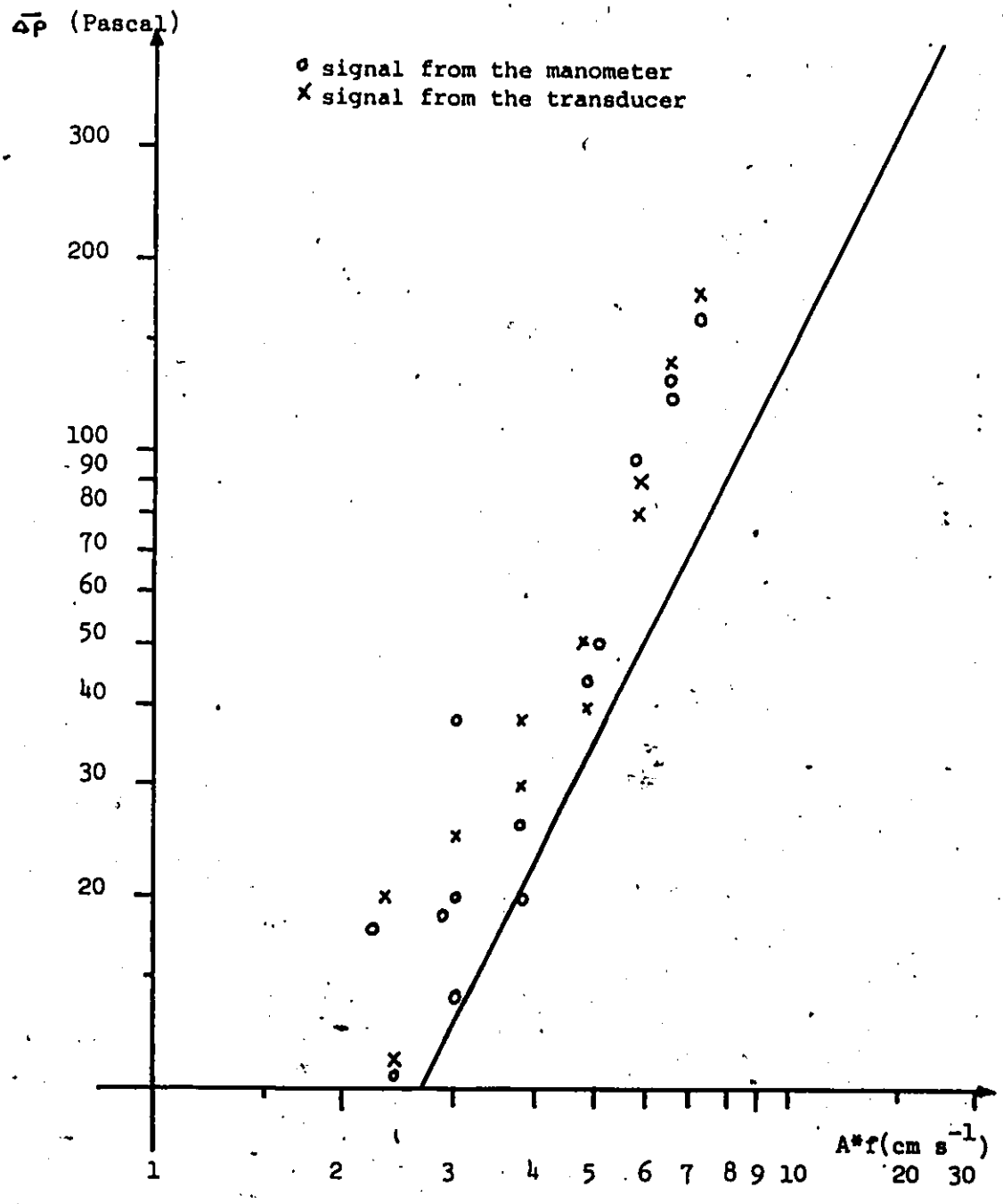

Fig. 4.3.3
A plot of (Af) vs $\overline{\Delta}$p at conditions $U_d = 0$, $U_c = 0$

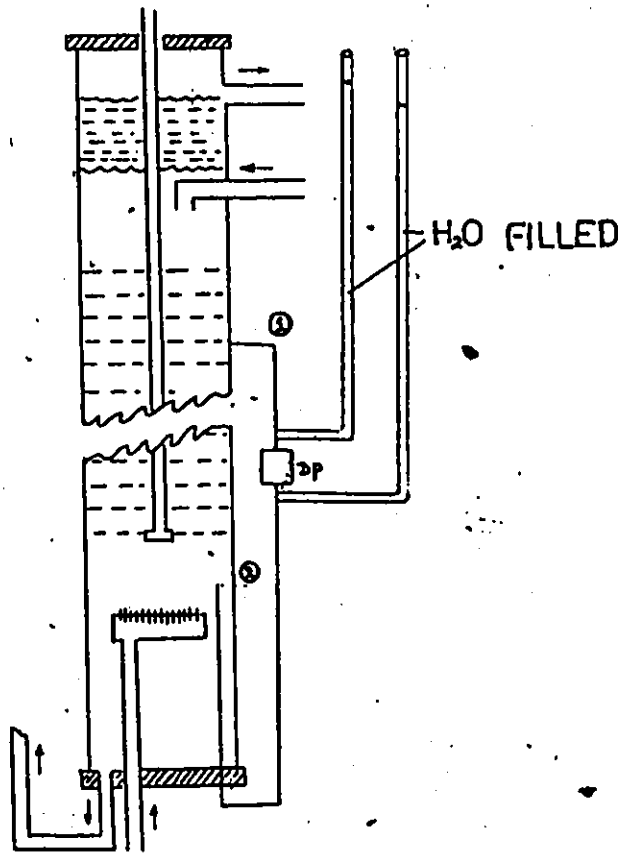

Fig. 4.3.4
Set up of simple manometer to check the $\overline{\Delta}$p signal of the transduces.

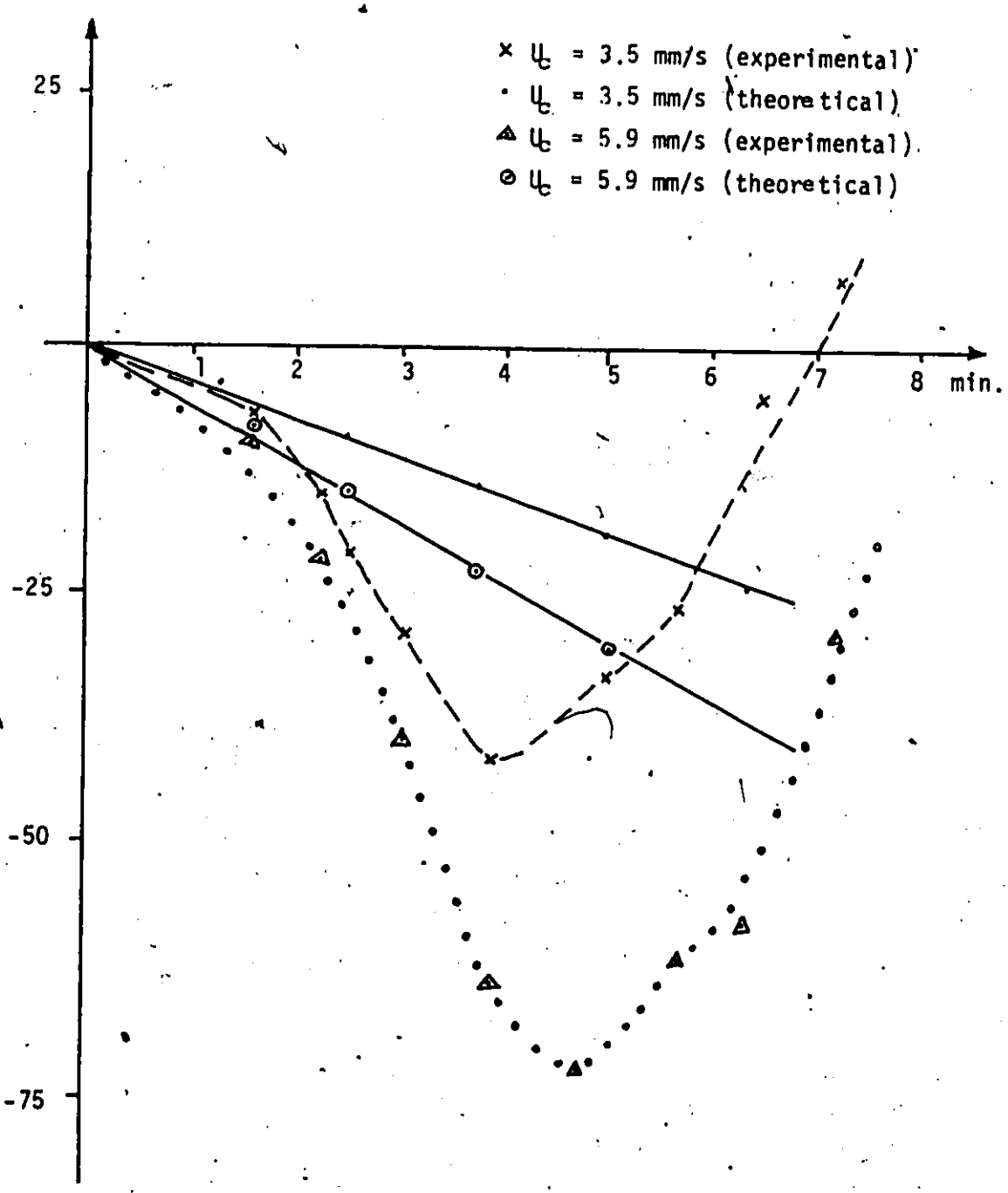

Fig 4.3.5 Δp Vs f at $U_d = 0$ and various U_c.

the theoretical prediction. In real case the combination effect of plate oscillating and phase flow is more complicated.

Case 3 : In the last series of experiments, U_d and f were zero, and the water flow U_c was varied. The results of $-\bar{\Delta}p$ measured and theoretical predictions Vs ε were again plotted and are shown in Fig. (4.3.6). The predicted and measured $\bar{\Delta}p$ values appear to agree well. The small discrepancy observed could be due to the assumption made on the orifice coefficient value. Furthermore, the accuracy of the measurement also contributes to the discrepancy, since the signals were so small that they lie within the error bound. It should be noted that the effect of U_c' (case 3) is 1-2 orders of magnitude smaller than the Bernouilli effect due to oscillation (case 1).

REGRESSION CORRELATION OF ε AND ΔP

To enable Δp measured to represent ε in the dynamic operation of the column, a linear regression is performed to relate ε to Δp, U_d, U_c and (A * f). This was considered preferable to the direct use of equations (4.3.6) to (4.3.8) for control purposes, because these equations did not represent the $\bar{\Delta}p$ data very accurately (see above).

The proposed regression model is:

$$\varepsilon = b_1 * \bar{\Delta}p + b_2 * U_d + b_3 * U_c + b_4 (A * f) + b_0 \qquad (4.3.10)$$

A 2 level factorial design was used to aid in planning the operating condition of each run. The range of each variable was selected so that it would give the widest possible range without

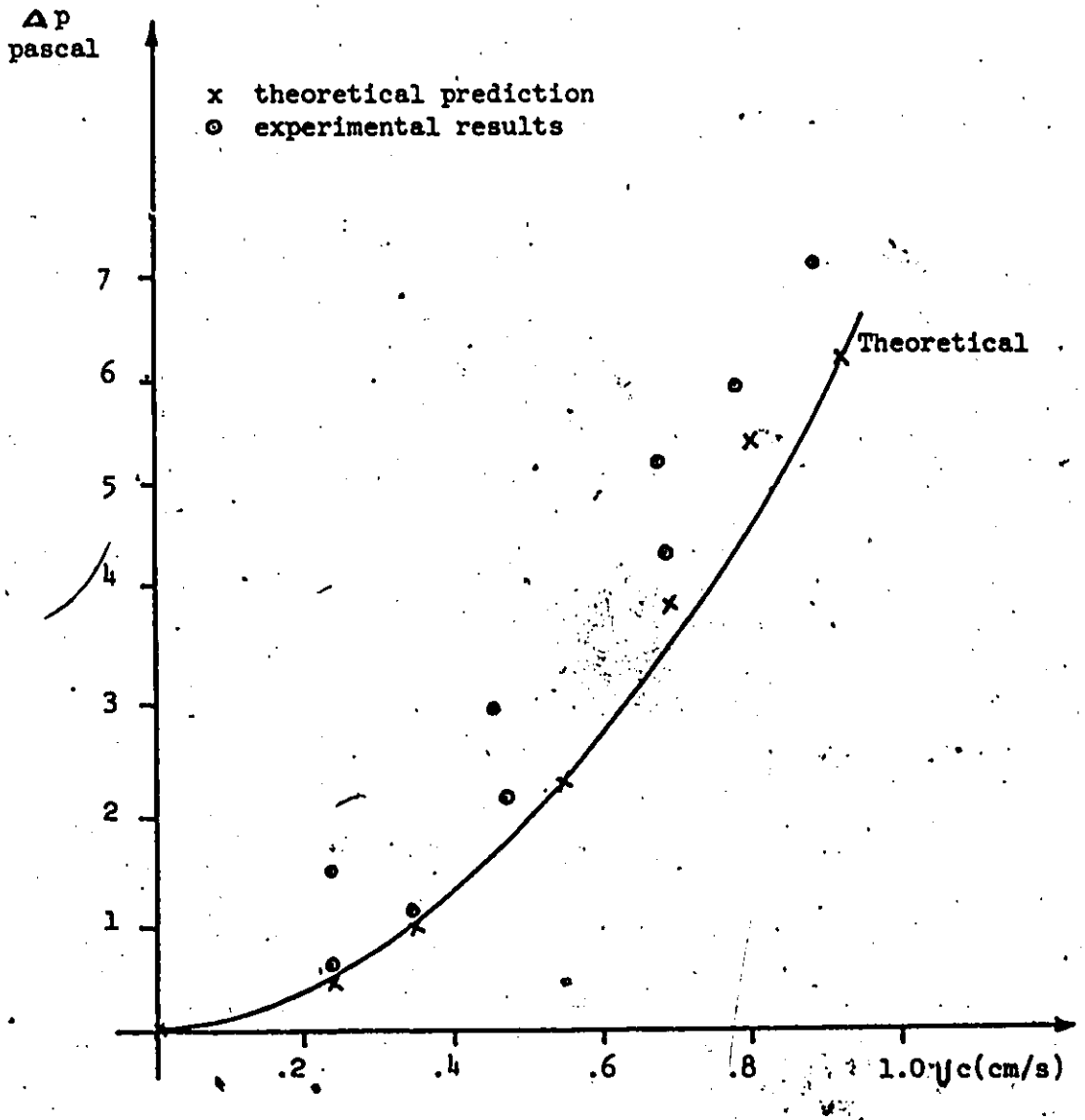

Fig. 4.3.6
Δp vs Uc at f = 0 and Ud = 0

flooding the column. Thus the range of U_d is: 0.0313 m/s - .0027 m/s

that of U_c is: .0035 m/s - .0093 m/s

and that of f is: 1.8 HZ - 3.8 HZ

The operating condition of 8 runs chosen by the design matrix were as follows:

U_d(m/s)	U_c(m/s)	f(HZ)
.0027	.0035	1.8
.00135	.0035	1.8
..00135	.0093	1.8
.0027	.0093	1.8
.00135	.0035	3.8
.0027	.0035	3.8
.00135	.0093	3.8
.0027	.0093	3.8

In eqn (4.3.10) above, $\bar{\Delta p}$ and ϵ were both response variables, thus the magnitude of the error in $\bar{\Delta p}$ is about the same as in ϵ. In this work, the ordinary least square method was used to estimate the parameters.

The above 8 runs (replicated three times) with other ϵ data collected previously were fed into a multiregression computer program. Other data were included to extend the range of each variable.

The parameters estimated by the regression program give the equation:

$$\epsilon = .00023\ \Delta p + 2.289\ U_d - 2\ U_c - .016\ (A * f) + .00476 \quad (4.3.11)$$

with individual confident interval on b_i's as:

$$-.00024 < b_1 < -.0023$$

$$1.01 < b_2 < 3.56$$

$$-2.38 < b_3 < -1.63$$

$$-0.31 < b_4 < -.01$$

$$.00069 < b_0 < .00884$$

wher: Δp is in Pascal with the difference always $P_2 > P_1$

U_d is in m/s

U_c is in m/s

f is in HZ

A is in m

It should be noted that A was constant in all experiments as .0127 m. It has been assumed that the agitation parameter is (A*f) and that amplitude and frequency independently have no other effect.

Since negative holdup has no physical meaning, when using eqn. (4.3.11) to calculate ϵ, one should keep in mind that the lowest possible value of ϵ is zero.

To test the accuracy of the model, residual analysis was perforemd. ϵ predicted by the regression line ($\hat{\epsilon}$) were plotted against direct measured ϵ, (calculated from eqn (4.2.1), ϵ_i or observed ϵ), in Fig. (4.3.7). The deviation of this line from the 45^o line represents the residual $(\epsilon_i - \hat{\epsilon})$. It can be seen that the residual, $(\epsilon_i - \hat{\epsilon})$ over all i is approximately 10% of the observed ϵ. In 10 repeated individual measurements of ϵ the variation is also $\pm$ 10%. This means that the sum

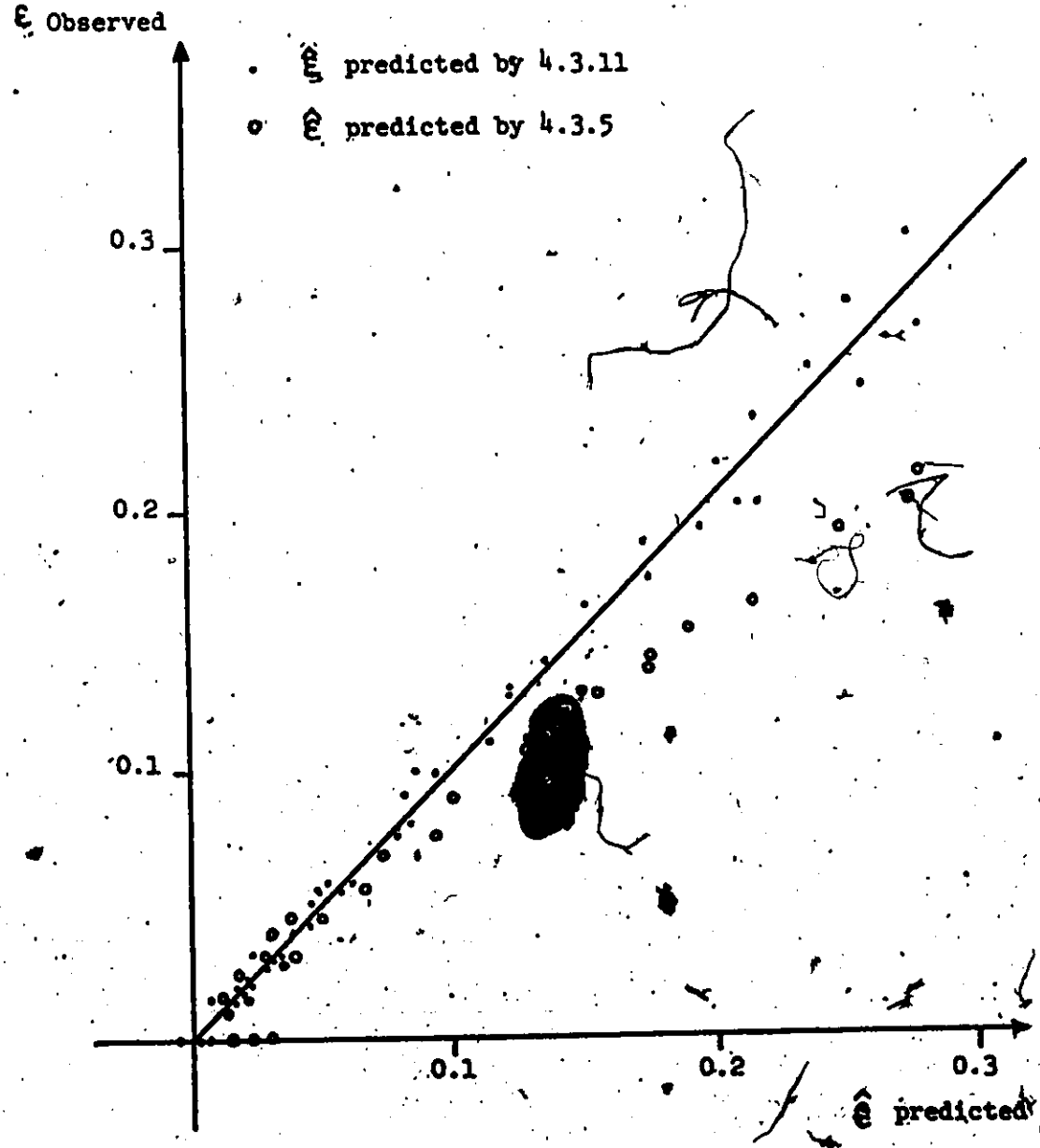

Fig. 4.3.7
Plot of ε observed vs $\hat{\varepsilon}$ predicted.

of squares due to regression is about the same as sum of square due to pure error, since:

S.S. Residual = S.S. pure error + S.S. L.O.F. (Lack of fit)

we can conclude that expectation of mean square L.O.F. is smaller than mean square pure error, which means that there is no lack of fit observed.

In the same graph, the ϵ values predicted from eqn (4.3.5) which neglected friction effects, were also plotted against ϵ_i. Compared with the ϵ calculated from eqn (4.3.5), $\hat{\epsilon}$ predicted by regression is a much better representation of the observed ϵ.

However, since the errors in both Δp and ϵ have the same magnitude, a better way of estimating the coefficients of the regression equation would be "parameter estimation using error in variable model". Due to time limitations, the regression equation obtained from least squares was accepted as sufficient. Thus, from here on, ϵ was determined from Δp measurement and the empirical correlation developed above as equation (4.3.11).

CHAPTER 5

5. COMPUTER CONTROL OF THE COLUMN

In extraction research, there have been very few reports on direct computer control specifically related to solvent extraction applications. While the viability of the computer for off-line and on-line studies for process monitoring, logging of data and supervision of alarm systems, etc., has been confirmed, the application of the computer to actual on-line process control studies in extraction process has still to be developed.

In this work, an extensive computer control study of a 15 cm diameter Karr column was carried out. A control strategy was initially developed before step tests were done on the column. After that various controllers were tested, from the conventional PI to sophisticated SELF-TUNING-REGULATOR. Brief discussions of each control scheme and the test results are also presented below. The evaluation of the controllers is done in Chapter 6.

5.1 DEVELOPMENT OF CONTROL STRATEGY

To develop a controller strategy, operating objectives of the process need to be established. The basic operating objective of any processing unit is the profitable production of a specified product.

In the liquid-liquid extraction operation, the separation of the constituents of a liquid solution is accomplished by contacting with

another insoluble liquid. Thus, the more complete the separation the more profitable the operation. This separation may be enhanced by maximizing the mass transfer rate of solute.

Thus the operating objective of the process is to maximize the mass transfer rate so as to maintain a desired concentration of solute in the extract and raffinate.

As noted on section 2.5, in this kind of extraction column, the local mass transfer rate of solute at any stage n can be expressed by eqn. (2.5.3), from which it is clear that An can be varied to maximize Q_n.

It can be shown that the ϵ of the system can be directly related to A_n as follows;

$$A_n = \frac{6\epsilon}{d_m} \qquad (5.1.1)$$

where d_m = sauter mean diameter, defined as the diameter such that if all the dispersed organic phase consisted of droplets of uniform diameter d_m, the interfacial area would be that of the actual dispersion.

From eqn (5.1.1), one can see that A_n can be maximized by maximizing ϵ. As shown in Figure (4.2.2), ϵ will increase with increasing (A*f) and U_d. With increasing U_c, ϵ will only increase near the flooding region. This suggests that U_c is not an ideal manipulated variable as it is only effective near the flooding zone. Furthermore, ϵ is the least sensitive to changes in U_c. In real operation, it is not advisable to change U_d very often, as a large surge tank will have to be used. Rather the changes in U_d and U_c should be taken as load changes.

Thus the (A*f) is the prospective manipulated variable. Since it is difficult to change the amplitude on-line, f was then selected to be the manipulated variable. f will be varied to maintain ϵ at a desired set point under various load changes. However, as can be seen from figure 4.2.2, with this choice of manipulated variable, the system would be highly non-linear. Thus, the operating range is critical.

The suggested control scheme is the feedback of $\hat{\epsilon}$, which is obtained from Δp measured using the regression eqn (4.3.11), and the use of f as manipulated variable. If changes in U_d are known, a feed-forward mode can be implemented.

One problem concerning the operation of the column has yet to be tackled; there is no automatic system to keep track and control the interface level. During this research, the interface level was left free to vary. Some degree of built-in control was provided by the overflow arrangement shown in Fig. 3.1. Care was taken to ensure that it did not go above the kerosene overflow.

5.2 STEP TESTS TO FIND PROCESS TRANSFER FUNCTIONS

In order to design a control algorithm using Z-transform, a process model is required. Although the PI and PID algorithms are frequently tuned by trial-and-error approaches, a model can be used to give initial estimates of the tuning parameters, information about the order of the process and hence lead to an intelligent choice of control structure. Furthermore, the model can help one in understanding the closed-loop behaviour.

The process model in this case is determined from the open-loop step response of the process using the Reaction Curve Method [24]. Determination of the model parameter is via a graphical construction and simple calculation. The accuracy of models so determined is not generally the best possible, but it is acceptable in this case.

A step change was made in the manipulated input (f), and the output $\hat{\epsilon}$ of the column was observed. A first-order plus dead time transfer function was then fitted to the response as follows:

$$\frac{\hat{\epsilon}(s)}{f(s)} = \frac{K\, e^{-\theta s}}{\tau s + 1}$$

where, θ = dead time of the process (the non minimum phase period is model as deadtime in this work)

τ = time constant of process (time for process to achieve 63.2% of its steady state value).

K = gain of the process.

Figure (5.2.1) shows a typical response of $\hat{\epsilon}$ to changes in f from 1.33 HZ to 3.3. HZ with U_d = 1.35 mm/s and U_c = 0 mm/s.

As the system is non-linear, K, θ and τ vary with varying level of U_d, U_c and f. The general trends in the variation of K, θ and τ are:

θ, increases as f increases, significantly larger for a decrease in f rather than for an increase.

τ, increases as f increases. Reduces for lower direction of agitation

K, increases as f increases.

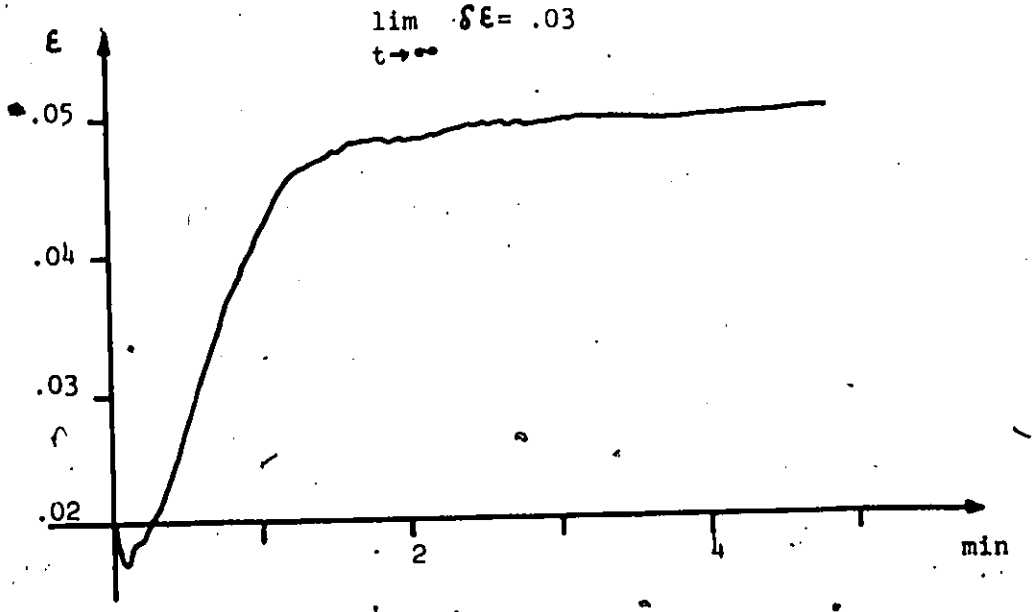

Fig. 5.2.1 Open loop ε response to a positive step change in δf (1.33 - 3.3 Hz).

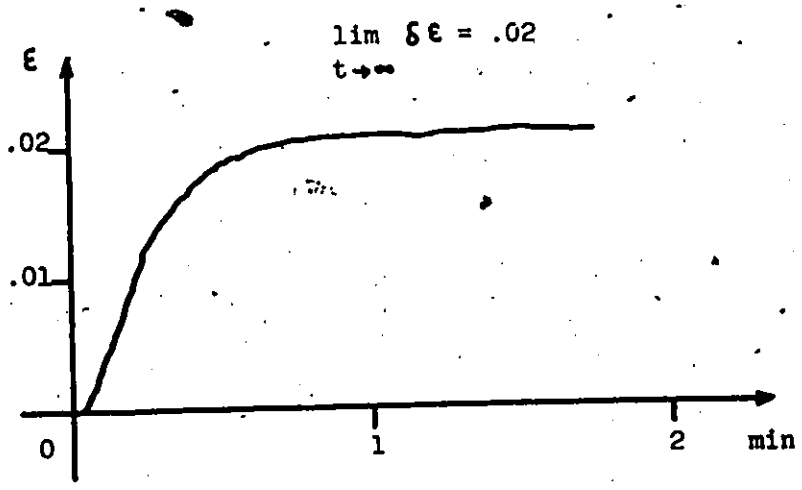

Fig. 5.2.2 Open loop ε response to a positive step change in δU_d (0.00135 m/s — .0027 m/s)

Table 1: Estimation of the ε transfer function G_p using step changes in δf

U_d (m/s)	U_c (m/s)	Step changes δf (HZ)	ε(Hold-up) Response	Process parameters K	τ (sec)	θ (sec)	Figure
.00135	0	+1.97 (1.33→3.3)	+.03	.014	33	15	5.2.1
.0027	0	-2.14 (3.4→1.25)	-.0526	.0246	24	18	C.1*
.00135	0	+ .47 (2.5→2.97)	$\pm$.02	.0426	43	10	
.00135	.0035	+ .47 (2.5→2.97)	+.03	.065	62	4	

*Fig. C.1 is given in Appendix C.

The results of the estimation of transfer function at various levels of U_d, U_c and f are presented in table 1.

A step change was also made in the disturbance input(U_d), and the output $\hat{\varepsilon}$ of the column was again fitted to a first-order plus dead-time transfer function as discussed above. Figure (5.2.2) shows a typical response of $\hat{\varepsilon}$ to changes in U_d from .00135 m/s to .0027 m/s. Where U_c = 0 and f = 1.3 Hz.

In this case K, θ and τ are all constant at low U_d but vary at higher U_d. They are also functions of U_c and f.

The results of the estimation of transfer functions at various levels of U_d, U_c and f are presented in table 2.

The nominal transfer functions used in the control testing are:

$$\underline{\varepsilon(s) \text{ with respect to } f(s)} \quad : \quad \frac{.015, e^{-15s}}{33\ s + 1}$$

where the holdup is in the region of .02 to .05 and U_d = 1.35 mm/s, U_c = 0.

$$\underline{\varepsilon(s) \text{ with respect to } Ud(s)} \quad : \quad \frac{22\ e^{-5s}}{14\ s + 1}$$

where the holdup is in the region of .05 to .08 and U_d change was from 1.25 mm/s to 2.7 mm/s, U_c = 0 and f = 3.3 HZ

5.3 FEEDBACK P+I FOR SET POINT CHANGES IN $\hat{\varepsilon}$

A basic classical control configuration is shown in Fig. 5.3.1. Where $G_p(Z)$ is the Z-transform of $(G_p(s) * H(s))$ and $G_{FF}(Z)$ is the Z-transform of $G_{FF}(s)$. The P+I algorithm was used in this case, and the

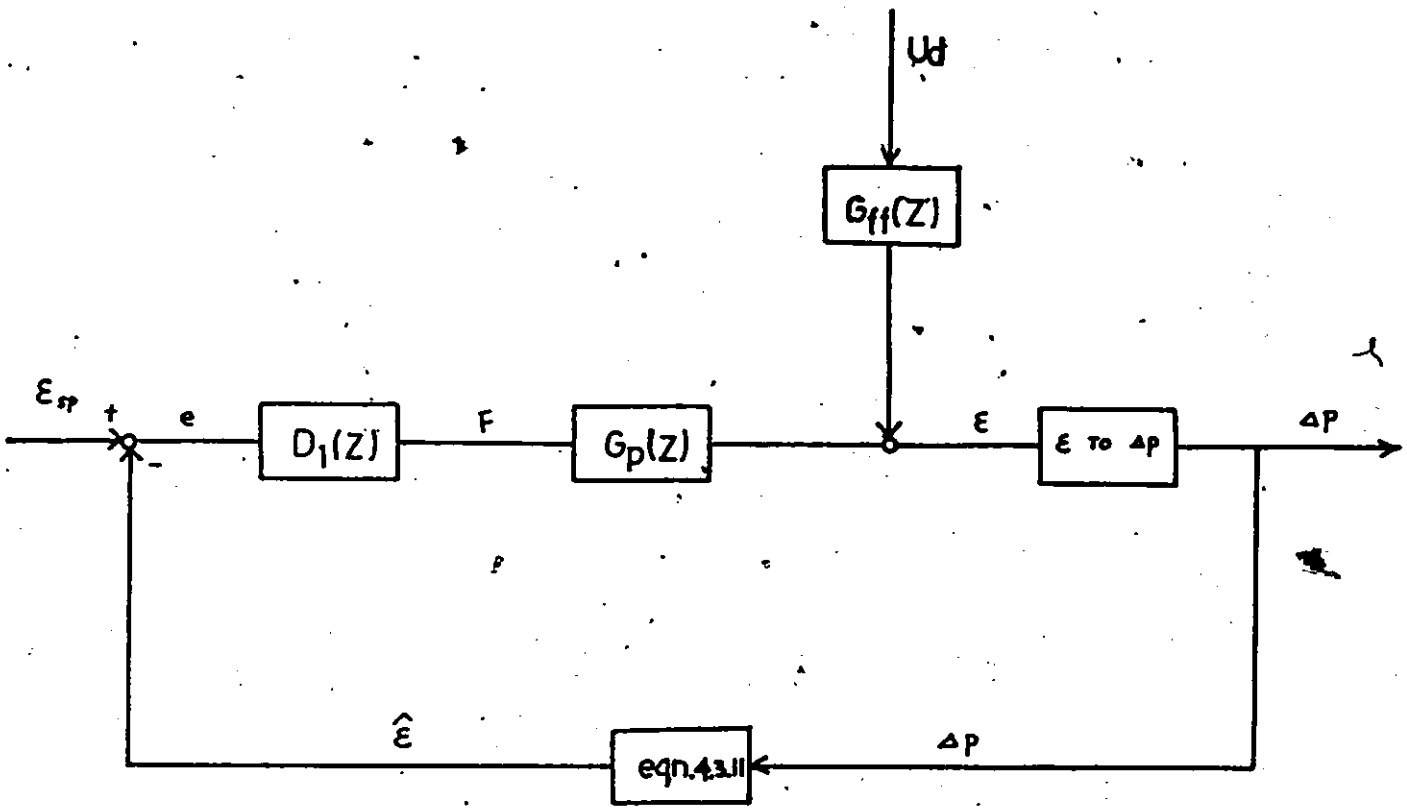

Fig. 5.3.1 Basic Classical Control Configuration

Table 2: Estimation of the ε transfer function G_f using step changes in δU_d.

U_c (m/s)	f (Hz)	step changes δUd (m/s)	ε response	process parameters K	τ (sec)	θ (sec)	Fig.
0	0	.00135 (.00135+.0027)	+.02	15	13	3	5.2.2
0	0	.00075 (.00135+.00195)	+.0145	24	12	4.5	C.2*
0	0	.00045 (.00033+.0038)	+.022	49	19	4	
.0059	0	.00045 (.0033+.0038)	.01	22	20	3	
.0059	1.33	.00045 (.0033+.0038)	.018	42	26	16.5	

*Fig. C.2 is given in Appendix C.

control interval was 1 minute. The presence of varying deadtime, up to 60 sec, in the f loop prevented the use of smaller control intervals.

5.3.1 DIGITAL P+I ALGORITHM

Referring to Fig. 5.3.1. the digital form of P+I algorithm is expressed as:

$$Fn = K_c \left(e_n + T/T_R \sum_{i=0}^{n-1} e_i\right) + M_R \qquad (5.3.1)$$

where : Fn = controller output at instant n.

e_n = error term defined as the difference between the set pt and the measured value

K_c = proportional gain

T_R = reset time

T = sampling time

MR = initial setting of Fn.

both K_c and T_R were determined by on-line tuning.

Anti reset windup was also incorporated in eqn (5.3.1) by specifying the upper and lower limits of the controller output.

The values of K_c and T_R of the ε controller were determined by on-line trial-and-error tuning. The ε controller was tuned with respect to a .03 setpoint change in ε.

The following steps were used in order to find the optimal proportional gain K_c and reset time T_R:

(1) take out the integral action initially

(2) set K_c at high value and make the set-point change, keep increasing K_c until the loop becomes very underdamped and oscillatory. The gain at which this occurs is called the ultimate gain.

(3) Back off on K_c to half of this ultimate gain

(4) Bringing in the integral action by reducing T_R by factor of 2 and making the set-point change.

(5) Find the value of T_R which makes the loop very underdamped and set T_R at twice this value.

5.3.2 RESULTS AND DISCUSSION

The best values of K_c and T_R found by trial and error method were: K_c = 40 and T_R = 120 sec. A lower value of K_c and higher value of T_R were observed to give a sluggish response whereas a higher Kc and lower T_R made the controller oscillatory.

Fig. (5.3.2) shows the close-loop response of ε when ε set-point was changed from .02 to .05 (U_d = 1.35 mm/s, U_c = 0), using K_c of 40 and T_R of 120 sec.

The performance of the controller in load regulation is illustrated in Fig. (5.3.3), in which the Kerosene flowrate U_d was increased by .00135 m/s. Following that increase, ε deviated from its steady state value, and the controller was brought back to its original value in an oscillatory manner.

This is because the change in U_d presented a dynamics different

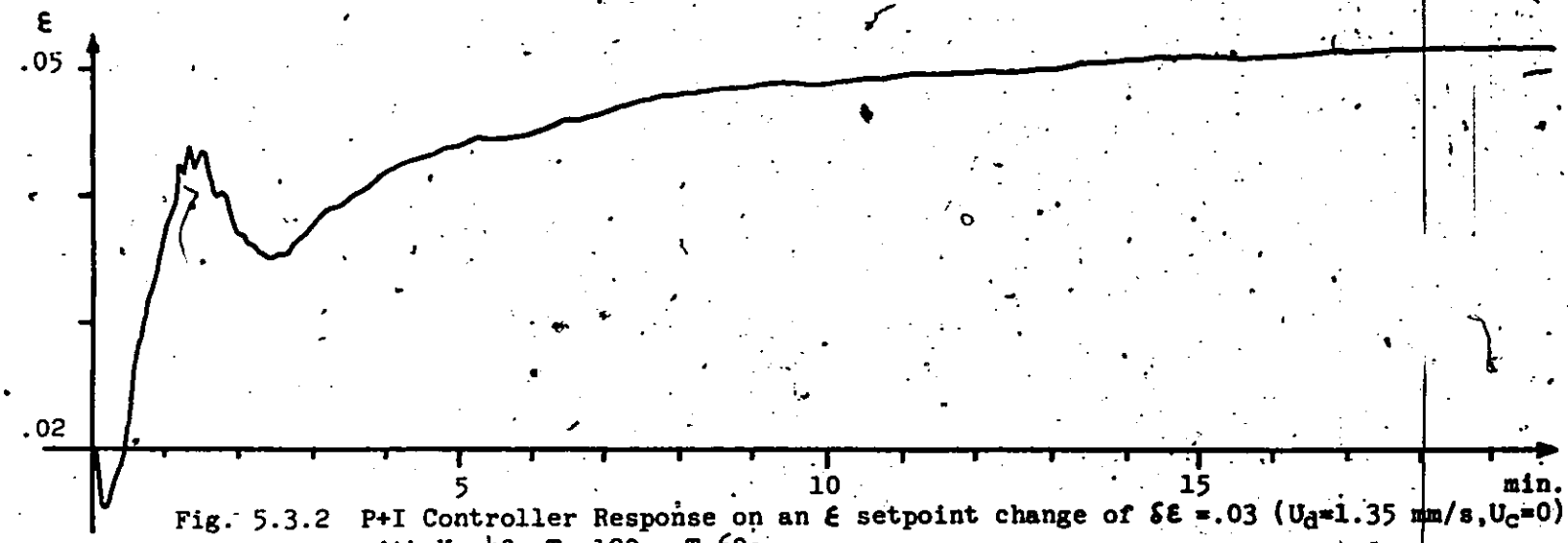

Fig. 5.3.2 P+I Controller Response on an ε setpoint change of $\delta\varepsilon$ =.03 (U_d=1.35 mm/s, U_c=0) with K_c=40, T_R=120s, T=60s

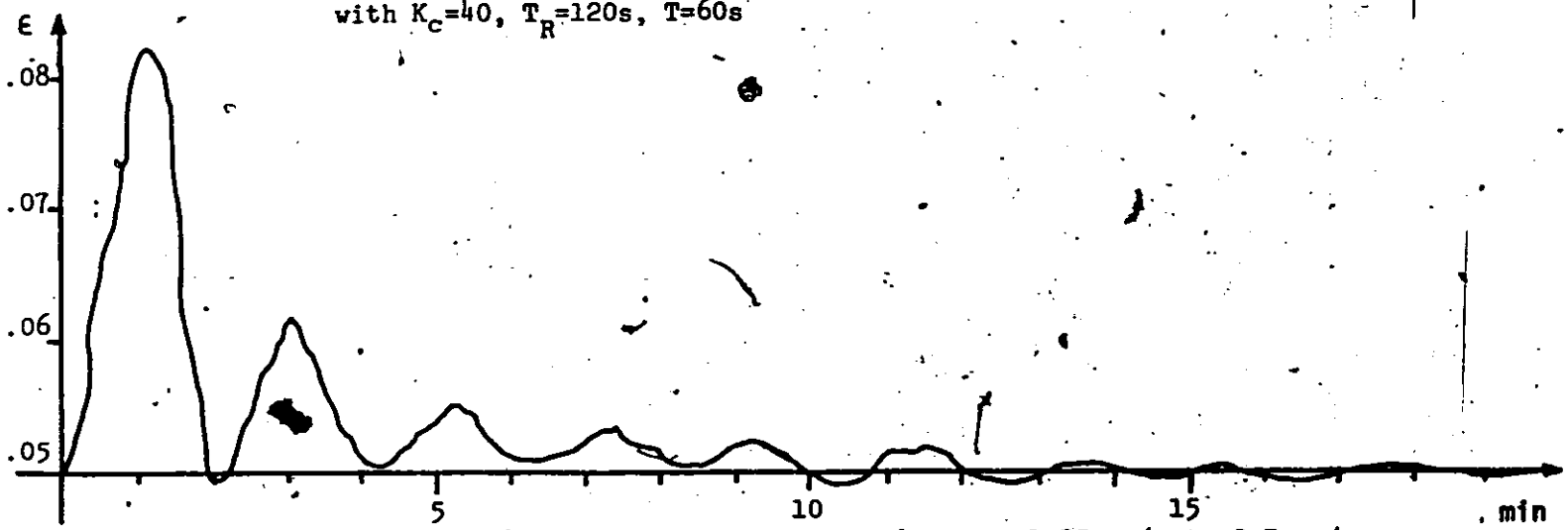

Fig. 5.3.3 P+I Controller Response on a U_d change from 1.35 mm/s to 2.7 mm/s with K_c=40, T_R=120s, T=60s

from that due to the change in f. Thus, even under the best tuning to track ε set point change, changes in U_d could make the system behave as an underdamped system.

The response of ε set point tracking for other setting of K_c = 50, T = 60 sec and T_R = 120 sec is shown on Fig. (5.3.4). It can be seen that by increasing Kc a little bit, the response became oscillatory with a much longer settling time.

When there was water flow, the dynamics of ε with respect to changes in f and Ud were different from that without water flow as can be seen in tables 1 and 2. Using the same setting, the controller was tested with ε set point change from .02 to .05 (U_d = 1.35 mm/s; U_c = 3.5 mm/s) and later a U_d change from 1.35 mm/s to 2.7 mm/s was introduced. The results are shown in Fig. (5.3.5). The set point response exhibited little difference from that shown in Fig. (5.3.2), where there was no water flow. The U_d change gave a more oscillatory response with a different period. In this case, the controller needed to be tuned specifically for overcoming the U_d (load) change.

To illustrate the problem with fixed parameter controllers, the P+I controller with the same setting of K_c = 40, T = 60 and T_R = 120 was tested on a ε set point change of .03 but in a different region, i.e. ε initial of .05 to .08. This result was shown on Fig. (5.3.6); as can be seen, the performance of the controller was very poor and a retuning was necessary. This is due to the nonlinearity of the process.

The computer program used for implementing PI controller is given in Appendix D.1.

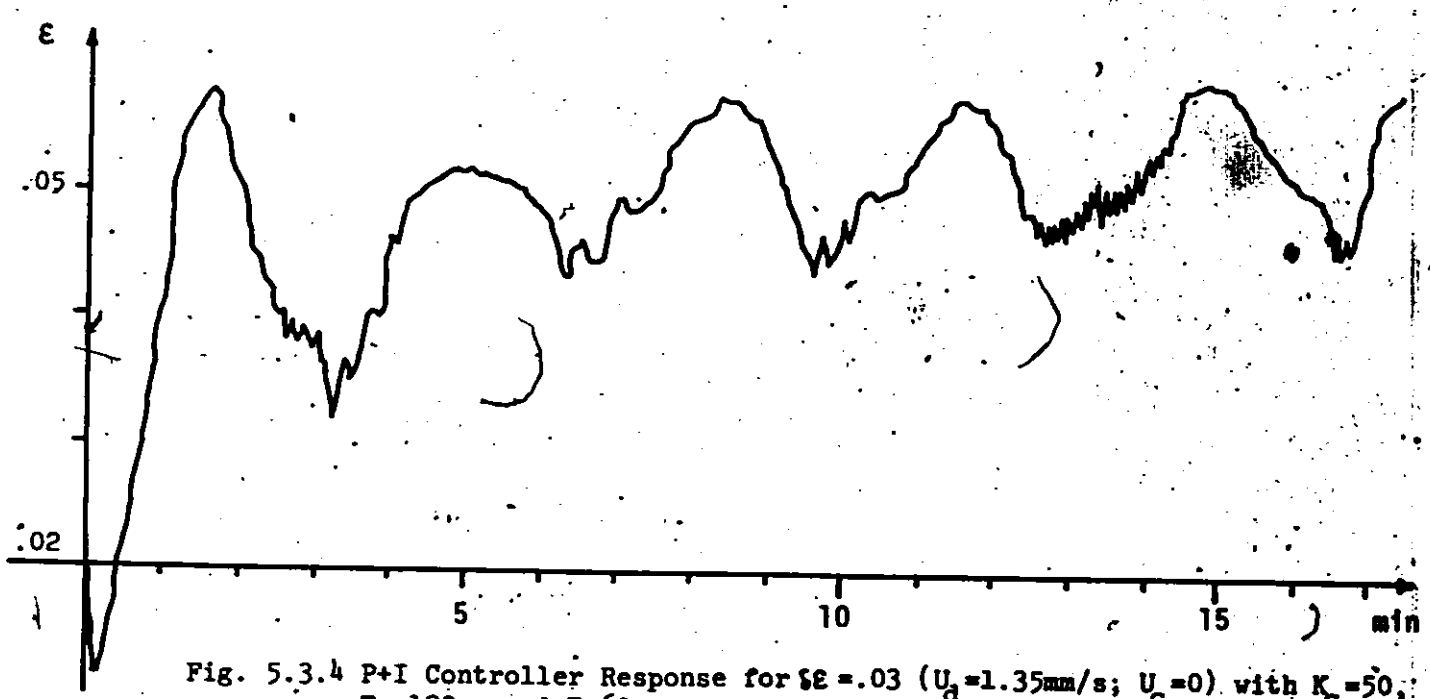

Fig. 5.3.4 P+I Controller Response for $\delta\varepsilon = .03$ ($U_d = 1.35$mm/s; $U_c = 0$) with $K_c = 50$, $T_R = 120$s, and $T = 60$s

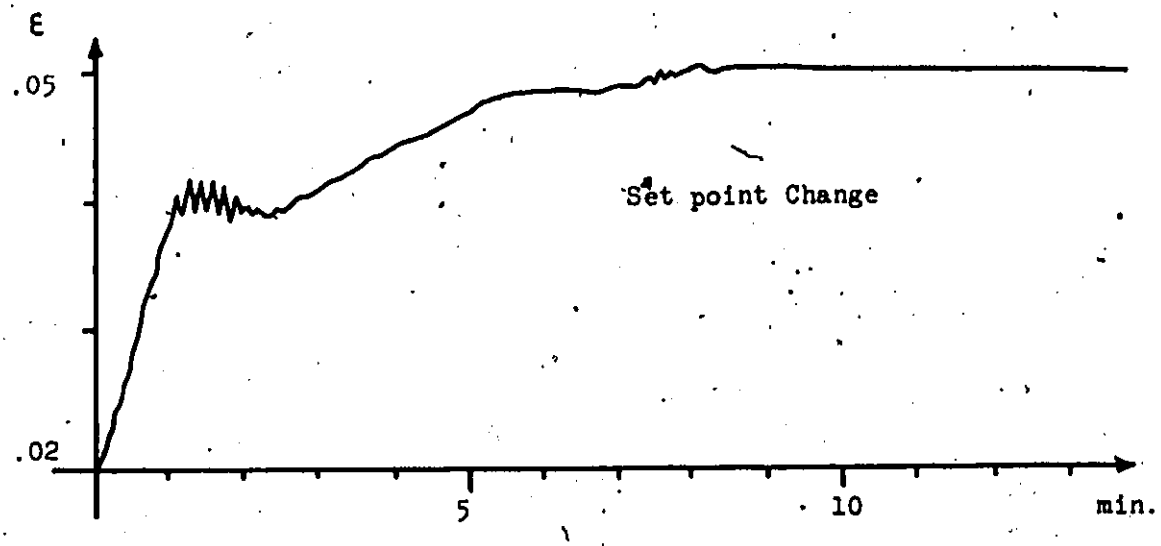

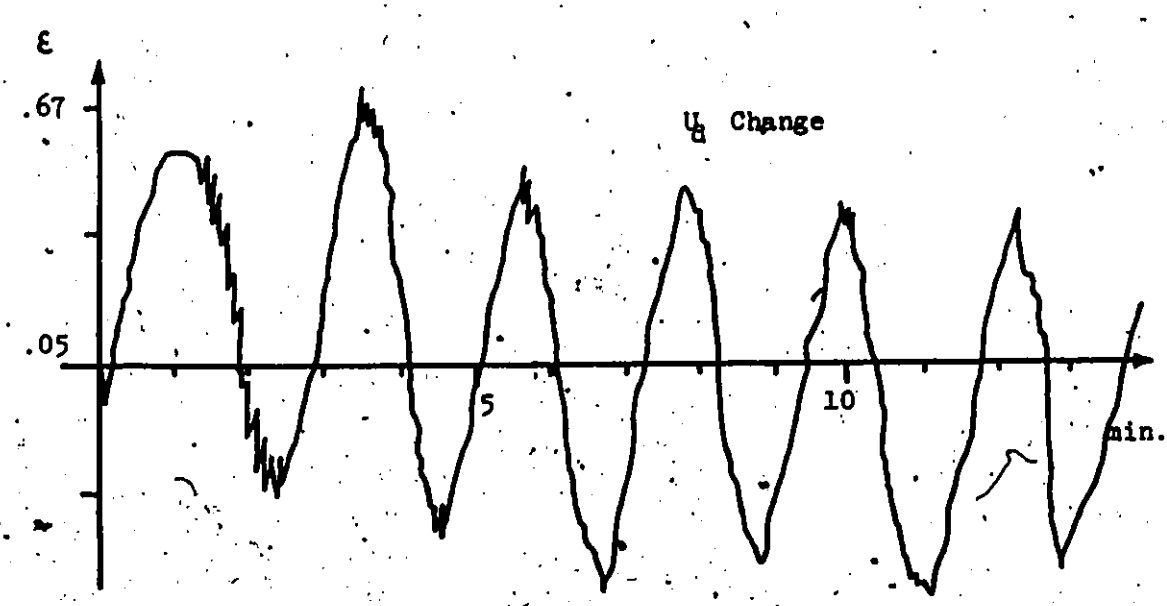

Fig. 5.3.5 P+I Controller (K_c=40, T=60, T_p=120) Response to $\delta\varepsilon$=.03 (U_d=1.35 m/s, U_c=3.5 mm/s) and U_d change from 1.35 mm/s to 2.7 mm/s.

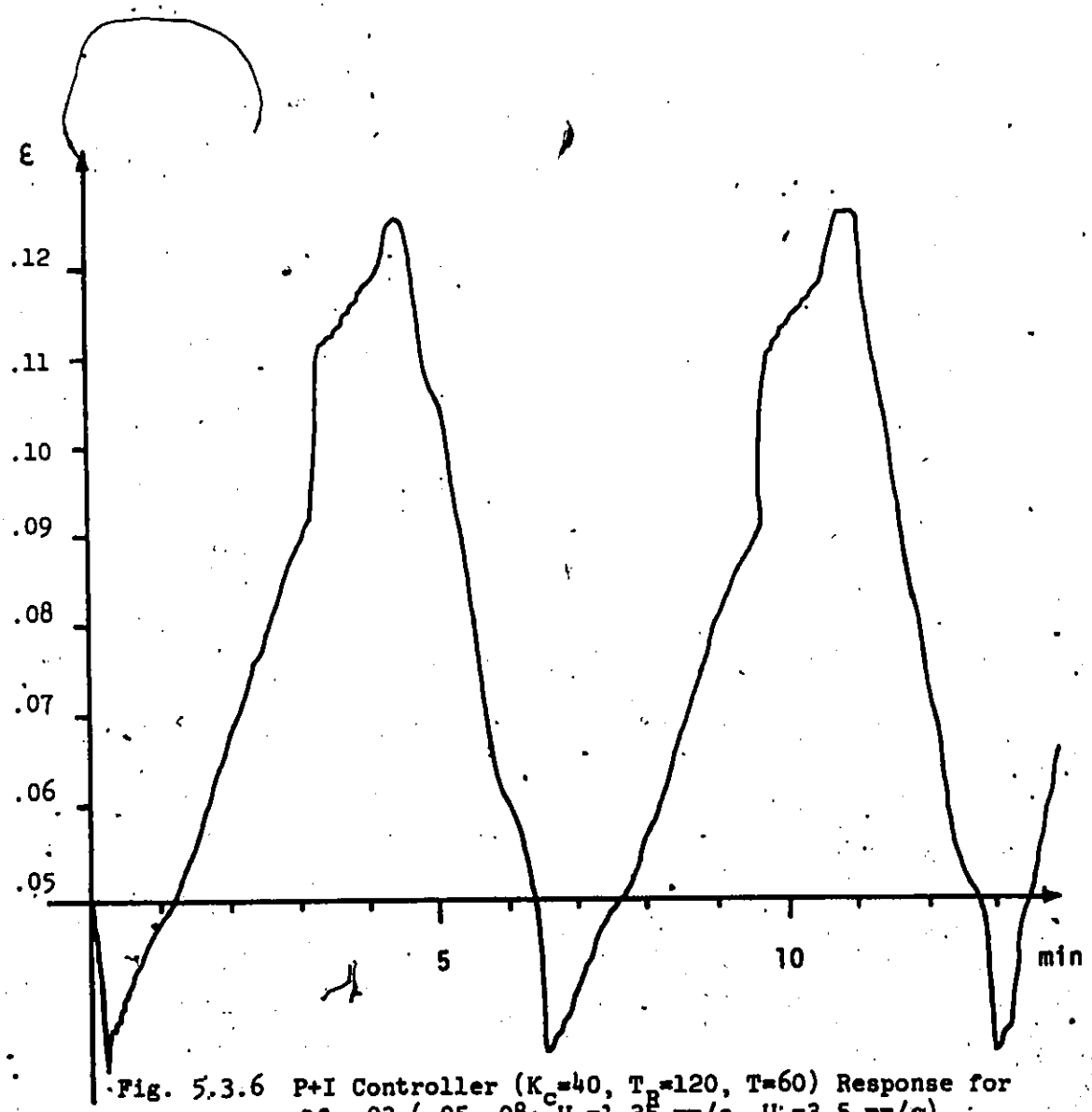

Fig. 5.3.6 P+I Controller (K_c=40, T_R=120, T=60) Response for $\delta\varepsilon$=.03 (.05-.08; U_d=1.35 mm/s, U_c=3.5 mm/s)

5.4 FEEDBACK/FEEDFORWARD ON SET POINT CHANGES IN ε [25]

As the dynamics of ε with respect to changes of f and changes of U_d are different, one needs more than just a feedback controller. A combined servo/regulator controller is necessary.

An alternate method [25] of compensation for sampled-data control systems subjected to set point change is to make use of feed-forward control, as illustrated in Fig. 5.4.1. The feedback loop then can be tuned for overcoming U_d change.

In the block diagram (Fig. 5.4.1), D1(Z) and D3(Z) are the pulse-transfer functions of the digital compensators which are to be determined. C(Z) can be expressed in terms of R(Z) as follows:

$$C(Z) = \frac{G(Z)\,[D_1(Z) + D_3(Z)]}{1 + G(Z)\,D_1(Z)} * R(Z) \qquad (5.4.1)$$

$D_1(Z)$ was in this case designed as a P+I controller, were as $D_3(Z)$ was designed as described below. First, look at the overall pulse-transfer function $G_0(Z)$ of the system with the set point input acting on it:

$$G_0(Z) = \frac{C(Z)}{R(Z)} = \frac{G(Z)\,[D_1(Z) + D_3(Z)]}{1 + G(Z)\,D_1(Z)} \qquad (5.4.2)$$

The design of the required digital compensator $D_3(Z)$ is essentially reduced to the specification of a suitable overall pulse-transfer function $G_0(Z)$. $D_3(Z)$ is a function of $G_0(Z)$ as well as $D_1(Z)$.

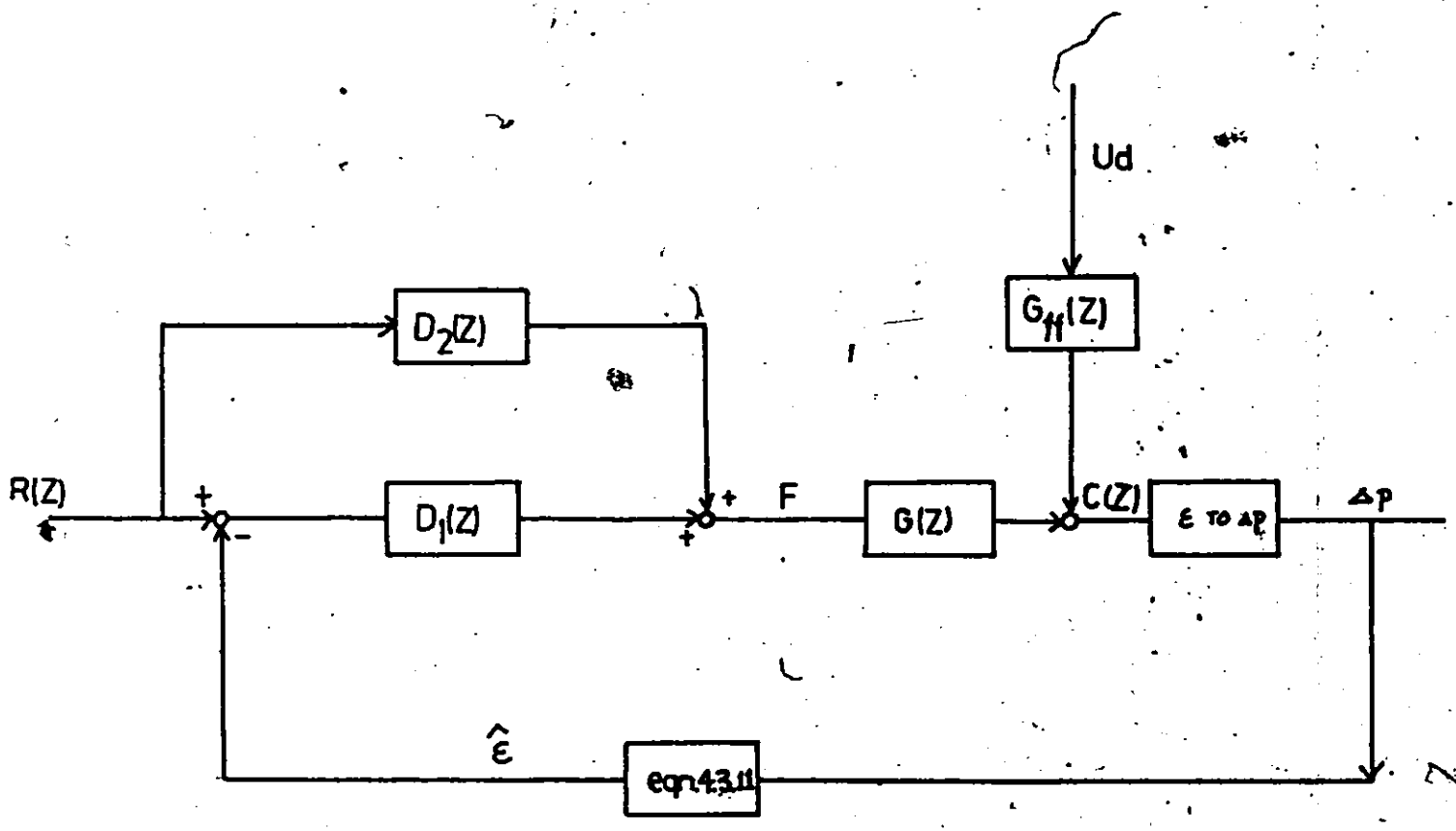

Fig. 5.4.1 A Sampled-data Feedback Control System Employing Feed-forward Control on Set point Change

The pulse-transfer function $D_3(Z)$ of the desired digital compensation follows immediately from eqn (5.4.2). Solving for $D_3(Z)$ from eqn. (5.4.2) yields:

$$D_3(Z) = \frac{[1 + G(Z)\, D_1(Z)]\, G_0(Z)}{G(z)} - D_1(Z) \qquad (5.4.3)$$

A restriction imposed upon the determination of the overall pulse-transfer function $G_0(z)$ is that $G_0(z)$ must contain as its zero(s) all the zero(s) of $G(Z)$ which lie outside the unit circle in the Z-plane. If the zeros of $G(Z)$ lying outside the unit circle were not cancelled by the zeros of $G_0(Z)$, the pulse-transfer function $D_3(Z)$ would become unstable. The pulse transfer function $D_3(Z)$ is then obtained from eqn (5.4.3) by proper substitution.

$G(Z)$ can be expressed as $(K * B(Z))$, where K is the gain term and $B(Z)$ is the dynamic term. By choosing $G_0(Z) = G(Z)/K$, one will expect a closed loop dynamic that behaves like that of an open loop response. $D_3(Z)$ is obtained from eqn (5.4.3) as:

$$D_3(Z) = [\tfrac{1}{K} + B(Z) * D_1(Z)] - D_1(Z)$$

Ignoring the dynamic term $B(Z)$, one gets:

$$D_3(Z) = \frac{1}{K} \qquad (5.4.4)$$

where $K = .015$ for nominal $G(Z)$

Using this static gain term for $D_3(Z)$, and using the P+I setting tuned for U_d change for the P+I feedback loop (i.e. $K_c = 20$, $T = 60$, $T_R = 90$), the controller was tested with a change of ϵ from .02 to .05 ($U_d = 1.35$ mm/s, $U_c = 0$). Fig. 5.4.2. shows the result and it exposes a problem with this scheme when used to track the setpoint; the double control

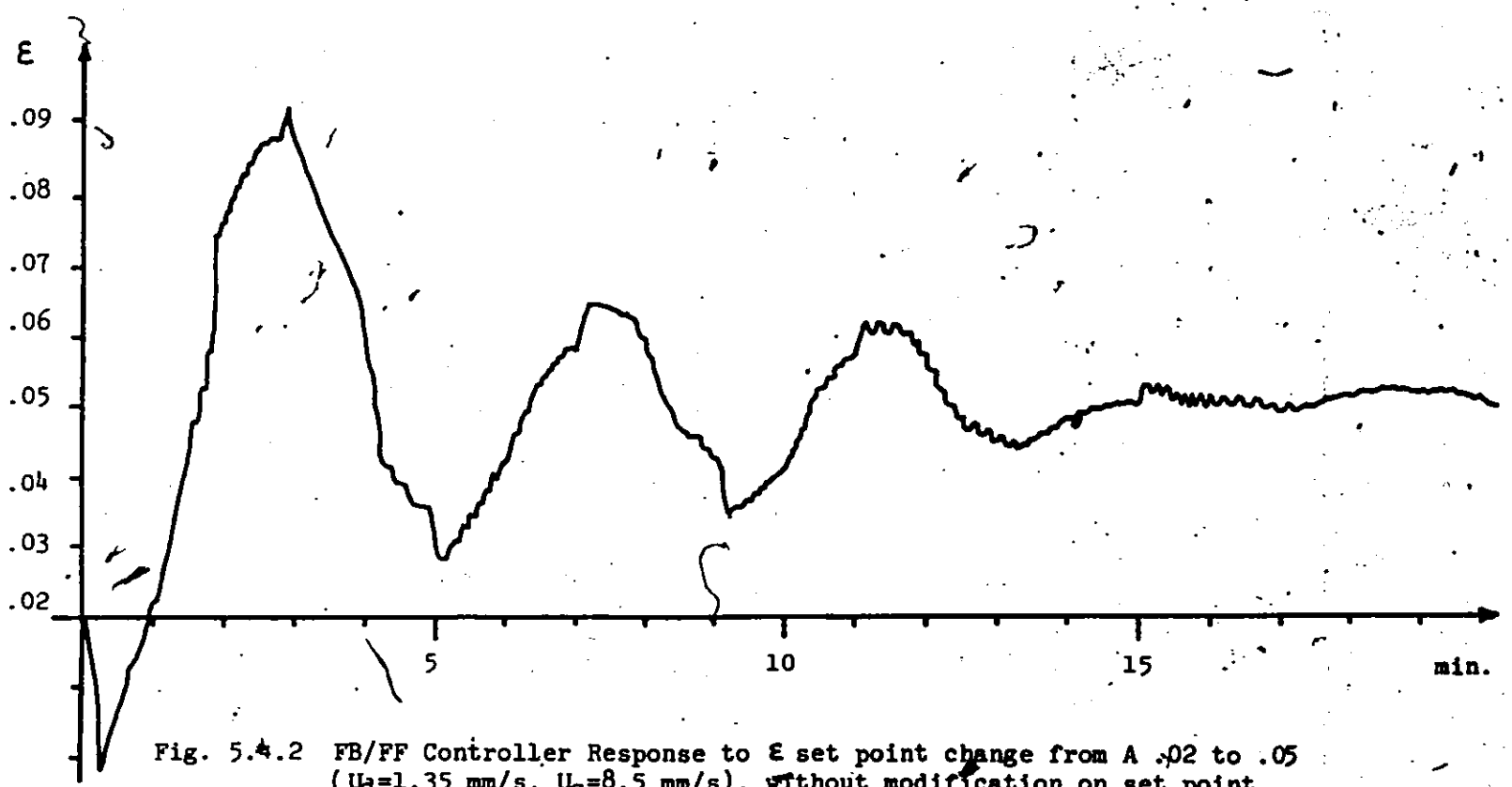

Fig. 5.4.2 FB/FF Controller Response to ε set point change from A .02 to .05 (U_d=1.35 mm/s, U_c=8.5 mm/s), without modification on set point.

action at the initial control interval gives the system a large overshoot. This large overshoot is also due to the chosen sampling interval of 60 sec. If smaller sampling time is used, the overshoot should be less. However, since PI controller has no deadtime compensator and the system deadtime varies up to 60 sec., it is not feasible to use sampling time smaller than 60 sec.

5.5 MODIFIED FB/FF ON SET POINT CHANGES IN ϵ.

The double control action encountered in sec. 5.4 can be overcome by making the overall-pulse-transfer function $G_0(Z)$ independent of $D_1(Z)$. This can be achieved by introducing an additional compensator $D_2(Z)$ as demonstrated in Fig. 5.5.1.

Referring to Fig. 5.5.1, it can be shown that the system output is related to the input by:

$$C(Z) = \frac{G(Z)\ [D_1(Z)\ D_2(Z) + D_3(Z)]}{1 + G(Z)\ D_1(Z)} * R(Z) \qquad (5.5.1)$$

and the over-all pulse-transfer function for servo problem is then given by

$$G_0(Z) = \frac{G(Z)\ [D_1(Z)\ D_2(Z) + D_3(Z)]}{1 + G(Z)\ D_1(Z)} \qquad (5.5.2)$$

If $D_2(Z)$ is so chosen that:

$$D_2(Z) = D_3(Z)\ G(Z) \qquad (5.5.3)$$

the eqn (5.5.2) reduces to the following very simple expression

$$G_0(Z) = D_2(Z) = D_3(Z)\ G(Z) \qquad (5.5.4)$$

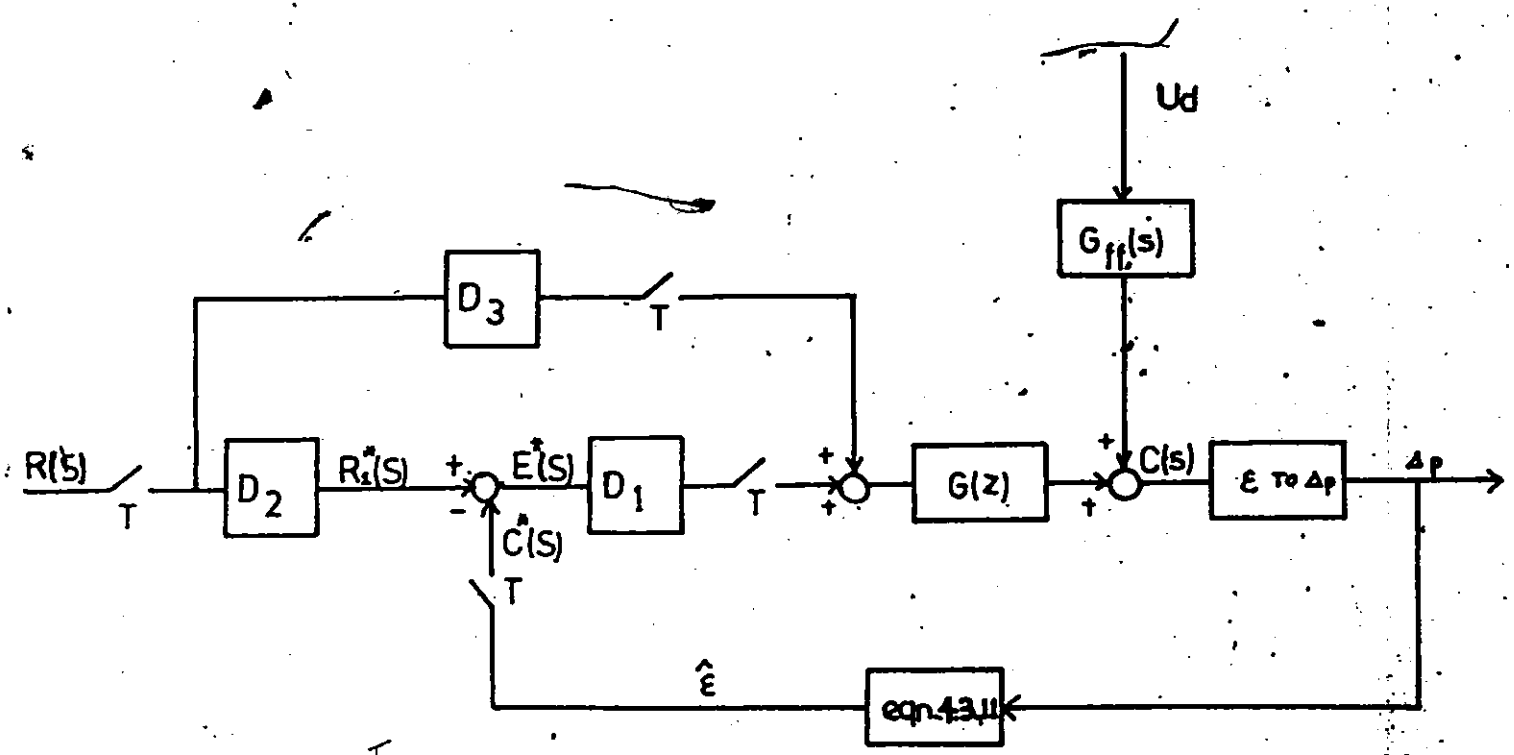

Fig. 5.5.1 Block Diagram illustrating A Conditional Feedback Control System (Reprinted from Ref. 17)

which is independent of $D_1(Z)$. Such a system is usually referred to as a Conditional Feedback System.

In Fig. 5.5.1, if all the samplers are assumed to be synchronized, it can readily be seen from the block diagram that if $D_2(Z) = D_3(Z) * G(Z)$ is satisfied, then $R_1^*(S)$ is equal to $C^*(S)$ and the actuating signal $E^*(S)$ is zero. This implies that the feedback loop is inoperative and the input signal R(S) is transmitted through the compensator $D_3(Z)$ to the holding device and the controlled system G(Z). Thus, the pulse-transfer function $D_1(Z)$ does not appear in the over-all pulse-transfer function C(Z)/R(Z), and the feedback loop is in control only when $C^*(S)$ is not equal to $R_1^*(S)$.

A sampled-data control system with a closed-loop response like that of the open-loop can be achieved by choosing $G_0(Z)$ as:

$$G_0(Z) = \frac{1}{K} * G(Z) \qquad (5.5.5)$$

and choosing $D_2(Z)$ according to eqn. (5.5.3). $D_3(Z)$ is then obtained from eqn (5.5.2) as follows:

$$D_3(Z) = \frac{1}{K} \qquad (5.5.6)$$

where K is the gain term in G(Z).

So for nominal transfer function in ϵ region of .02 to .05 the controller can be described by the following equations:

$$D_3(Z) = 1/.015$$

$$D_2(Z) = G_0(Z)$$

$$= Z\{\frac{e^{-15S}}{33S + 1} * (\frac{1 - e^{-TS}}{S})\}$$

If $R_1^*(Z)$ = modified ϵ set point
$R_1(Z)$ = ϵ set point

$$D_2(Z) = \frac{Z^{-1}(1 - e^{-1/33(1-f)T} - e^{-1/33T} Z^{-1} + e^{-1/33(1-f)T} Z^{-1})}{1 - e^{-1/33T} Z^{-1}}$$

where N and f are the whole and fractional numbers of periods of delay in θ, respectively, i.e. $\theta = NT + fT$.

In difference equation, $R_1^*(Z)$ can be expressed in term of $R_1(z)$ as follows: $R_1^*(t)=(1-Q)\ ^*R(t-1) + (Q-p)\ ^*R(t-2) + p\ ^*\ R(t-1)$

where $p = e^{-1/33T}$

$Q = e^{-1/33(1-f)T}$

the error term then is defined as follows:

$$E^*(Z) = R_1^*(Z) - C^*(Z)$$

where $C^*(Z)$ is the predicted ϵ from Δp measurement.

The computer program used in implementing this mode of controller is given in Appendix D.2. This scheme was tested for a set point change of $\delta\epsilon$ = .03, i.e. .02 to .05 (U_d = 1.35 mm/s, U_c = 3.5 mm/s). The results for the scheme using an ordinary Z-transform and the scheme using a modified Z-transform [24] are shown in Figs. (5.5.2) and (5.5.3) respectively. Comparing these two responses, one can see that using the modified Z-transform gave a better response. Hence, it is evident that the process model used is critical in this case. In Fig. (5.5.3), when the system was in steady state, there was some noise in the Δp signal. The same observation was made during the step tests when open-loop system was used (see Fig. C.1 in appendix C). Thus, the noise could not have been generated by the controller.

This scheme was also tested for U_d change from 1.35 mm/s to 2.7 mm/s. The result shown in Fig. 5.5.4 illustrates that optimum tuning

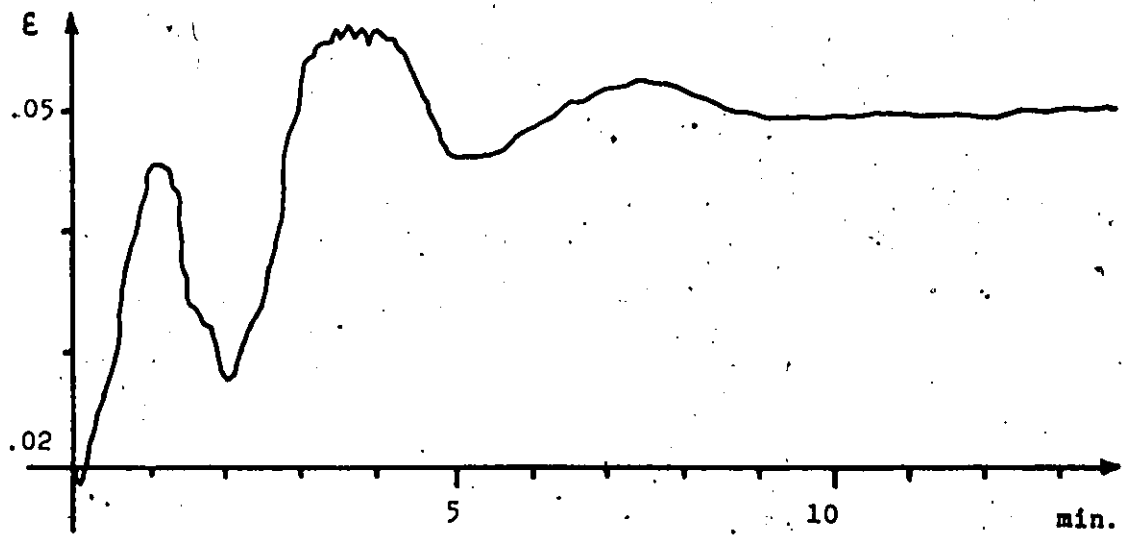

Fig. 5.5.2 FF/FB Controller Response to set point change of $\delta\varepsilon$=0.3 (U_d=1.35 mm/s, U_c=3.5 mm/s) using ordinary Z-transform with K_c=40, T_R=120, T=60

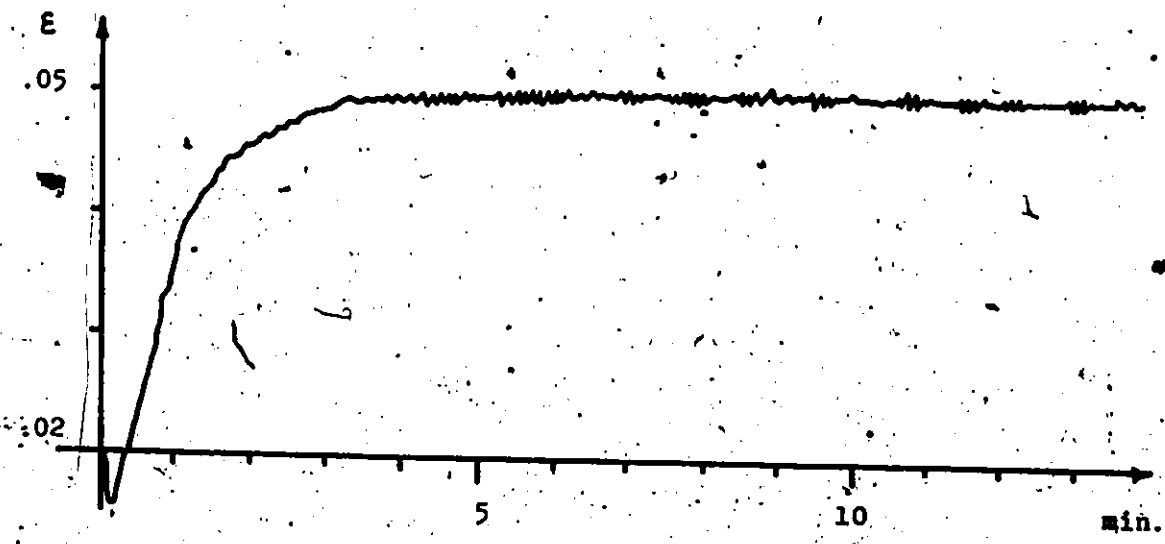

Fig. 5.5.3 FF/FB Controller Response to set point change of $\delta\varepsilon$=.03(U_d=1.35 mm/s, U_c=3.5 mm/s) using modified Z-transform with K_c=40, T_R=120, T=60.

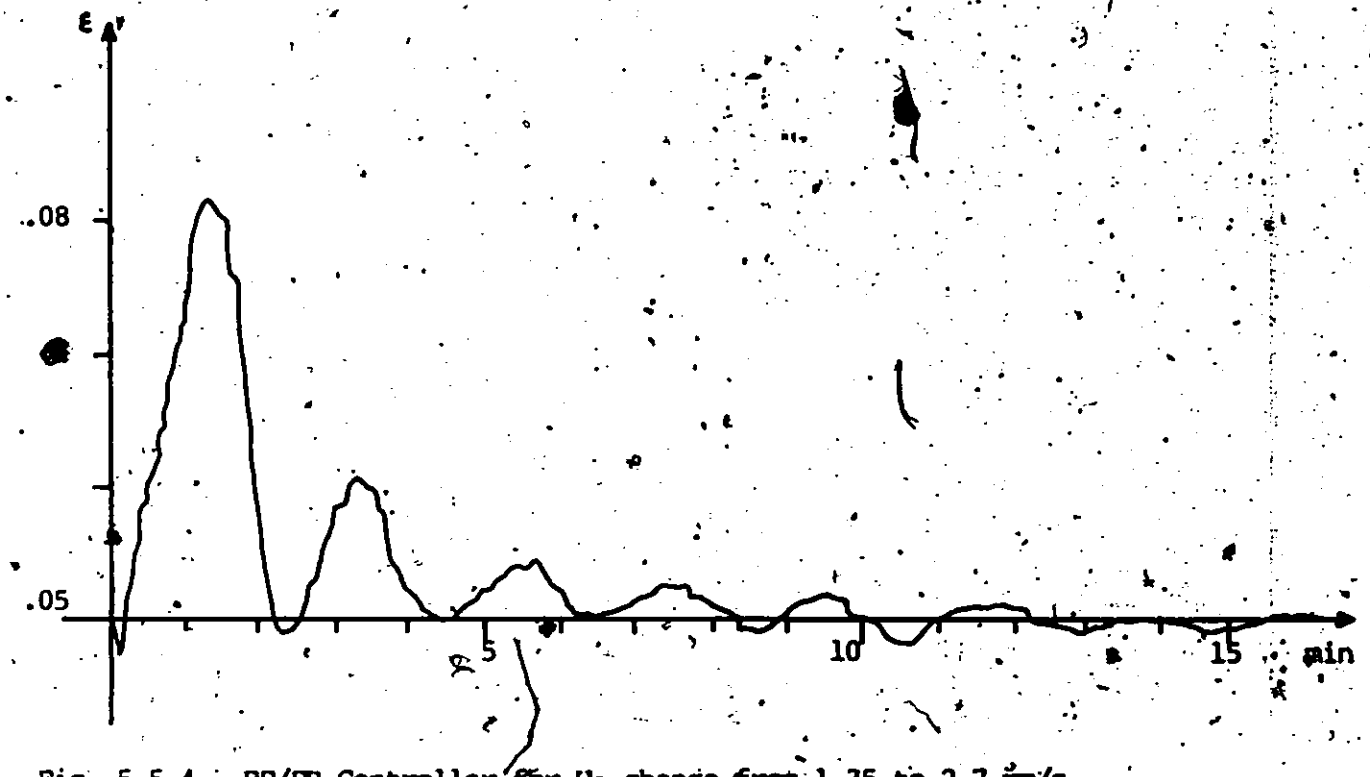

Fig. 5.5.4. FF/FB Controller for U_d change from 1.35 to 2.7 mm/s
$K_R = 40$, $T_R = 120$, $T = 60$

for set point changes is not optimum for load changes, as already pointed out in sec. 5.3.

However, in this case, since $G_0(Z)$ is independent of $D_1(Z)$, $D_1(Z)$ can then be tuned for load changes. It was found by the Ziegler-Nichols method [24] that the best tuning for U_d change was $K_c = 20$, $T_I = 60$ sec, $T_R = 90$ sec. With these $D_1(Z)$ parameters and using the same $D_3(Z)$ and $D_2(Z)$, the controller was tested again for the same ϵ set point and Ud changes. Results are shown in Fig. (5.5.5) & (5.5.6). It can be seen that the set point tracking performance is as good as before (see Fig. 5.5.2) but the disturbance rejection is more acceptable.

An alternate $G_0(Z)$ is:

$$G_0(Z) = 1 \qquad (5.5.6)$$

in this case a sampled-data control system with zero settling time and no error at the sampling instants is obtained. This requires a digital compensator having the pulse transfer function given by:

$$D_3(Z) = \frac{1}{G(Z)} \qquad (5.5.7)$$

Unfortunately, the pulse-transfer function defined in eqn (5.5.6) is not physically realizable, because the pulse transfer functions of all digital controlled systems or plants contain the factor Z^{-1}. For a system with dead time (n*T), $G_0(Z)$ should at least be Z^{-n-1}, i.e.

$$G_0(Z) = Z^{-n-1} \qquad (5.5.8)$$

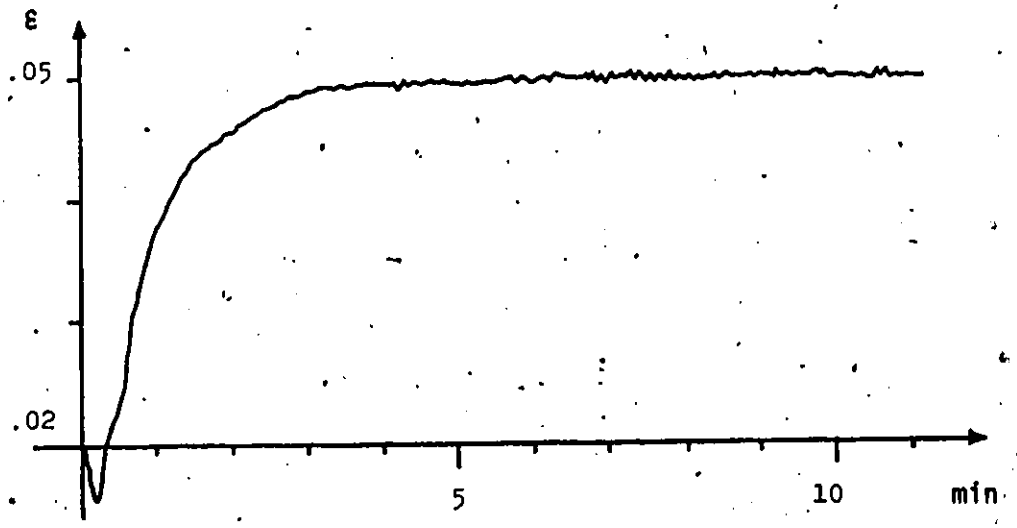

Fig. 5.5.5 FF/FB Controller Response to set point change of $\delta\varepsilon$=.03 (U_d=1.35 mm/s, U_c=3.5 mm/s) with K_c=20, T_R=90, T=60

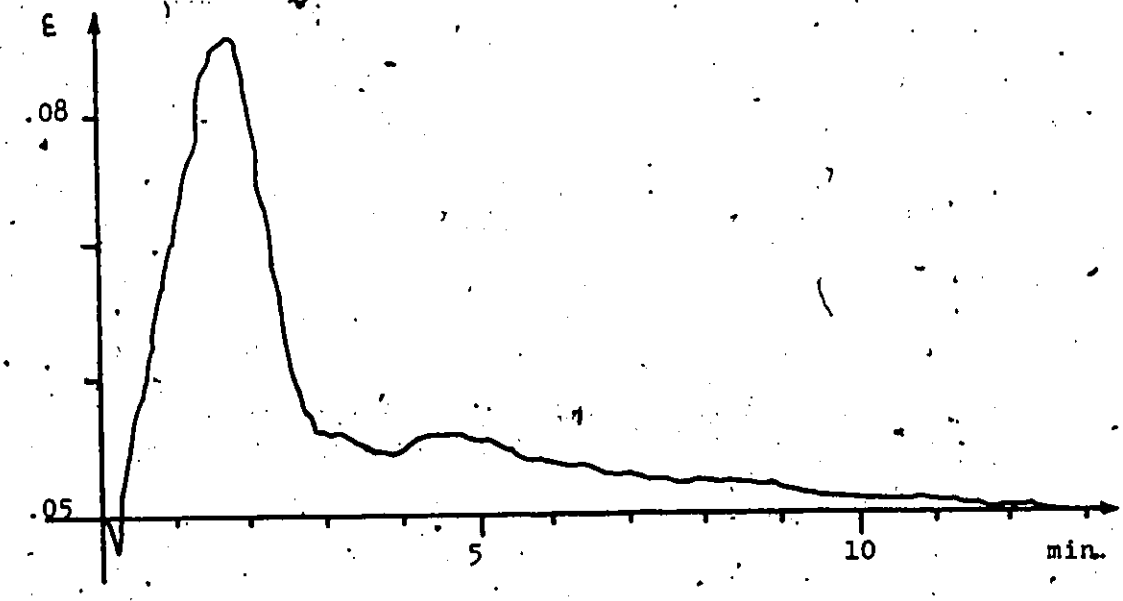

Fig. 5.5.6 FF/FB Controller Response to U_d Change from 1.35-2.7 mm/s with K_c=20, T_R=90, T=60.

The sampled data control system characterized by an input output relation given in eqn (5.5.8) can be obtained with getting of:

$$D_3(Z) = \frac{Z^{-n-1}}{G(Z)} \qquad (5.5.9)$$

and $$D_2(Z) = Z^{-n-1} \qquad (5.5.10)$$

This control scheme was tested on an ϵ set point change of .02 - .05 (U_d = 1.35 mm/s; U_c = 0); the result was not acceptable as the controller behaved like an on-off controller. Since this controller is the equivalent of a dead-beat controller, it is too powerful for a non-minimum phase system. To detune the controller in this case one can set:

$$D_3(Z) = Z\left(\frac{\tau_{FF}\, s+1}{K} * H(s)\right) \qquad (5.5.11)$$

and $$D_2(Z) = G_0(Z) = Z^{-N-1}\, D_3(Z) * G(Z) \qquad (5.5.12)$$

$$D_2(Z) = G_0(Z) = Z^{-N-1}\, \frac{Z[(\tau_{FF}\, s+1)*H(s)]}{Z[\tau_p\, s+1 * H(s)]} \qquad (5.5.13)$$

where τ_p = process time constant

τ_{FF} = tuning parameter, which can vary from 0 to τ_p.

The responses for τ_{FF} = .5 and .1 are shown in Fig. 5.5.7. The responses with the $\tau_{FF} > 0$ are more oscillatory and give more overshoot, but the rise time is slightly faster. The oscillatory response in this case is attributed to the fact that the process is non-linear. Thus, when a large overshoot was encountered, the model error became very significant resulting in the activation of the feedback loop. Furthermore the sampling time of 60 s chosen also contributes the large overshoot as discussed before. The response with τ_{FF} = .5 is not

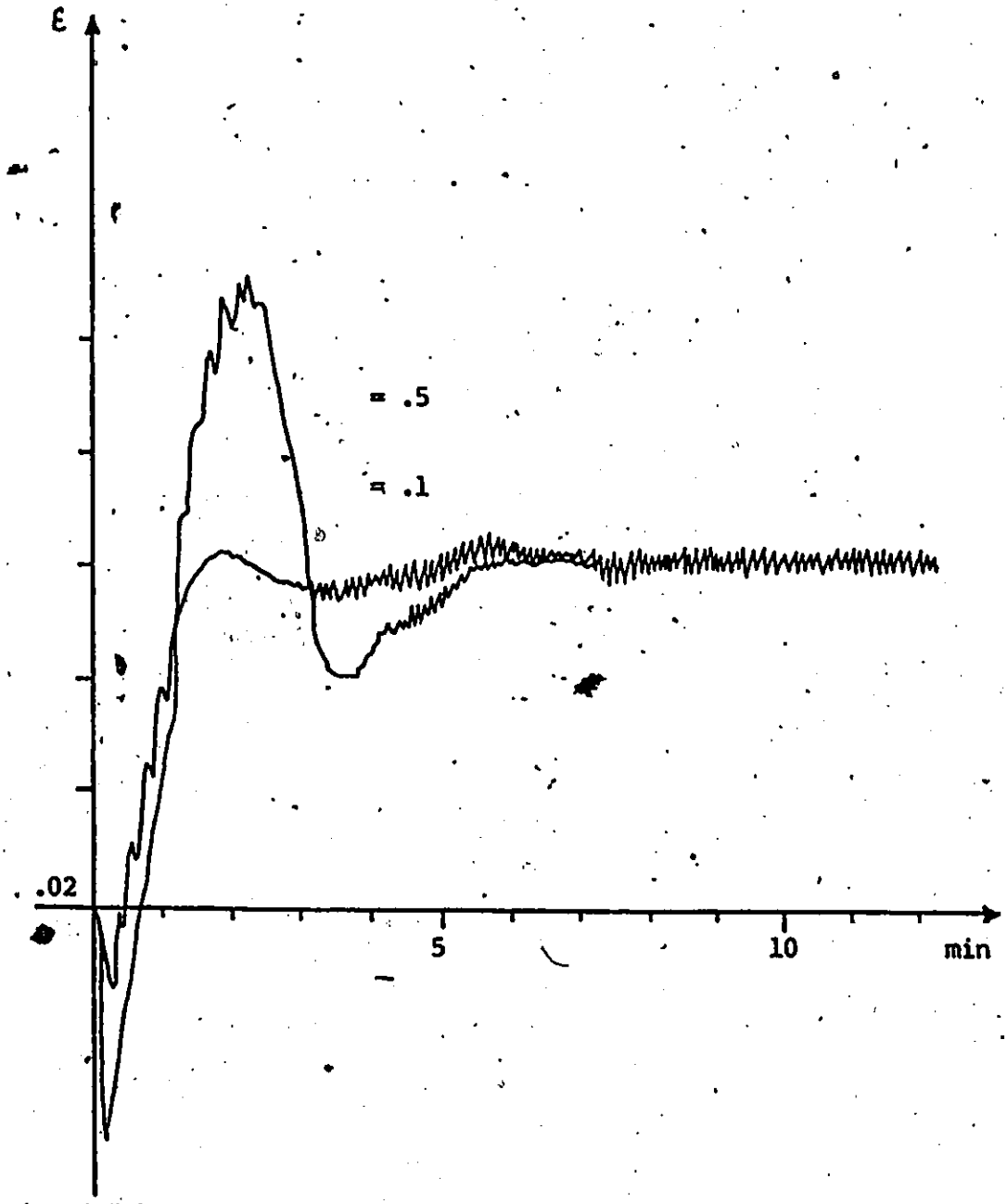

Fig. 5.5.7. Responses of Controller Characterized by Eqn (5.5.11) + (5.5.13) with $\tau_{ff} = .5$ and $\tau_{ff} = .1$

acceptable, because it gave 75% overshoot. With $\tau_{FF} = .1$, the response is more oscillatory with just slightly faster rise time compared to that in Fig. 5.5.3.

For an ϵ set point change from .02 to .05, the control scheme which used Feedback/Feedforward on set point and specified servo problem overall pulse transfer function as that of open loop (characterized by eqn (5.5.5) and eqn (5.5.6)) is therefore considered the best one. However, this controller is heavily dependent on the accuracy of the model used, as already pointed out earlier. Hence, the performance of the controller in handling the non-linearity of the process is expected to be poor. This can be seen in Fig. 5.5.8 where the response of the same controller was tested with a set point change of .05 to .08.

5.6 FB/FF FOR DISTRUBANCES

In the case where load response is the main concern, the controller would be designed specifically for load changes. One possible scheme for this case is to incorporate both feed-forward and feed-back in the controller as shown in Fig. 5.6.1.

Feed-forward has the advantage that it uses the manipulative inputs before the controlled variable have deviated from their desired values. However, the use of feed-forward control required the accurate measurement of disturbances and information on their dynamics. These are usually difficult to obtain exactly, and inaccuracy will result in the presence of an offset.

Therefore, a combined feedforward/feedback controller seems much

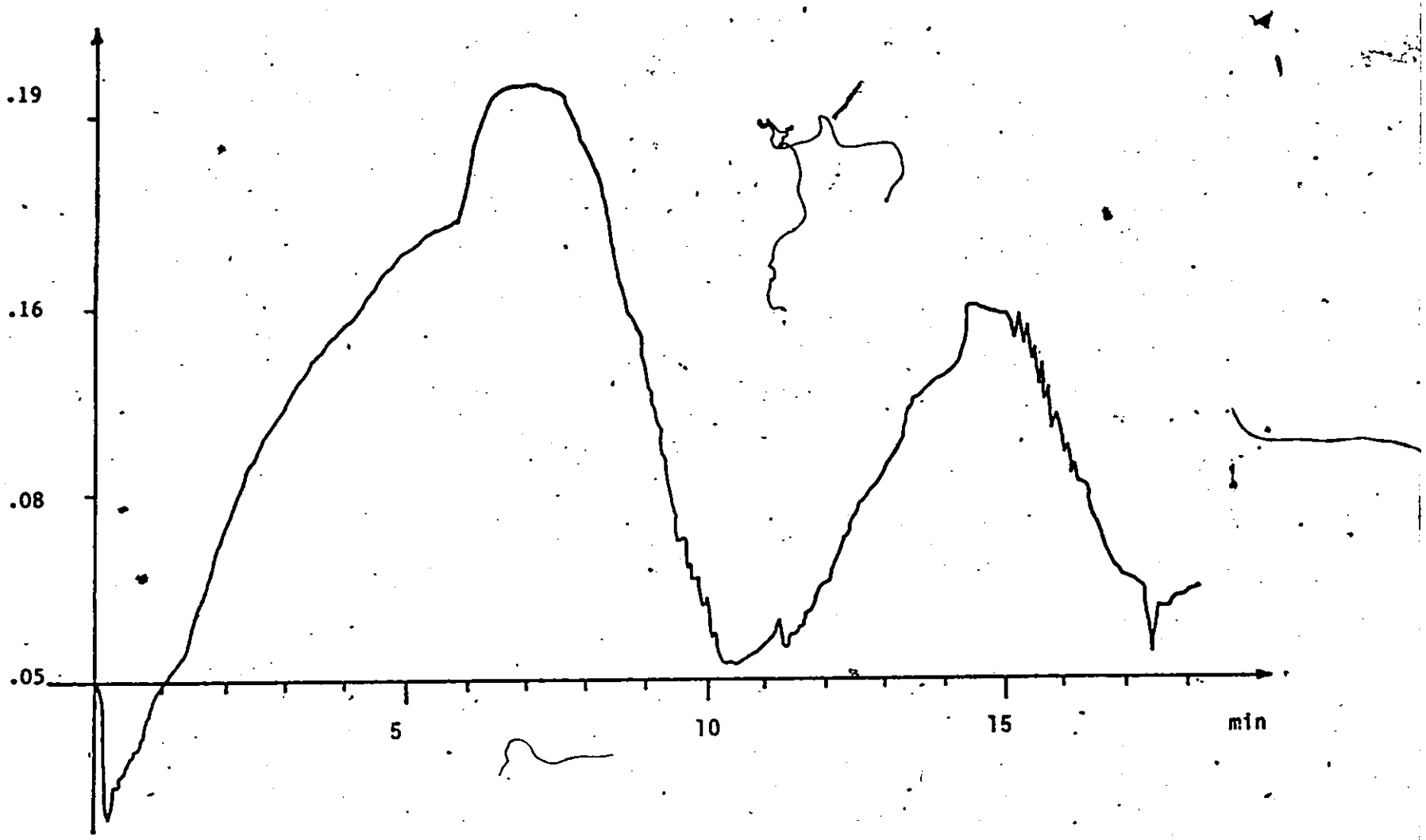

Fig. 5.5.8 Response of the Controller Characterized by equn. (5.5.5) and (5.5.6), Using Transfer Function of $\hat{\epsilon}$ between .02 to .05 to overcome a $\hat{\epsilon}$ Set point Change from .05 to .08.

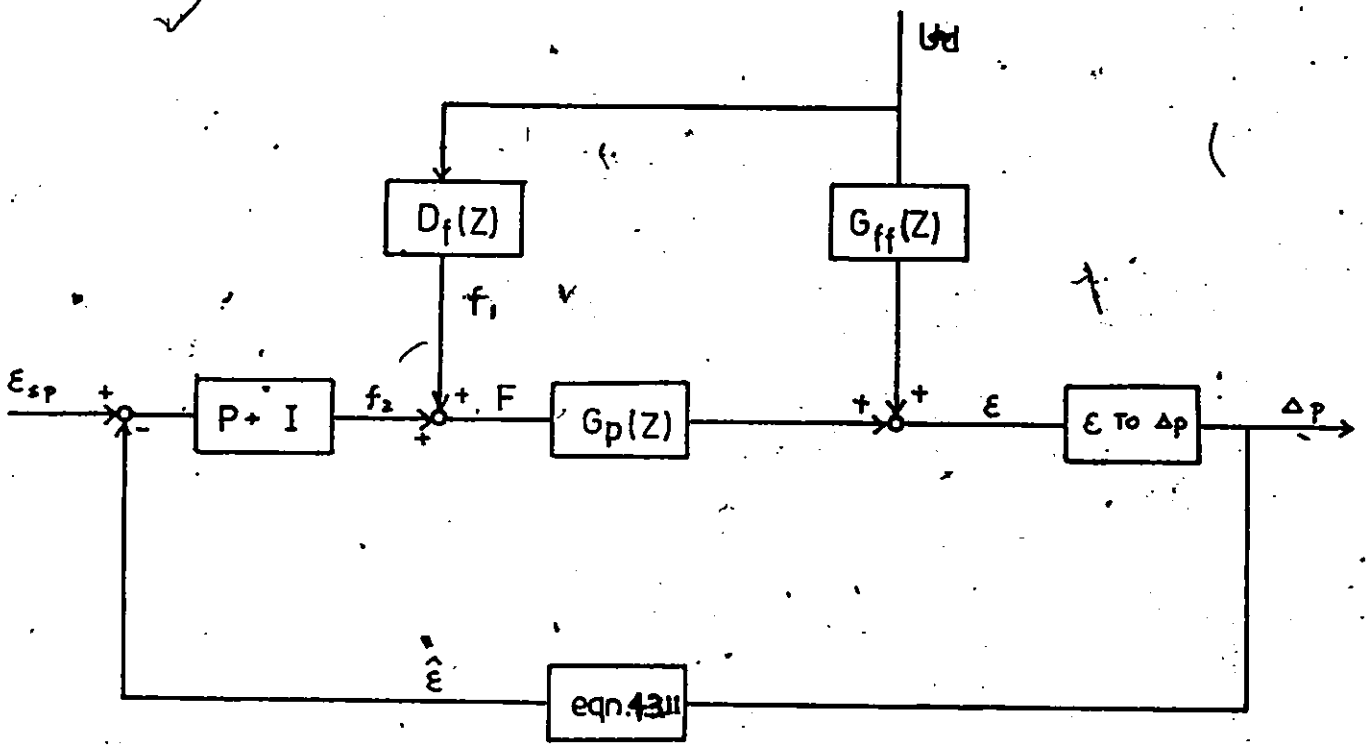

Fig. 5.6.1 Block Diagram for FF/FB Controller Scheme for Ud Change

more desirable than just a feed forward one alone. This is because the feed-back system will initiate corrective action once the system deviates from the target, regardless of how the deviation occured.

The controller scheme in Fig. (5.6.1) with feedback PI loop, and feedforward dynamic compensator:

$$D_f(Z) = -\frac{G_{ff}(Z)}{G_p(Z)} \qquad (5.6.1)$$

where $G(Z) = Z(H(s) \cdot G(s))$

was tested with a U_d change from 1.35 mm/s to 2.7 mm/s, the steady state ϵ before the change was made was equal to .05. At this operating region, i.e. ϵ between .02 to .05 and U_d between 1.35 mm/s to 2.7 mm/s.

$$G_{ff}(Z) = Z(H(s) * \frac{22e^{-5S}}{14s + 1})$$

The controller therefore become:

$$D_f(Z) = -\frac{G_{ff}(Z)}{G_p(Z)}$$

$$\frac{f_1(Z)}{U_d(Z)} = \frac{-22}{.028} \quad (\frac{1 - e^{-1/4T} - e^{-1/30T} Z^{-1} + e^{-1/4T} e^{-1/30T} Z^{-1}}{1 - e^{-1/30T} - e^{-1/14T} Z^{-1} + e^{-1/14T} e^{-1/30T} Z^{-1}})$$

In difference equation,

$$f_1(t) = \frac{-22}{.028} * \frac{1}{(1 - M)} * [(1-L)Ud(t) + (ML-M)Ud(t-1) + (ML-L)f_1(t-1)$$

where $M = e^{-1/30T}$; $L = e^{-1/14T}$

The total control action is:

$$F(Z) = f_1(Z) + f_2(Z)$$

where $f_2(Z)$ is from the PI feedback loop. The result with P+I

parameters tuned for U_d change (i.e. K_c = 20, T_R = 90 s, T = 60s) is shown in Fig. 5.6.2. It shows that the performance in overcoming load changes is the best one obtained so far in this work, in the sense that the deviation from steady state value is less or the ($\int e\,dt$) is less.

To show the importance of the feedback loop parameters, the PI loop parameters tuned for set point changes (i.e. K_c = 40, T_R = 120s, T = 60s) was used instead. From the result shown in Fig. 5.6.3, one can see that the performance of the controller is poor. The roots of the problem are the following:

(i) referring to eqn (5.6.1), since $G_{ff}(s)$ and $G_p(s)$ were both non-linear, the accuracy of $D_f(Z)$ was inherently poor; and

(ii) $D_f(Z)$ involved a predictor term which presented a physical realizability problem. This predictor was omitted in the implementation of the controller.

the consequence then was that $D_f(Z)$ did not cancel the U_d change exactly, giving an offset which activated the feed back loop. Therefore, the selection of feedback parameters is critical.

The program used to implement this mode of controller is presented in Appendix D.3.

5.7 DAHLIN CONTROLLER

The traditional P+I controller has the draw-back that it cannot take into account the process deadtime. Whenever deadtime occurs one has to detune the controller or else oscillation will occur.

The Z-transform design technique has been found useful for the

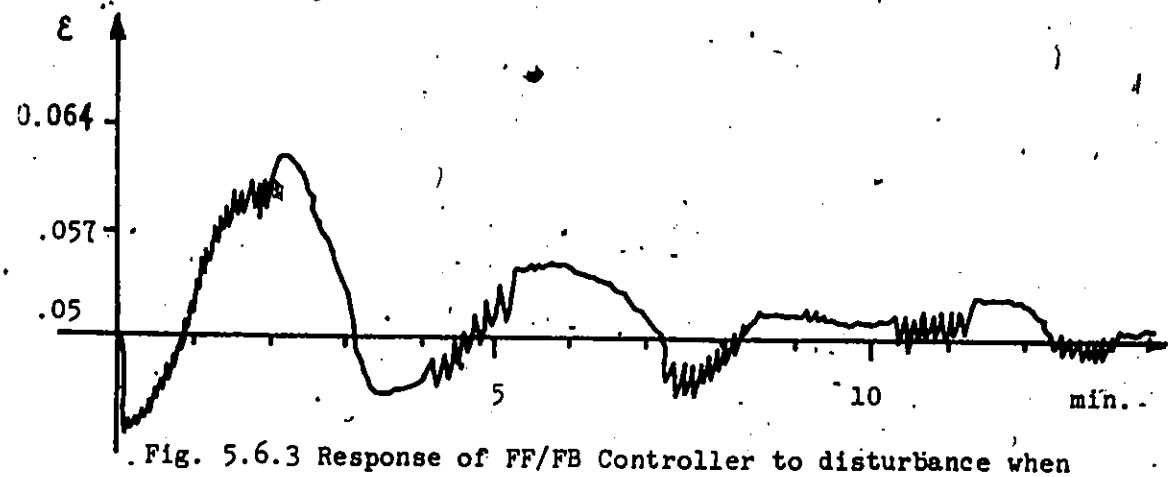

Fig. 5.6.3 Response of FF/FB Controller to disturbance when U_d was changed from 1.35-2.7 mm/s with PI parameters: K_c=40, T_R=120, T=60.

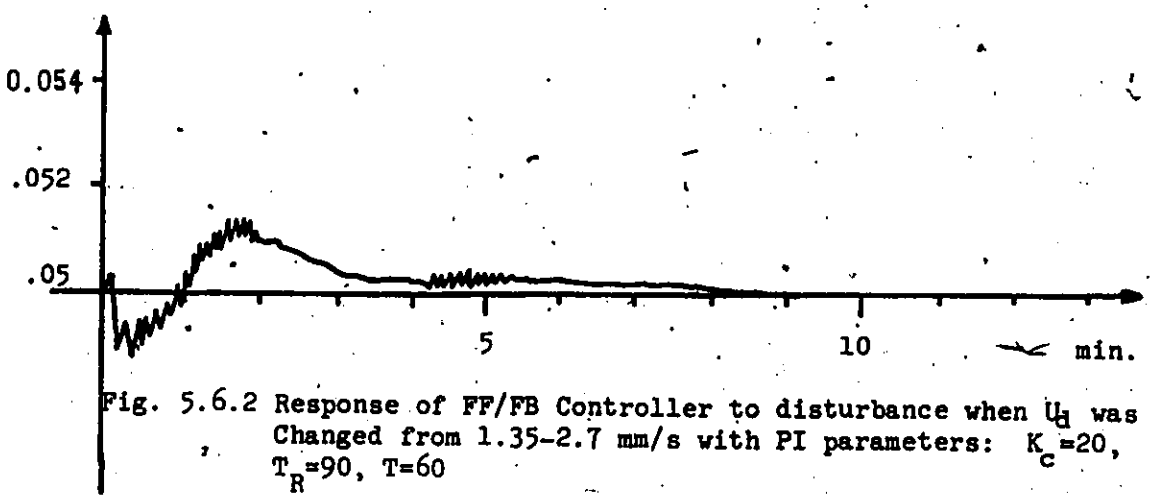

Fig. 5.6.2 Response of FF/FB Controller to disturbance when U_d was Changed from 1.35-2.7 mm/s with PI parameters: K_c=20, T_R=90, T=60

accommodation of process model. This type of controller is readily implemented using digital control.

5.7.1 Dahlin Algorithm

Consider the block diagram of a digital control loop in Fig. 5.7.1 R(Z), M(Z) and C(Z) are the Z-transform of the set point, the output and the input. The closed-loop transfer function of the process is:

$$\frac{C(Z)}{R(Z)} = \frac{HG(Z)\ D(Z)}{1 + HG(Z)\ D(Z)} \tag{5.7.1}$$

where $HG(Z) = Z[(\frac{1 - e^{-ST}}{S}) \cdot G(s)]$

T = sampling time

D(Z) is the controller in Z-domain and it can be determined by specifying a desired closed-loop response, D(Z) then can be calculated from the closed-loop expression C(Z)/R(Z) as follows:

$$D(Z) = \frac{C(Z)/R(Z)}{1 - C(Z)/R(Z)} \cdot \frac{1}{HG(Z)} \tag{5.7.2}$$

The approach initiated by Dahlin [24] was to consider the closed-loop system as a continuous first order lag with deadtime. Thus, using this approach

$$\frac{C(s)}{R(s)} = \frac{e^{-\theta S}}{\lambda s + 1} \tag{5.7.3}$$

The closed-loop time constant λ is the tuning parameter of the algorithm. The chosen deadtime θ should be no less than the actual process deadtime so that no predictive terms are incurred in the

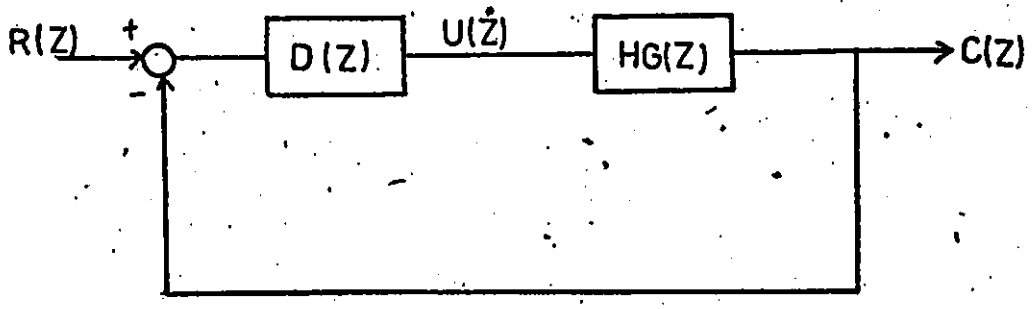

Fig. 5.7.1 Block Diagram of a Digital Control Loop Using Z-transforms

expression of D(Z).

The Z-domain equivalent of C(s)/R(s) is obtained by taking the modified Z-transform of the product of C(s)/R(s) and H(s):

$$\frac{C(z)}{R(z)} = Z[H(s)\frac{C(s)}{R(s)}]$$

$$= Z[\frac{1 - e^{-TS}}{s} * \frac{e^{-\theta s}}{\lambda s + 1}]$$

$$\frac{Z^{-(n+f)}[(1 - e^{-(1-f)T/\lambda}) + (e^{-(1-f)T/\lambda} - e^{-T/\lambda})Z^{-1}]}{1 - e^{-T/\lambda} Z^{-1}} \quad (5.7.4)$$

where N and f are the whole and fractional numbers of periods of delay in θ, respectively. i.e. $\theta = NT + fT$

Substituting C(z)/R(z) into eqn (5.7.2) yields the Dahlin controller D(z) as follows:

$$D(z) = \frac{Z^{-(n+1)}(1 - e^{-1/\lambda T} Z^{-1} - e^{-(1-f)T/\lambda}(1 - Z^{-1}))}{(1 - e^{-1/\lambda T} Z^{-1}) - Z^{-(N+1)}(1 - e^{-1/\lambda T} Z^{-1} - e^{-(1-f)T/\lambda}(1 - Z^{-1}))} \quad (5.7.5)$$

$$D(z) = \frac{Z^{-(N+1)} - PZ^{-(N+2)} - QZ^{-(N+1)} + QZ^{-(N+2)}}{1 - PZ^{-1} - Z^{-(N+1)} + PZ^{-(N+2)} - QZ^{-(N+1)} + QZ^{-(N+2)}} \quad (5.7.6)$$

where $P = e^{-1/\lambda T}$

$Q = e^{-(1-f)T/\lambda}$

Since R(Z) = F(Z)/E(Z), where F is the manipulated variable, frequency, and E is the error term, in difference equation F can be related to E as:

$$F(t) = p * F(t-1) + (1+Q) F(t-N-1) - (P+Q) F(t-N-2) +$$

$$(1-Q) * E(t-N-1) + (Q-P) E(t-N-2) \quad (5.7.7$$

the value of F then is a function of T, sampling time and λ, the tuning parameter.

The computer program written to implement controller in eqn (5.7.7) is listed in Appendix D.4.

5.7.2 Results and Discussion

The controllers parameter, λ, was tuned on line with respect to set point changes from .02 to .05 (U_d = 1.35 mm/s, U_c = 0 mm/s). Tuning results of the ε controller with sampling time of 60 sec. are shown in Fig. 5.7.2. The Dahlin controller was tested starting with an initial value of λ = 33 sec, which is the process time constant. The response in this case was very fast but oscillatory with a rather large overshoot. When λ was increased to 90, the rise time of the response was still fast; however, there was hardly any oscillation. Thus, λ = 90 is considered the best tuning and the response to δc of .03 is shown in Fig. 5.7.3.

With the setting of λ = 90, T = 60, the controller was tested against a change of U_d from 1.35 mm/s to 2.7 mm/s. The response is shown in Fig. (5.7.4). Unlike the response of the PI controller (shown in Fig. 5.3.5), the response of the Dahlin controller to load change is acceptable even though it was designed for set point change.

In the case where water was flowing the dynamics of the system are different as pointed out in sec (5.3.2). Using the appropriate transfer function the Dahlin controller was also tested with a set point change from .02 to .05 (U_d = 1.35 mm/s, U_c = 3.5 mm/s). Next, a change of U_d from 1.35 mm/s to 2.7 mm/s was also introduced. These results are shown in Fig. 5.7.5. It appears that the controller works just as well

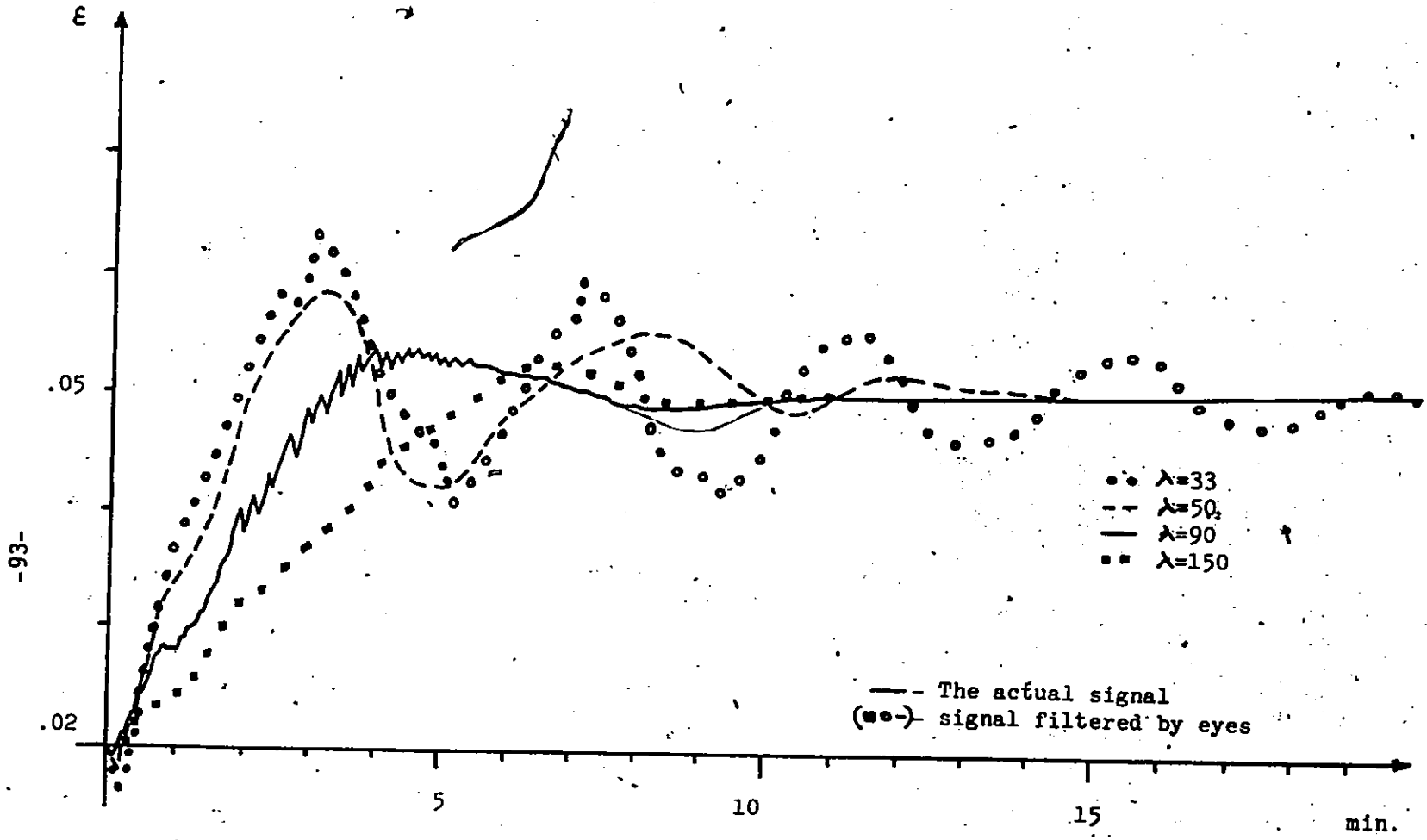

Fig. 5.7.2 On-line Tuning of the Dahlin Controller with respect to a set point change of =.03 (U_0=1.35 mm/s, U_c=0 mm/s) with T=60 sec.

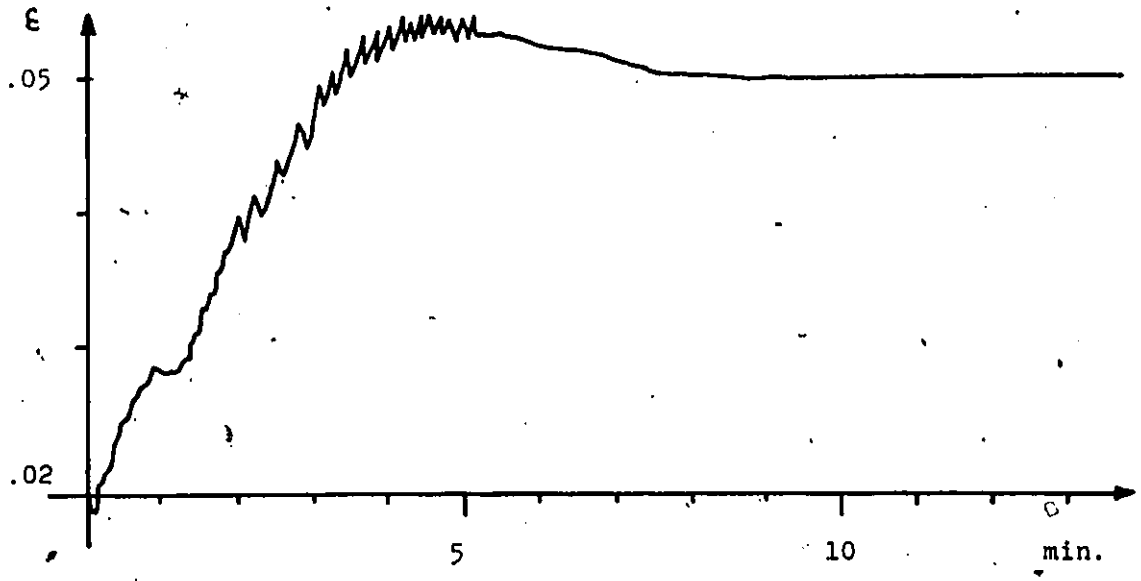

Fig. 5.7.3 Response of Dahlin Controller (with λ=90, T=60) to set point change of $\delta\varepsilon$=.03 (U_d=1.35 mm/s, U_c=0 mm/s)

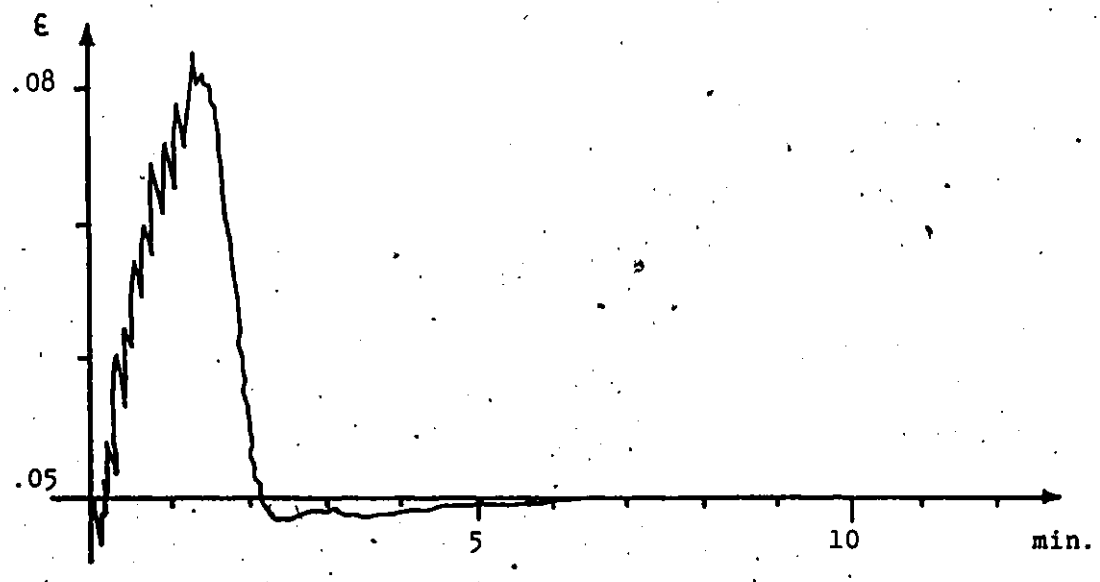

Fig. 5.7.4 Response of Dahlin Controller (with λ=90, T=60) to U_d change from 1.35 mm/sec. to 2.7 mm/s.

with or without water flowing, as long as the appropriate model is used.

Since the Dahlin controller is a fixed parameter controller, it suffers from the same drawback as the PI controller when the process is non-linear, i.e. when the operating region is moved, the controller needs to be retuned or redesigned. Fig. (5.7.6) shows the response of the controller designed for ε in the region of .02 to .05, when ε is changed from .05 to .08. It can be seen that the controller performance is very poor and unacceptable.

5.8 MINIMUM VARIANCE CONTROLLER AND RESULTS

The previous controllers tested were all deterministic with fixed parameters, and were found to be unsatisfactory. The fact that the process is non-linear and has a varying deadtime, suggests the use of a controller which has tracking ability and deadtime compensation. Thus, the self-tuning-regulator (S.T.R.), which is a minimum variance controller plus a parameters estimator, presents itself as a possible controller for the Karr column.

But before the S.T.R. is tested, the minimum variance (M.V.) controllers performance must be verified. The theories for M.V. controller and S.T.R. are presented in books by Box and Jenkins [26] and Astrom and coworkers [27 - 33]. The theory of the M.V. Controller is briefly outlined below.

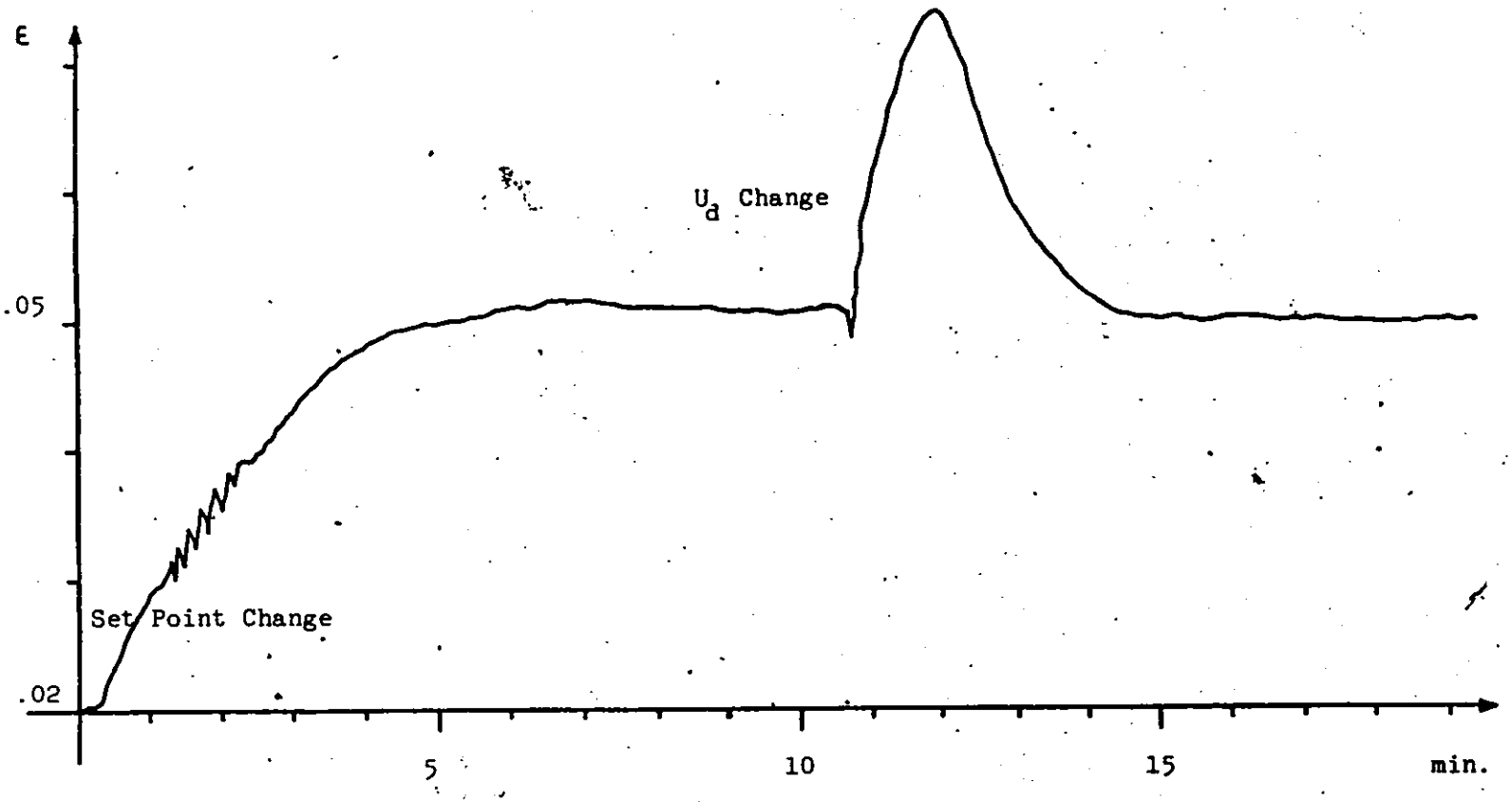

Fig. 5.7.5 Dahlin controller response (with λ=90, T=60) to ε set point change from 0.2 to 0.5 (U_d=1.35 mm/s, U_c=3.5 mm/s). Later U_d was changed from 1.35 mm to 2.7 mm/s.

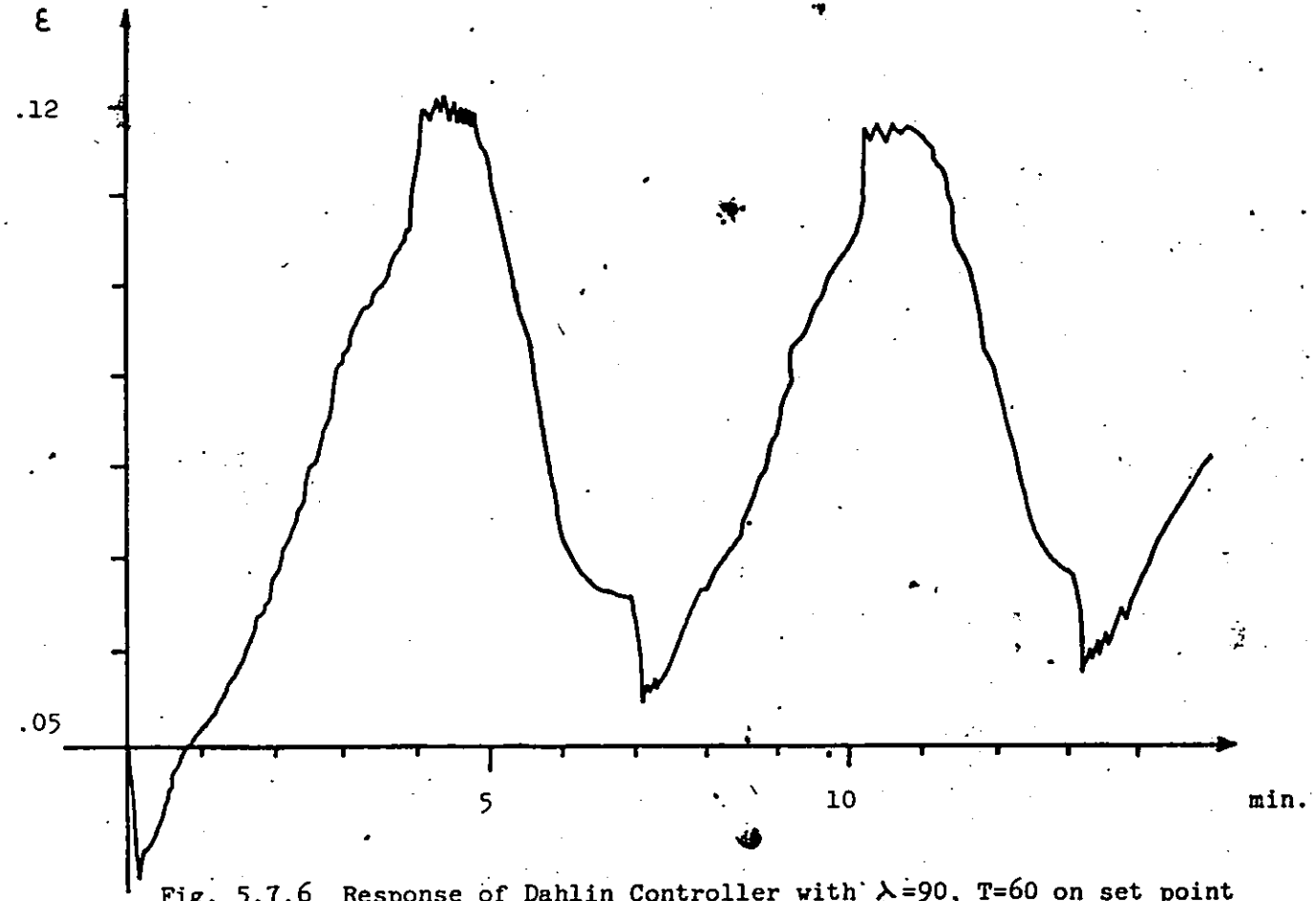

Fig. 5.7.6 Response of Dahlin Controller with λ=90, T=60 on set point change from .05 to .08 (ψ_d=1.35 mm/s, ψ_c=0)

5.8.1 M.V. controller algorithm

Assume that the dynamics of the process to be controlled can be described by a linear transfer function model and that the effect of the stochastic disturbances on the output can be represented by an (ARIMA) model.

$$Y_{t+f+1} = \frac{W(Z^{-1})}{\delta(Z^{-1})} U_t + N_{t+f+1} \tag{5.8.1}$$

$$\text{where } N_{t+f+1} = \frac{\theta(Z^{-1})}{\phi(Z^{-1})\nabla^d} a_{t+f+1} \tag{5.8.2}$$

Y_t is the output deviation from its target value at time t and U_t is the input deviation from a correspondence steady state value. The term $w(Z^{-1})$, $\delta(A^{-1})$, $\theta(Z^{-1})$ and $\phi(Z^{-1})$ in the discrete transfer function represents polynomials in the backward shift operator, Z^{-1}, and f>1 represents the number of whole period of time delay in the system. N_t is the disturbance representing the total effect at the output of all unobserved disturbances acting within the system [26].

Optimal control is usually designed by optimizing some function. In the Minimum Variance case, the controller is derived by minimizing $E(y_{t+f+1})^2$.

In this work, no time series identification of the dynamic was done. The discrete transfer function in the Z^{-1} domain $W(Z^{-1})/\delta(Z^{-1})$ was obtained by relating the continuous models obtained from step-test to discrete models. The continuous models obtained were of first-order plus deadtime form as shown below:

$$\frac{y(s)}{U(s)} = \frac{g\, e^{-T_D s}}{\tau s + 1} \tag{5.8.8}$$

where g = gain term

τ = time constant

$T_D = f + c$

f = whole periods of delay

C = fractional period of delay

The continuous transfer function in eqn (5.8.3) can be represented in discrete domain [26] as:

$$(1 - \delta Z^{-1})\, Y_t = (W_0 - W_1\, Z^{-1})\, U_{t-f-1} \tag{5.8.4}$$

where $\delta = e^{-h/\tau}$ (5.8.5)

h = sampling interval

$$W_0 = g\,(1 - \delta^{1-c}) \tag{5.8.6}$$

$$W_1 = g\,(\delta - \delta^{1-c}) \tag{5.8.7}$$

The noise considered in this case is the deterministic set point change

$$Nt = \frac{1}{1-Z^{-1}}\, \alpha_t \tag{5.8.8}$$

where α_t represents impulse shock. Thus the process described by eqn (5.8.1) can be represented as:

$$Y_{t+f+1} = \frac{W_0 - W_1\, Z^{-1}}{1 - \delta\, Z^{-1}}\, U_t + \frac{1}{1 - Z^{-1}}\, \alpha_{t+f+1} \tag{5.8.9}$$

where Y_t = (c - c steady state). The term N_{t+f+1} can be represented by the (1 + f) step ahead forecast and the forecast error as follows [26]:

$$N_{t+f+1} = \frac{1}{1 - Z^{-1}} \alpha_{t+f+1} \tag{5.8.10}$$

$$\text{but} \quad \frac{1}{1 - Z^{-1}} \alpha_{t+f+1} = \psi_1(B) \alpha_{t+f+1} + \frac{T(B)}{\nabla^d} \alpha_t \tag{5.8.11}$$

where $\psi_1(B) \alpha_{t+f+1}$ = the forecast error

and $\frac{T(B)}{\nabla^d} \alpha_t$ = the (1+f) step ahead forecast

$\psi_1(B)$, a polynomial of order f, and T(B) can both be found by equating the coefficients on L.H.S. and R.H.S. of eqn (5.8.1), and after some calculation yields:

$$\psi_1(B) = 1 \tag{5.8.12}$$

$$T(B) = 1 \tag{5.8.13}$$

Thus eqn (5.8.11) becomes:

$$\frac{1}{1 - Z^{-1}} \alpha_{t+f+1} = \alpha_{t+f+1} + \frac{1}{1 - Z^{-1}} \alpha_t \tag{5.8.14}$$

Substituting eqn (5.8.14) into eqn (5.8.9) yields,

$$Y_{t+f+1} = \frac{w_0 - w_1 Z^{-1}}{1 - \delta Z^{-1}} U_t + \alpha_{t+f+1} + \frac{1}{1 - Z^{-1}} \alpha_t \tag{5.8.15}$$

The M.V. controller can be derived by minimizing $E(Y_{t+f+1}^2)$. Taking expectation of the square of eqn (5.8.15) gives:

$$E(Y_{t+f+1}^2) = E\{\frac{w_0 - w_1 Z^{-1}}{1 - \delta Z^{-1}} U_t + \frac{1}{1 - Z^{-1}} \alpha_t\}^2 + E\{\alpha_{t+f+1}\}^2 +$$

$$2E[(\frac{w_0 - w_1 Z^{-1}}{1 - \delta Z^{-1}}) U_t + \frac{\alpha_t}{1 - Z^{-1}})(\alpha_{t+f+1})] \tag{5.8.16}$$

the third term on the R.H.S. of eqn (5.8.16) is equal to zero, thus eqn (5.8.16) becomes:

$$E(Y_{t+f+1}^2) = E\{\frac{w_0 - w_1 z^{-1}}{1 - \delta z^{-1}} U_t + \frac{1}{1 - z^{-1}} \alpha_t\}^2 + E\{\alpha_{t+f+1}\}^2 \qquad (5.8.17)$$

$E(Y_{t+f+1}^2)$ can then be minimized by setting:

$$\frac{w_0 - w_1 z^{-1}}{1 - \delta z^{-1}} U_t = - \frac{1}{1 - z^{-1}} \alpha_t \qquad (5.8.18)$$

$$\text{Thus, } \nabla U_t = - \frac{(1 - \delta z^{-1})}{w_0 - w_1 z^{-1}} \alpha_t \qquad (5.8.19)$$

where $\nabla U_t = (U_t - U_{t-1})$

Under this controller, $Y_{t+f+1} = \alpha_{t+f+1}$ or $Y_t = \alpha_t$. Substitute α_t in to eqn (5.8.19) gives:

$$\nabla U_t = \frac{(1 - \delta z^{-1}}{(w_0 - w_1 z^{-1})} * Y_t \qquad (5.8.20)$$

The advantage of this controller is it contains a deadtime compensator. Thus the choice of sampling time is unrestricted. However, M.V. controller sometimes calls for excessively large variation in the manipulated variable, because essentially this is the equivalent of a deadbeat controller. In situations where this manipulation is too severe, it is a common practice to calculate control laws which minimize the variance of Y subject to a constraint on the variance of ∇U_t, that is, to minimize

$$E\{Y_{t+f+1}^2 + \xi'' (\nabla U_t)^2\} \qquad (5.8.21)$$

this constraint is especially necessary when the system behaviour is non-minimum phase, as in the case of the Karr column.

However, the solution required to solve this linear quadratic control problem required spectral factorization (ref. 26, 27). An alternative and much simpler approach to constraining the variations in the manipulated variable has been proposed by Clarke and Hasting James [31] and Clarke and Gawthrop [32]. Rather than minimizing eqn (5.8.21), they treat the simpler problem of minimizing an instantaneous performance index [33].

$$I = \{\hat{Y}_{t+f+1/t} + \xi' (\nabla U_t)^2\} \qquad (5.8.22)$$

where $\hat{Y}_{t+f+1/t}$ is the minimum variance forecast of Y_{t+f+1} made at time t. This criterion usually results in a controller which, for the same constraint on the variance of ∇U_t, has only slightly larger variance for the output [33]. The resulting controller can be shown to be [31] & [32]:

$$\nabla U_t = - \frac{(1 - \delta Z^{-1})}{(w_o - w_1 Z^{-1}) + \frac{\xi'}{w_o}(1 - \delta Z^{-1})} Y_t \qquad (5.8.23)$$

ξ' is a tuning parameter. If $\xi' = 0$, a M.V. without constraint is obtained.

In difference equation:

$$(w_0 + \lambda) \nabla U_t + (- w_1 - \lambda\delta) \nabla U_{t-1} = - Y_t + \delta Y_{(t-1)}$$

$$\nabla U_t = - \frac{1}{(w_0 + \lambda)} Y_t + \frac{\delta}{(w_0 + \lambda)} Y_{t-1} + \frac{(w_1 + \lambda * \delta)}{w_0 + \lambda} \nabla U_{t-1} \qquad (5.8.24)$$

for a set point change from .02 to .05, the nominal transfer function

from ε with respect to frequency is:

$$\frac{K\, e^{-T_D S}}{\tau s + 1} = \frac{.015 * e^{-15S}}{33\, s + 1}$$

For sampling time of 60 sec, and $\lambda = .05$

$$c = 15/30$$

$$\delta = e^{-Ts/\tau} = .1623$$

$$w_0 = g\,(1 - \delta^{1-c}) = .01$$

$$w_1 = g\,(\delta - \delta^{1-c}) = -.0013$$

Equation (5.8.24) becomes:

$$\nabla U_t = -16.66\, Y_t + 2.7\, Y_{t-1} + .2\, \nabla U_{t-1}$$

where $Y_t = \varepsilon_t - \varepsilon$ set point

$$\nabla U_t = F_t - F_{t-1}$$

The computer program written to implement the controller in eqn (5.8.24) using the microcomputer is presented in Appendix D.5.

5.8.2 RESULTS AND DISCUSSION

The controller described in eqn (5.8.23) was tested with ε set point change from .02 to .05. (U_d = 1.35 mm/s; U_c = 0) various ξ' values were tried and the tuning results were shown in Fig. 5.8.1. Lower ξ' value gave a fast and underdampted response, and as ξ' increases the response became very sluggish. Of all those ξ' and Ts (sampling time) combinations tested, the best response was found at ξ' = .05 and Ts = 30 s. This response is presented in Fig. 5.8.2. The response of this controller when U_d was changed from 1.35 mm/s to 2.7 mm/s is shown in Fig. 5.8.3. It has almost the same disturbance

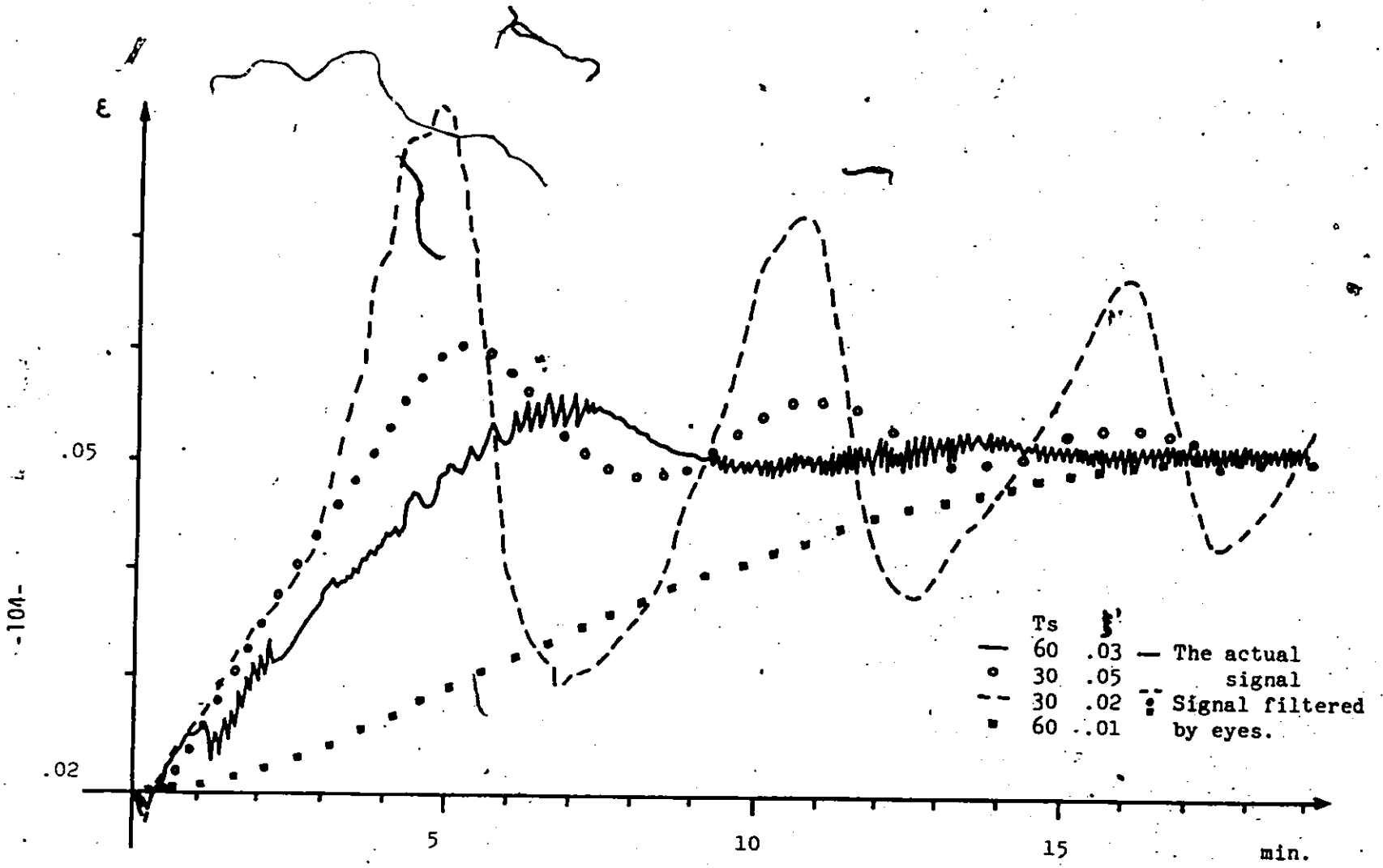

Fig. 5.8.1 Tuning Result of M.V. Controller

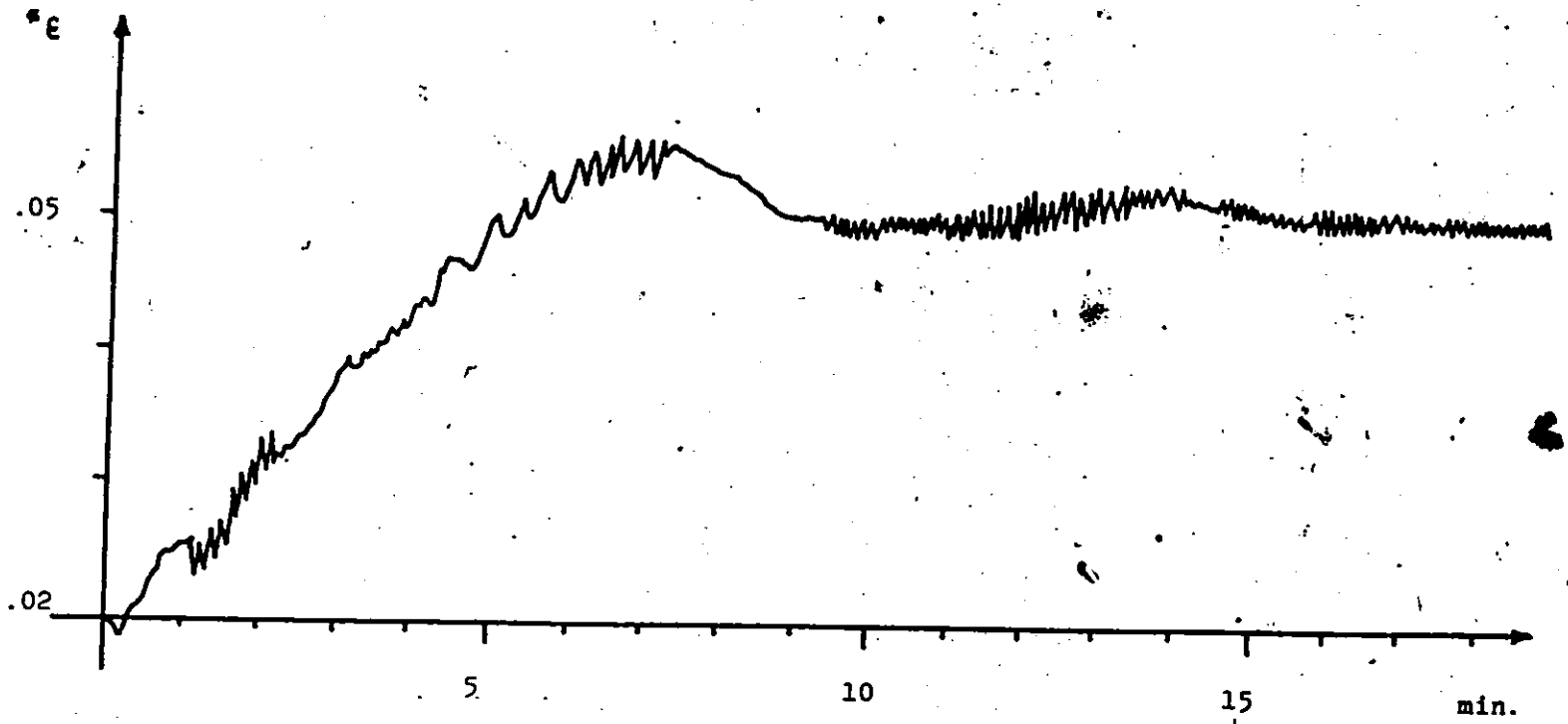

Fig. 5.8.2 Best Response of M.V. Controller with $\zeta'=.03$, T=60 sec. (U_d=1.35 mm/s, U_c=0) for ε set point change from .02 to .05

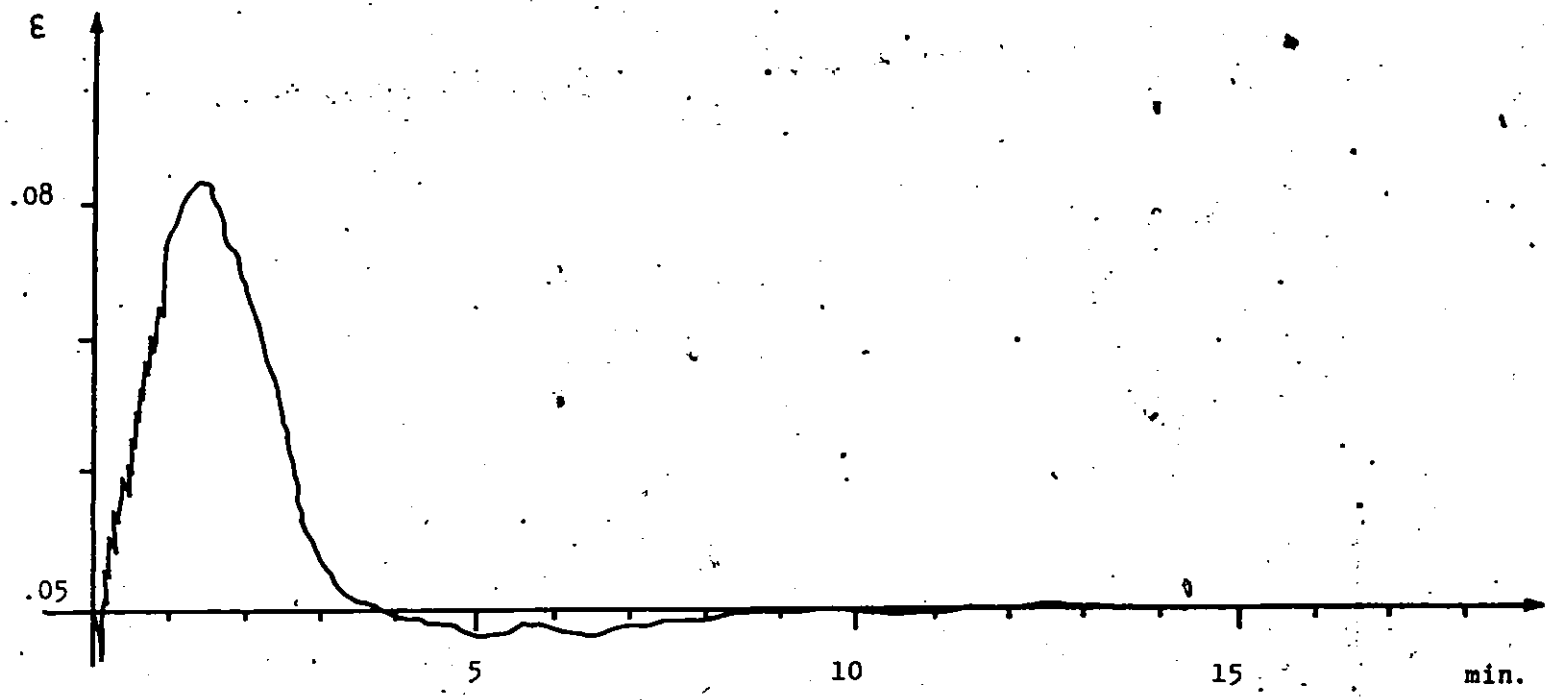

Fig. 5.8.3 Response of M.V. Controller with ζ'=.03, T=60 when U_d was changed from 1.35 mm/s to 2.7 mm/s (U_d=1.35 mm/s, U_c=0)

characteristic as that of the Dahlin controller. Unlike the PI controller, it overcomes the U_d change without oscillation, even though it was designed for set point change.

In the case where water was flowing, this controller was tested using the appropriate model, with a ϵ set point change from 0.018 to 0.05 (U_d = 1.35 mm/s, U_c = 3.5 mm/s). After this, it was subjected to a change of U_d from 1.35 mm/s to 2.7 mm/s. The results, shown in Fig. 5.8.4, indicate that the controller performance is independent of whether there is water flow or not. The same conclusion has been drawn in section 5.6.

The ability of the M.V. controller in handling this non-linear process was also checked using the same procedure as for the Dahlin controller. The result in Fig. 5.8.5 shows that when the operating region was changed, the controller needed to be redesigned using the appropriate model. This is as expected because the M.V. controller is a fixed parameter controller.

5.9 SELF-TUNING-REGULATOR (S.T.R) AND RESULT

S.T.R. is one modern controller which has had a great impact on the process industry. The self tuning controller and regulator involves the synthesis of a feedback rule which optimizes a quadratic function, couple with an on-line parameter estimator as shown in Fig. 5.9.1.

The on-line estimator has the capability of using the input-output information on the process to tune the controller directly. Because of this characteristic, it is suitable for use in a non-linear

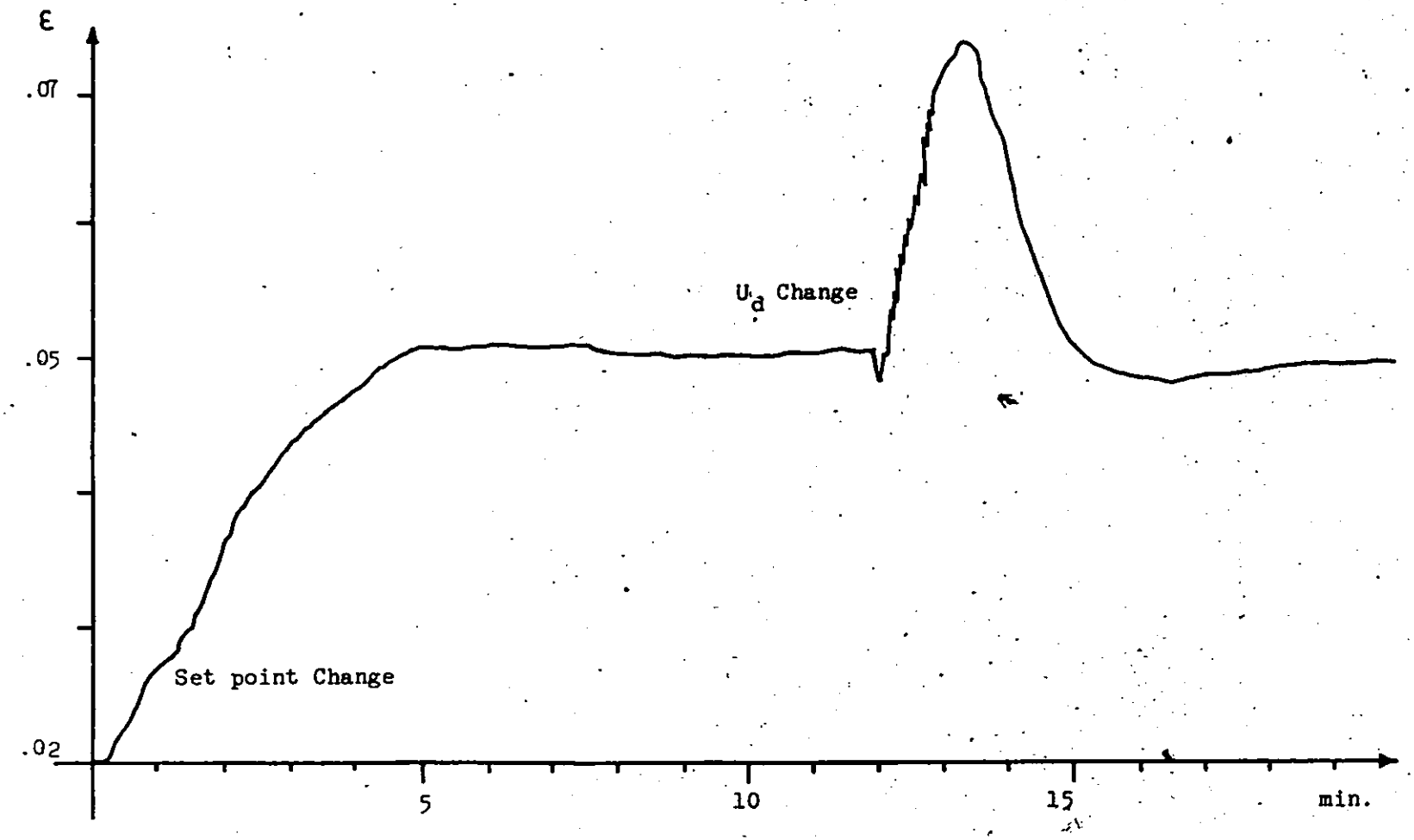

Fig. 5.8.4 Response of M.V. Controller (with ξ =.03, T =60) on ε set point change from .02 -.05 (U_d=1.35 mm/s; U_c =3.5 mm/s). Later, U_d was changed from 1.35 mm to 2.7 mm/s.

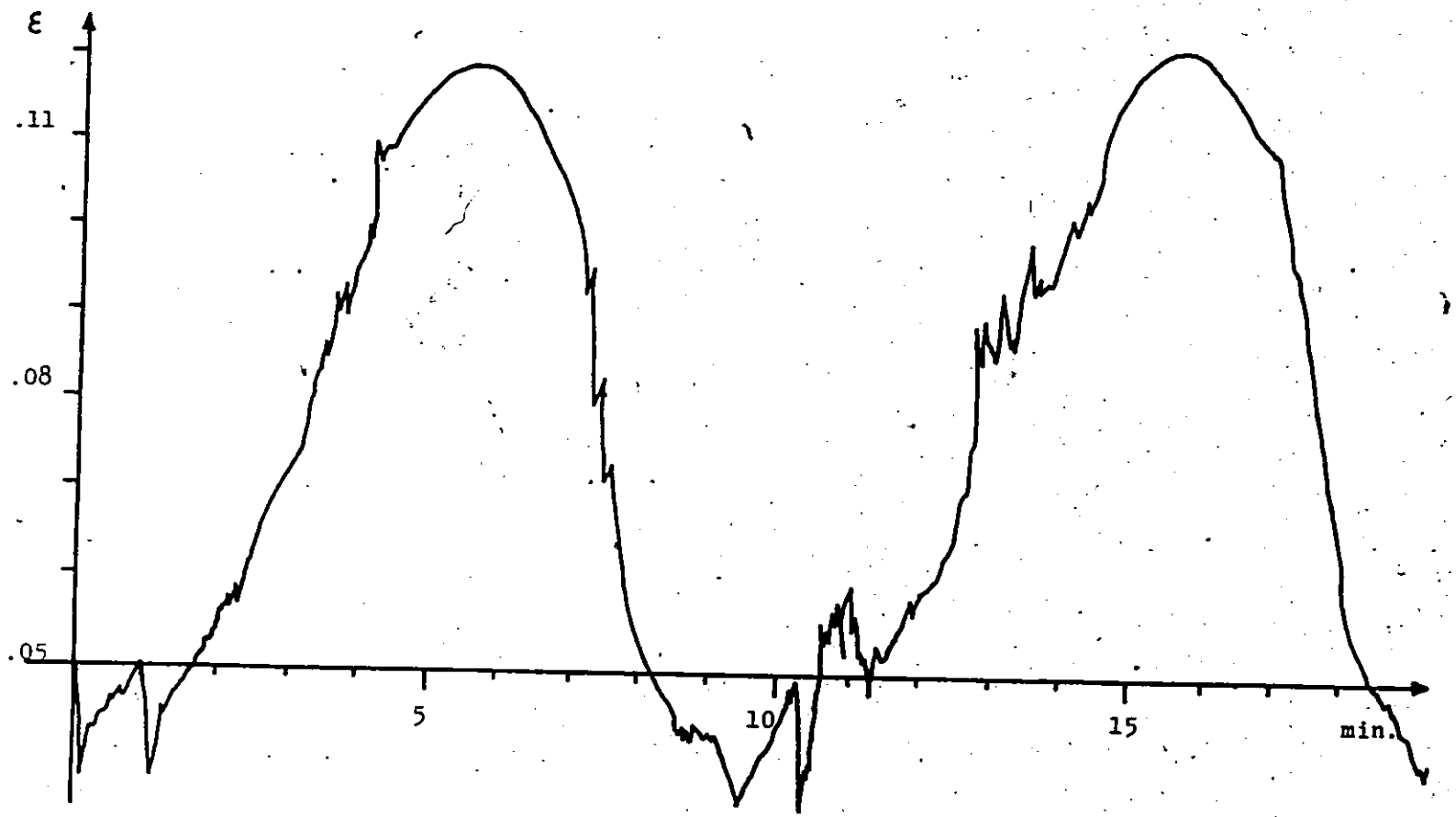

Fig. 5.8.5 Response of M.V. Controller for ε set point change from .05 to .08 (U_d=1.35 mm/s, U_c=0)

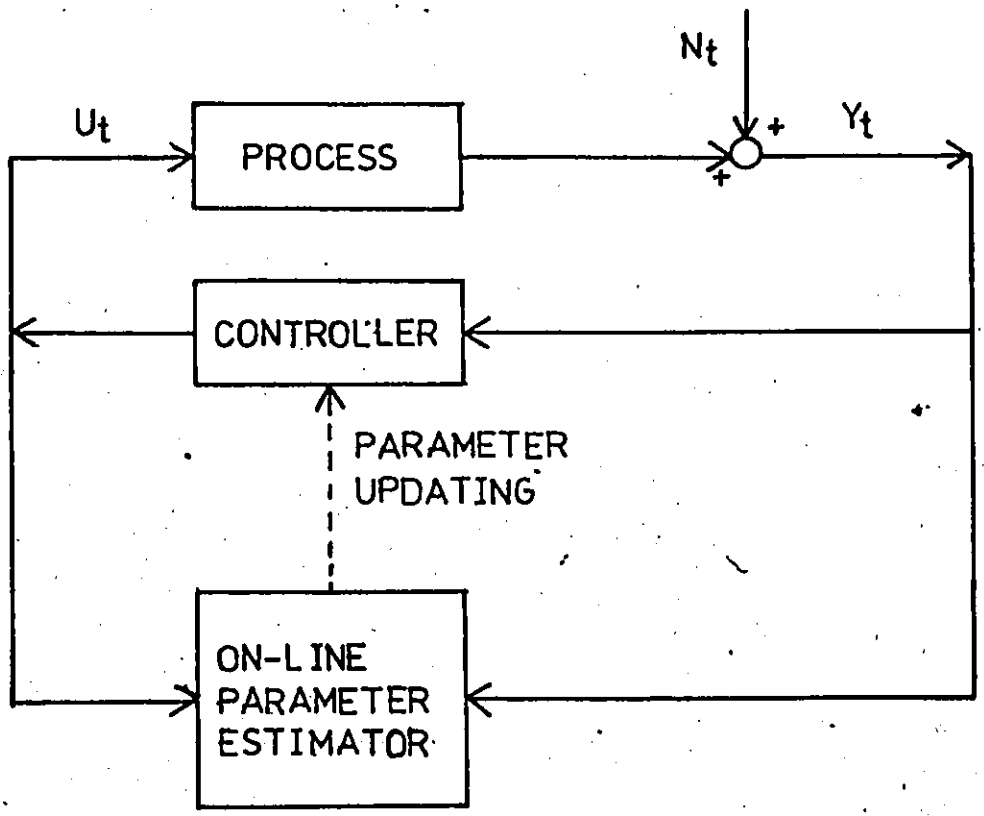

Fig. 5.9.1 S.T.R. Control Scheme

or time varying system.

5.9.1 S.T.R. Algorithm

Much of the theory on S.T.R. has developed by Astrom and Wittenmark and their coworkers, [28 - 33]. Consider the dynamics of the process as described by the following transfer function:

$$Y_{t+f+1} = \frac{w(Z^{-1})}{\delta(Z^{-1})} U_t + N_{t+f+1} \tag{5.9.1}$$

where $N_{t+f+1} = \frac{\theta(B)}{\phi(B)\ \nabla^d}\ \alpha_{t+1}$

$$= \psi_1(B)\ \alpha_{t+f+1} + \frac{T(B)}{\phi(B)\ \nabla^d}\ \alpha_t \tag{5.9.3}$$

$w(Z^{-1})$ and $\delta(Z^{-1})$ are polynomial of order s and r, respectively. $\phi(Z^{-1})\nabla^d$ is a polynomial of order (p+d) with p roots inside the unit circle and d roots equal to unity. Letting d roots equal to unity enables one to model the nonstationary disturbances. Also a value of d. > 0 always leads naturally to integral action in the controller.

Multiplying eqn (5.9.1) by $\psi(Z^{-1})\phi(Z^{-1})\nabla^d\delta(Z^{-1})$ and substitute eqn (5.9.2) into the result yields:

$$\delta(Z^{-1})\theta(Z^{-1})[Y_{t+f+1} - \psi_1(Z^{-1})\alpha_{t+f+1}] = \delta(Z^{-1})T(Z^{-1})Y_t + w(Z^{-1})\phi(Z^{-1})\nabla^d U_t$$

$$\text{or } \delta(Z^{-1})\theta(Z^{-1})\ [Y_{t+f+1} - \varepsilon_{t+f+1}] = \alpha(Z^{-1})\ Y_t + \beta(Z^{-1})\nabla^d\ U_t \tag{5.9.3}$$

where $\alpha(Z^{-1}) = \alpha_0 + \alpha_1 Z^{-1} + \ldots\ldots \alpha_m Z^{-m}$

$\beta(Z^{-1}) = \beta_0 + \beta_1 Z^{-1} + \ldots\ldots \alpha_\ell Z^{-\ell}$

$m = r + \max [q - f - 1, p + d - 1]$ (5.9.4)

$\ell = s + p + f$ (5.9.5)

If the parameters in eqn (5.9.3) were known, then the M.V. controller which minimizes $E(Y^2_{t+f+1})$ would be given by:

$$\nabla^d U_t = - \frac{\alpha(Z^{-1})}{\beta(Z^{-1})} Y_t \tag{5.9.6}$$

If $\delta(z^{-1})\theta(Z^{-1}) = 1$, then eqn (5.9.3) becomes:

$$Y_{t+f+1} = \alpha(Z^{-1}) Y_t + \beta(Z^{-1}) \nabla^d U_t + \varepsilon_{t+f+1} \tag{5.9.7}$$

In this case, the process output Y_{t+f+1} can be expressed explicitly in terms of the M.V. controller parameters (α_i, β_i). If the M.V. controller parameters were unknown, one might try to estimate them directly using linear least square on eqn (5.9.7) to obtain unbiase estimate of α's and β's. Furthermore, linear least square can be expressed in a recursive manner. Therefore the controller parameters can be updated in every sampling interval and one can use the controller in the form:

$$\nabla^d U_t = - \frac{\hat{\alpha}(Z^{-1})}{\hat{\beta}(Z^{-1})} Y \tag{5.9.8}$$

The restriction $\delta(Z^{-1})\theta(Z^{-1}) = 1$ appears to limit the use of this controller. Therefore if eqn (5.9.7) was used to update $\hat{\alpha}$'s and $\hat{\beta}$'s at each interval, one would get a biased estimate. However, Astrom and Wittenmark [28] proved that this algorithm would have desirable assymtotic property inspite of $\delta(Z^{-1})\theta(Z^{-1})$ being not equal to one.

Suppose that the following regression model was used to estimate α's, β's recursively:

$$Y_t = \underline{x}'_{t-f-1}\ \underline{\theta} + \epsilon_t \tag{5.9.9}$$

where, $\underline{x}'_{t-f-1} = [Y_{t-f-1}, \cdots Y_{t-f-1-m}, \nabla^d U_{t-f-1} \cdots \nabla^d U_{t-f-1-\ell})$ (5.9.10)

$$\underline{\theta}^T = [\alpha_0, \alpha_1, \cdots \alpha_m, \beta_0, \beta_1 \cdots \beta_\ell] \tag{5.9.11}$$

placket [28] showed that least square could be set up recursively:

$$\hat{\underline{\theta}}_t = \hat{\underline{\theta}}_{t-1} + \underline{K}_t \{Y_t - \underline{x}'_{t-f-1}\ \underline{\theta}_{t-1}\} \tag{5.9.12}$$

where $\underline{K}_t = \dfrac{\underline{P}_{t-1}\ \underline{x}_{t-f-1}}{(\lambda + \underline{x}'_{t-f-1}\ \underline{P}_{t-1}\ \underline{x}_{t-f-1})}$

$$\underline{P}_t = \underline{P}_{t-1} - \left\{\frac{\underline{P}_{t-1}\ \underline{x}_{t-f-1}\ \underline{x}'_{t-f-1}\ \underline{P}_{t-1}}{\lambda + \underline{x}'_{t-f-1}\ \underline{P}_{t-1}\ \underline{x}_{t-f-1}}\right\} * \frac{1}{\lambda} \tag{5.9.13}$$

$$\underline{P}_t = \frac{1}{\sigma_y^2}\ \mathrm{CoV}\ (\hat{\theta}) = (\underline{x}^T\ \underline{x})^{-1}$$

λ = "Forgetting factor" which calculates effective window length or effective number of observations included in estimating the parameters.

As the system is nonminimum phase, a constraint on the variance of $(\nabla^d U_t)$ needs to be imposed. Again the simplified Clarke method [31,37] which minimize the instantaneous performance index

$$I = (\hat{Y}_{t+f+t} + \xi^2\ (\nabla^d\ U_t)^2) \tag{5.9.14}$$

is used to derive the controller. Minimizing eqn (5.9.14) can be shown as equivalent to minimizing

$$I_1 = E\{Y_{t+f+1} + \xi\ \nabla^d\ U_t\}^2 = E(\pi_{t+f+1})^2 \qquad (5.9.15)$$

where $\xi = \xi'/w_0$

Clarke and Gawthrop [32] were able to show that this kind of constraint S.T.R. can be achieved by using an estimation model:

$$\pi_{t+f+1} = \alpha(Z^{-1})\ Y_t + \gamma(Z^{-1})\ \nabla^d\ U_t + \epsilon_{t+f+1} \qquad (5.9.16)$$

the controller eqn

$$\nabla^d\ U_t = \frac{-\alpha(Z^{-1})}{\gamma(Z^{-1})}\ Yt \qquad (5.9.17)$$

will have the same properties as controller in eqn (5.9.8). The value of ξ that will reduce the variance of $(\nabla^d U_t)$ will be found by on-line tuning. But one should keep in mind that since

$$\xi = \xi'/w_0 \qquad (5.9.18)$$

and since ξ is positive, the sign of ξ' must be equal to that of w_0. For non-minimum phase system a non-zero value of ξ' is needed to ensure that one does not have parametric sensitivity or instability.

In order to use the recursive least squares, λ is usually chosen to be between 1 - .95. λ value of .95 will give fast but noisy adaptation. High λ gives slow adaptation but more smooth tracking. $\underline{\theta}_0$ is the best guess of $\underline{\theta}$, one can use known M.V. controller or P+I controller parameters. $\underline{P}_0$ represents the uncertainty in $\hat{\underline{\theta}}_0$. If a poor guess of $\hat{\underline{\theta}}_0$ is anticipated, choose $\underline{P}_0 = \gamma\underline{I}$ where γ is a large number. If one is more confident in $\underline{\theta}_0$ then a smaller $\underline{P}_0$ should be chosen.

If the orders of $\alpha(Z^{-1})$ and $\beta(Z^{-1})$ used in eqn (5.8.9) are true orders m and ℓ, it can be shown that the S.T.R. will converge to the M.V. controller. In this work, the m and ℓ used are 1 and 1 as obtained

from the process discrete transfer function in eqn (5.8.3) and noise model of deterministic step described in eqn (5.8.8), respectively.

The subject of parameter estimation under closed-loop conditions has been extensively discussed in reference [34 - 38]. In this work, β_0 was fixed at 1 in all runs to ensure the system was within stability bounds, i.e. the requirement

$$0.5\, w_0 < |\beta_0| < \alpha$$

is satisfied. Also to ensure that the deadtime is not underestimated, which will also cause instability, the sampling time is chosen so as to be larger than the expected longest deadtime.

Since the S.T.R. in this case is mainly used to track the ϵ set point step change, the most satisfactory mode of operation in this situation is to allow tuning of the controller over a few periods where such step changes are present. Then the estimation portion of the regulator should be turned off when parameters are converging to avoid the $\underline{P}$ matrix growing excessively large due to the lack of information.

Also, in order for S.T.R. to be able to handle servo-tracking properly, some modifications of the variable $Y_{t-f-1}, \ldots, Y_{t-f-\ell}$ are required when a set point change is introduced. Because at steady-state $Y_{t-f-1}, \ldots, Y_{t-f-\ell}$ and elements of $\underline{x}_{t-f-1}$, are all at zero, and when a new set point is introduced $Y_{t-f-1}, \ldots, Y_{t-f-\ell}$ should be set at:

$$Y_{t-f-1} = \ldots\ldots = Y_{t-f-\ell} = \epsilon - \epsilon_{\text{setpoint new}} \qquad (5.9.20)$$

$\underline{X}_{t-f-1}$, therefore, become:

$$\underline{X}'_{t-f-1} = |Y_{t-f-1}, \ldots, Y_{t-f-\ell}, 0, \ldots, 0| \qquad (5.9.21)$$

The program written in basic used for implementing S.T.R. in this

case is given in Appendix D.6.

5.9.2 RESULTS AND DISCUSSION

As with the other controllers, the S.T.R. was first tested with an ϵ set point change from .02 to .05. Its initial parameters $\underline{\theta}_0$ were chosen as the approximate optimal parameters of the PI controller, i.e. $\hat{\underline{\theta}}_0^T = |10, -5, 1, -5|$. Since $\hat{\underline{\theta}}_0$ was expected to be a poor guess, $\underline{P}_0$ had to be made large. And because Y_t was of the order of 10^{-2}, to make $\underline{P}_0$ large ($\underline{P}_0 = \gamma \underline{I}$), γ was taken to be 100,000. ξ' used was .01 and throughout the experiments on the S.T.R., λ was set at .95, ℓ at 1 and m at 1. The result of the test is shown in Fig. 5.9.2, where it can be seen that the controller settles down after 23 min, and that ϵ set point of .05 was reached without an off-set. The plots of $\hat{\theta}_i$ Vs time for this test are shown in Fig. 5.9.3. It should be pointed out that the performance of the S.T.R. in Fig. 5.9.2. is not the best possible nor it is comparable with the M.V. controller in that ϵ range, because it is a process dynamic learning period for the S.T.R. to adapt its parameters. The overshoot can be reduced by increasing the λ value. In the same figure 5.9.2, the response for $\lambda = .05$ is also shown. At t = 30 min in Fig. 5.9.2, the ϵ set point was changed to .08, and the response of the controller to this change using $\epsilon = .25$ is shown in Fig. 5.9.4. Its $\hat{\theta}_i$ vs time graph is shown in Fig. 5.9.5. Compare with other controllers, the superiority of the S.T.R. is clearly demonstrated, since it can move ϵ, from .05 to .08 without difficulty.

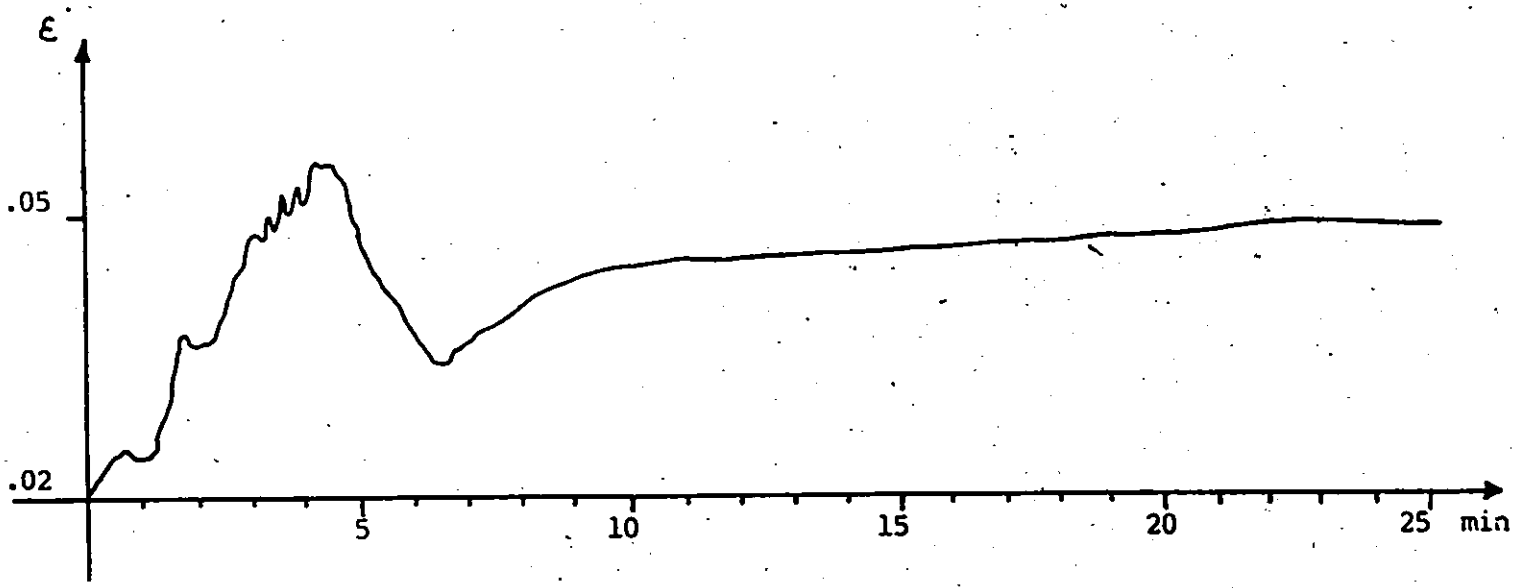

Fig. 5.9.2 S.T.R. Response on ε Set Point Change from .02 - .05 (U_d = 1.35 mm/s, U_c = 0) with $\hat{\theta}_o$=/10, -5, 1, -5/
$\underline{P}_o$= 100,000 $\underline{I}$
$\tilde{\gamma}'$ = 0.5

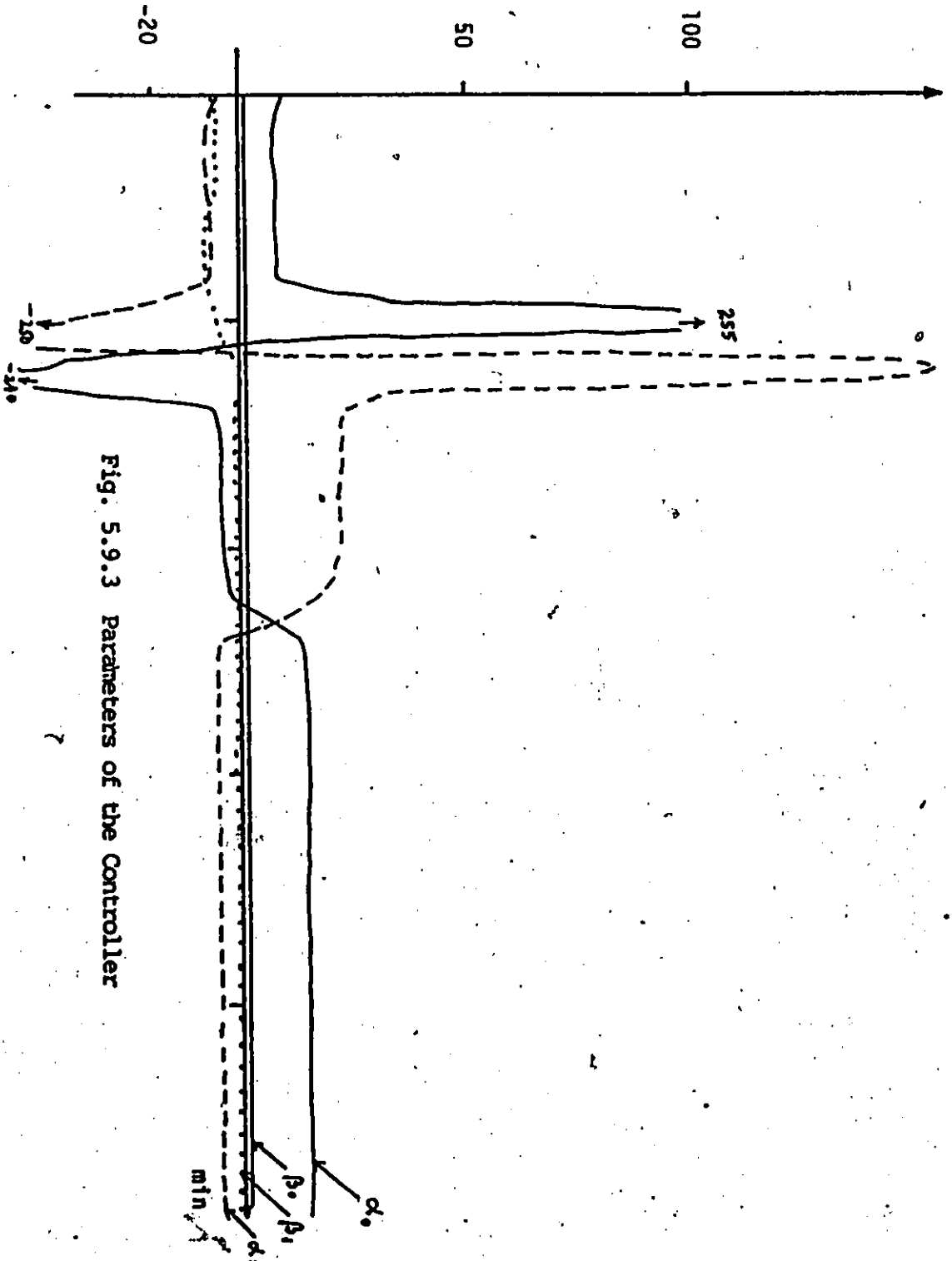

Fig. 5.9.3 Parameters of the Controller

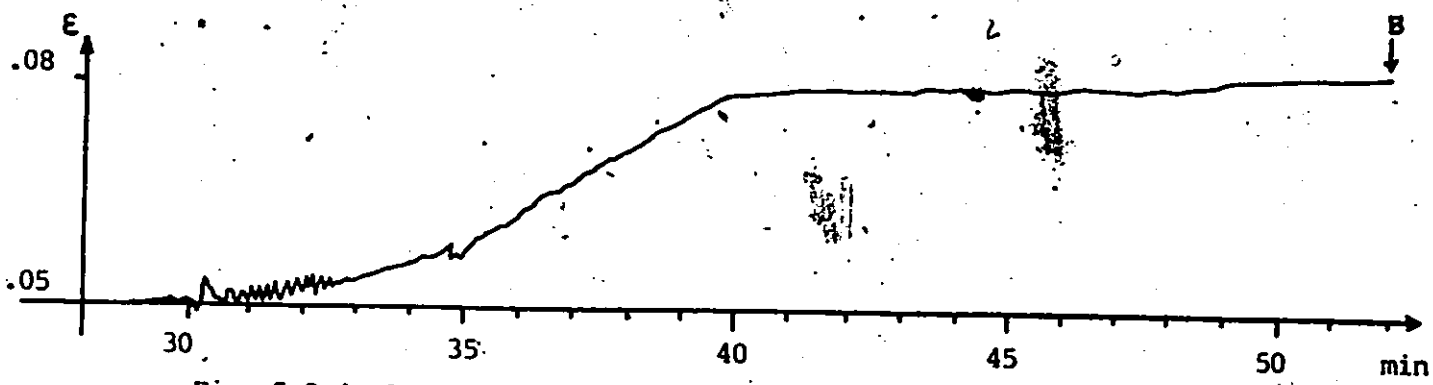

Fig. 5.9.4 S.T.R. Response for ε Set Point Change from .05 to .08
(U_d = 1.35 mm/s, U_c = 0)

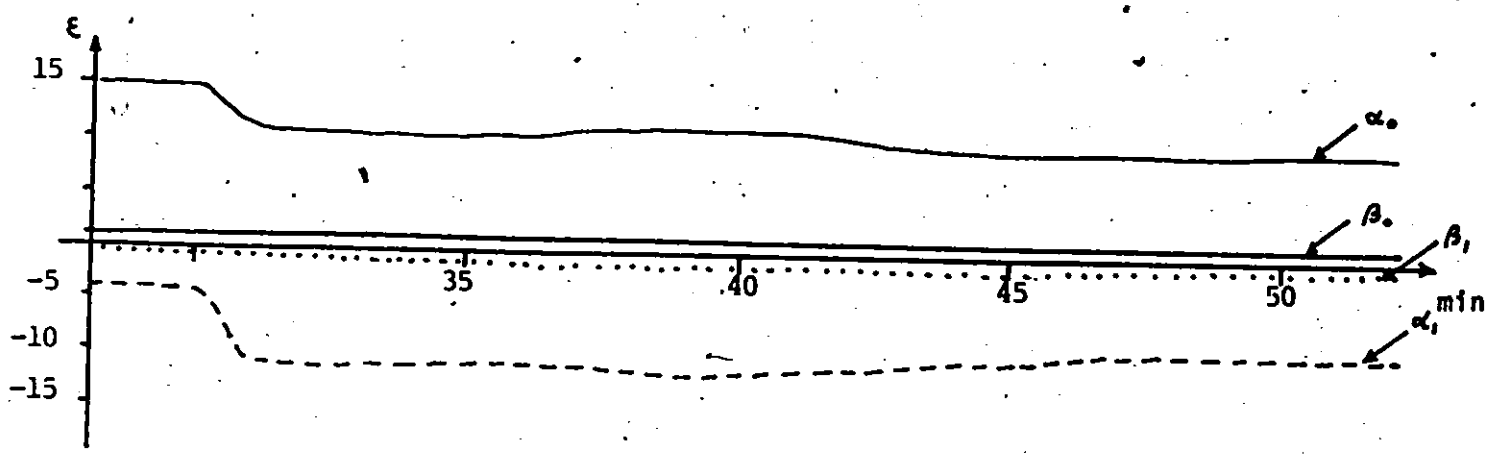

Fig. 5.9.5. The Controller Parameters Plot

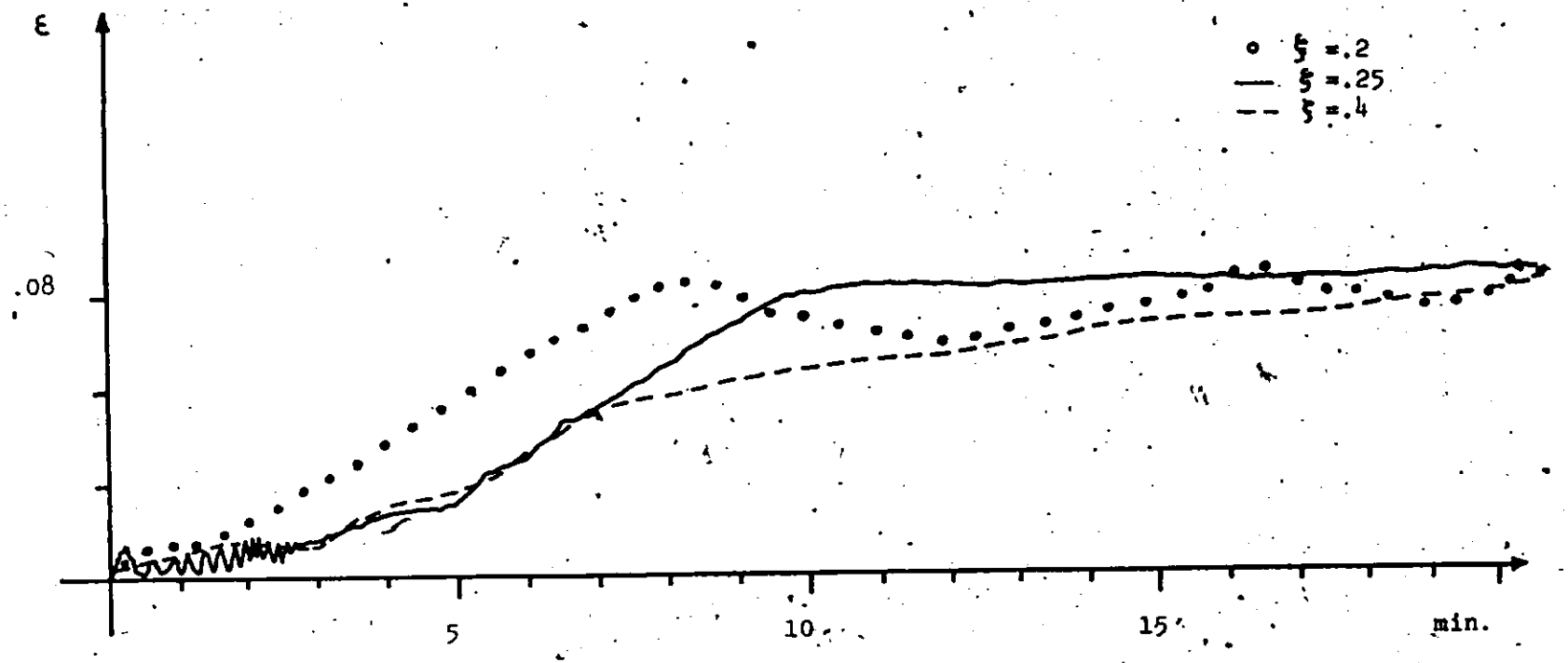

Fig. 5.9.6 Tuning of S.T.R. for ε set point change from .05 to .08 (U_d=1.35 mm/s, U_c=0)

Other tests were run with the S.T.R. The value of ξ is tuned on-line, and one typical tuning result for the change of ϵ set point from .05 to .08, is shown in Fig. 5.9.6. The procedure to obtain each graph in Fig. 5.9.6 was the same as before, i.e., first ϵ was changed from .02 to .05 using $\underline{\hat{\theta}}_0 = |10, -5, 1, -5|$, ... etc and after the parameters were converged, the ϵ set point was then changed to .08. As expected, a large ξ gives a slower but smoother response (see Fig. 5.9.6).

A high value of ϵ (i.e. near flooding) is of more interest in optimum operation, and with the S.T.R. it can be shown that ϵ can be changed to any level in the non-linear region without a problem. The result for an ϵ set point change from .04 to .12 (U_d = 1.35 mm/s, U_c = 0) with ξ = .3, $\underline{P}_0$ = 1000,000 $\underline{I}$ and $\underline{\hat{\theta}}_0 = |18, -7, 1, -.3|$, is shown in Fig. 5.9.7. With water flowing and setting ξ = .3, $\underline{P}_0$ = 1000,000 $\underline{I}$ and $\underline{\hat{\theta}}_0 = |18, -7, 1, -.3|$, the ϵ set point was changed from .03 to .20 (U_d = 2.7 mm/s, U_c = 3.5 mm/s), the result being shown in Fig. 5.9.8. In the last case, since the ϵ region involves a longest deadtime of up to 60 seconds, a sampling time of 90 second is necessary to ensure that the deadtime, f, is not underestimated.

The performance of the S.T.R. on U_d change was also tested. At point B (when ϵ = .08, $\underline{\hat{\theta}} = |13, -8.5, 1, -.126|$ in Fig. 5.9.4, a U_d change from 1.35 mm/s to 2.7 mm/s was introduced, the response with ξ = .5 is shown in Fig. 5.9.9. As expected the performance of the S.T.R. in this case is similar to that of the M.V. controller discussed in sec. 5.8. The $\hat{\theta}_i$ vs t in this case is plotted in Fig. 5.9.10.

In this work, the S.T.R. convergence was not tested using the theory discussed in ref [28]. It was only verified using the plot of $\hat{\theta}_i$ vs time.

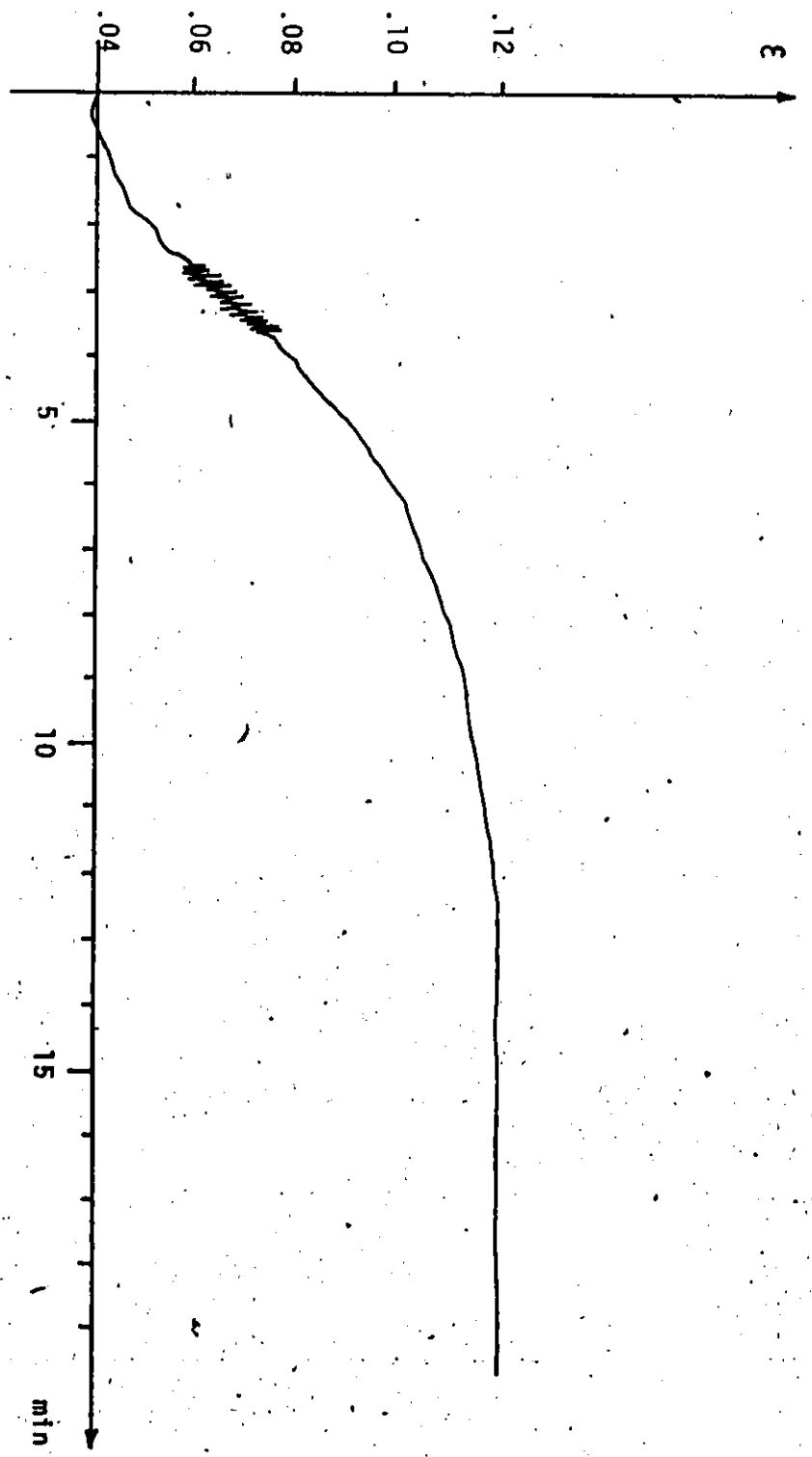

Fig 5.9.7. S.T.R. response for ε set point change from .04 to .12
(U_d = 1.35 mm/s, U_c = 0)

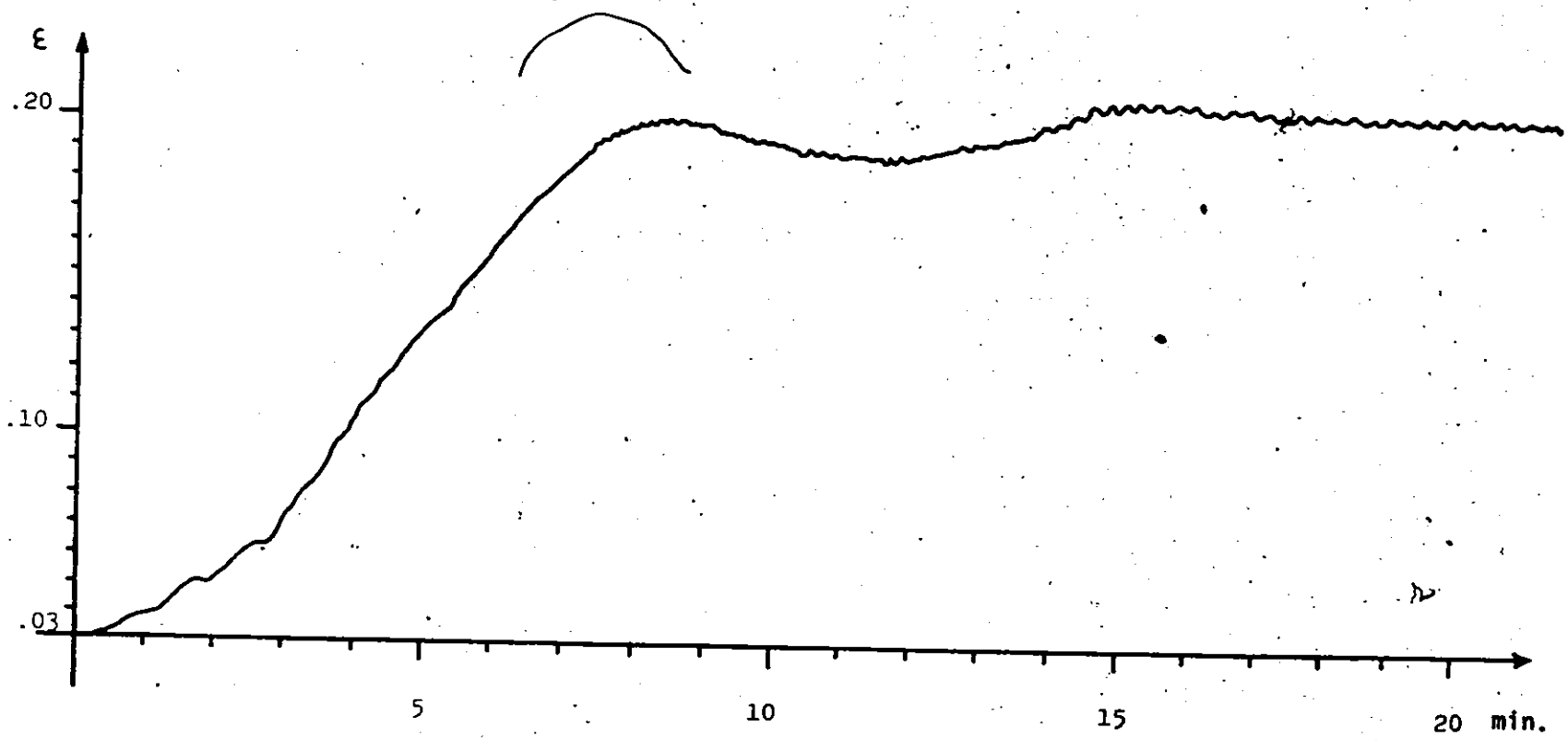

Fig. 5.9.8. S.T.R. Response for ε set point change from 0.3 to .020 (U_d=1.35 mm/s, U_c=3.5 mm/s)

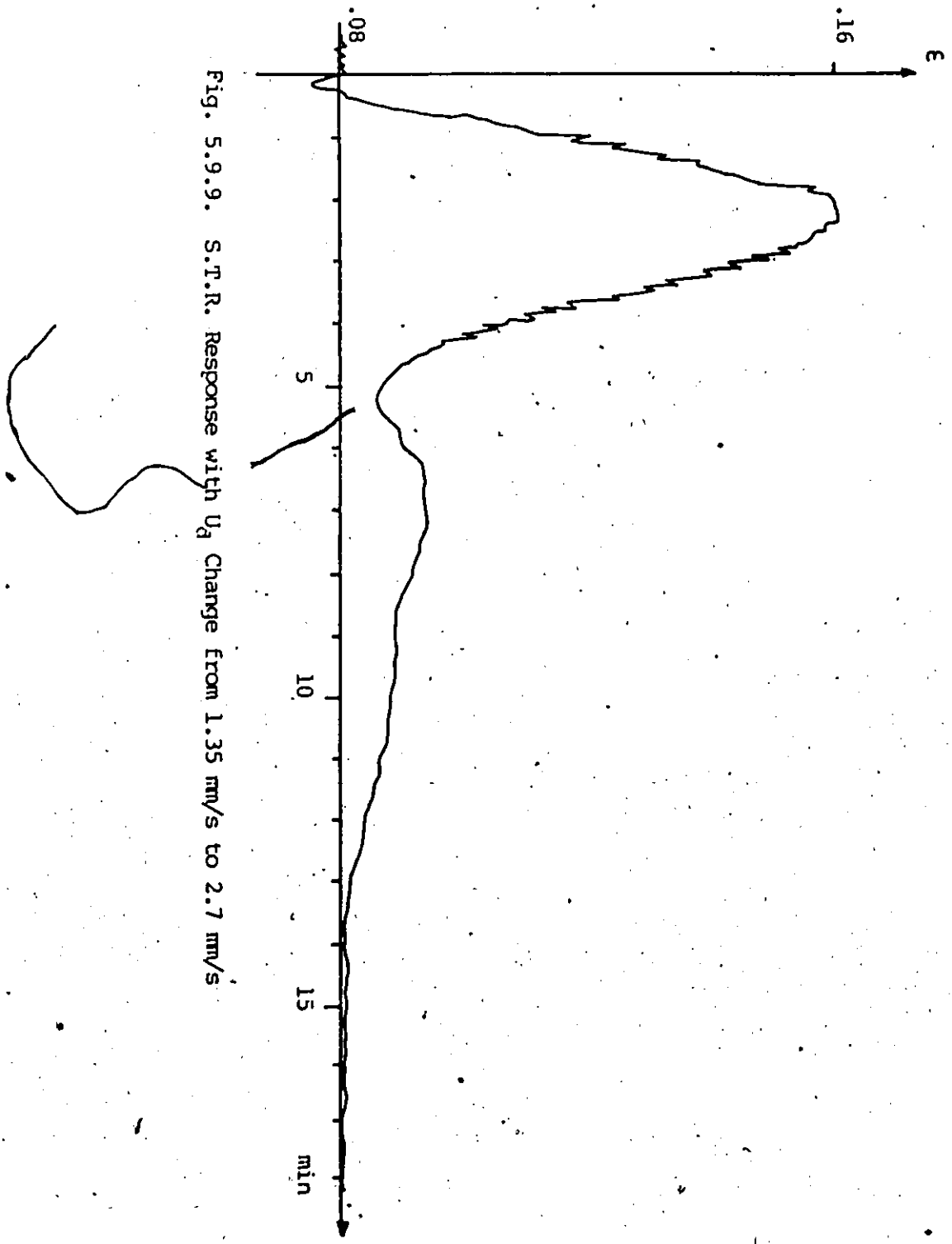

Fig. 5.9.9. S.T.R. Response with U_a Change from 1.35 mv/s to 2.7 mv/s

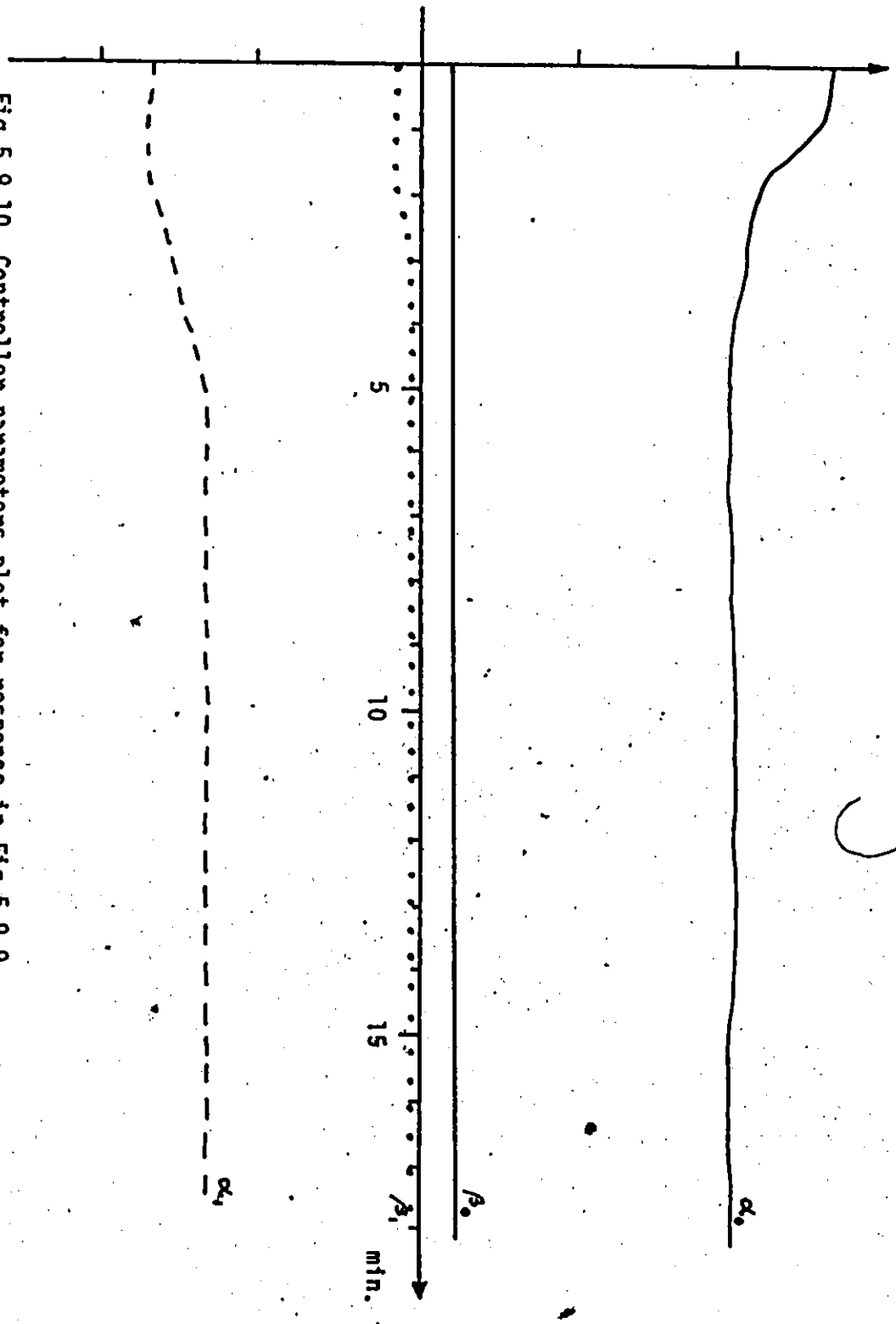

Fig 5.9.10. Controller parameters plot for response in Fig 5.9.9

ERRATA

Page]27 ,]28 and]29 are missing due to mistake in paging.

CHAPTER 6

6. EVALUATION OF THE CONTROLLERS

To find the most suitable controller for this process, which is highly non-linear, non-minimum phase and having varying dead-time, the controllers tested are compared on the basis of their servotracking and regulator performance.

6.1 COMPARISON OF THE CONTROLLERS PERFORMANCE ON SERVO PROBLEM

The controllers discussed in chapter 5 were initially compared with respect to each other's performance in a fixed operating region with set point change of $\delta\varepsilon = .03$, i.e. $\varepsilon = .02$ to $.05$ ($U_d = 1.35$ mm/s, $U_c = 0$). This is done by plotting the "best" response of each controller for the ε set point change in that region in Fig. 6.1.1. It can be seen that the best response, in terms of fastest rise time, fastest settling time and lowest % over-shoot, came from the PI controller using a feedback/feedforward on set point scheme. The next best response was obtained from the Dahlin controller. This controller can be tuned to give a response without overshoot. This is important especially when bringing ε near the flooding point, because overshoot in this case will flood the column. The M.V. controller has the third best response. Both the M.V. controller and the Dahlin controller have deadtime compensators and thus the choice of sampling time is less restrieted. The M.V. controller is optimum in the sense that it

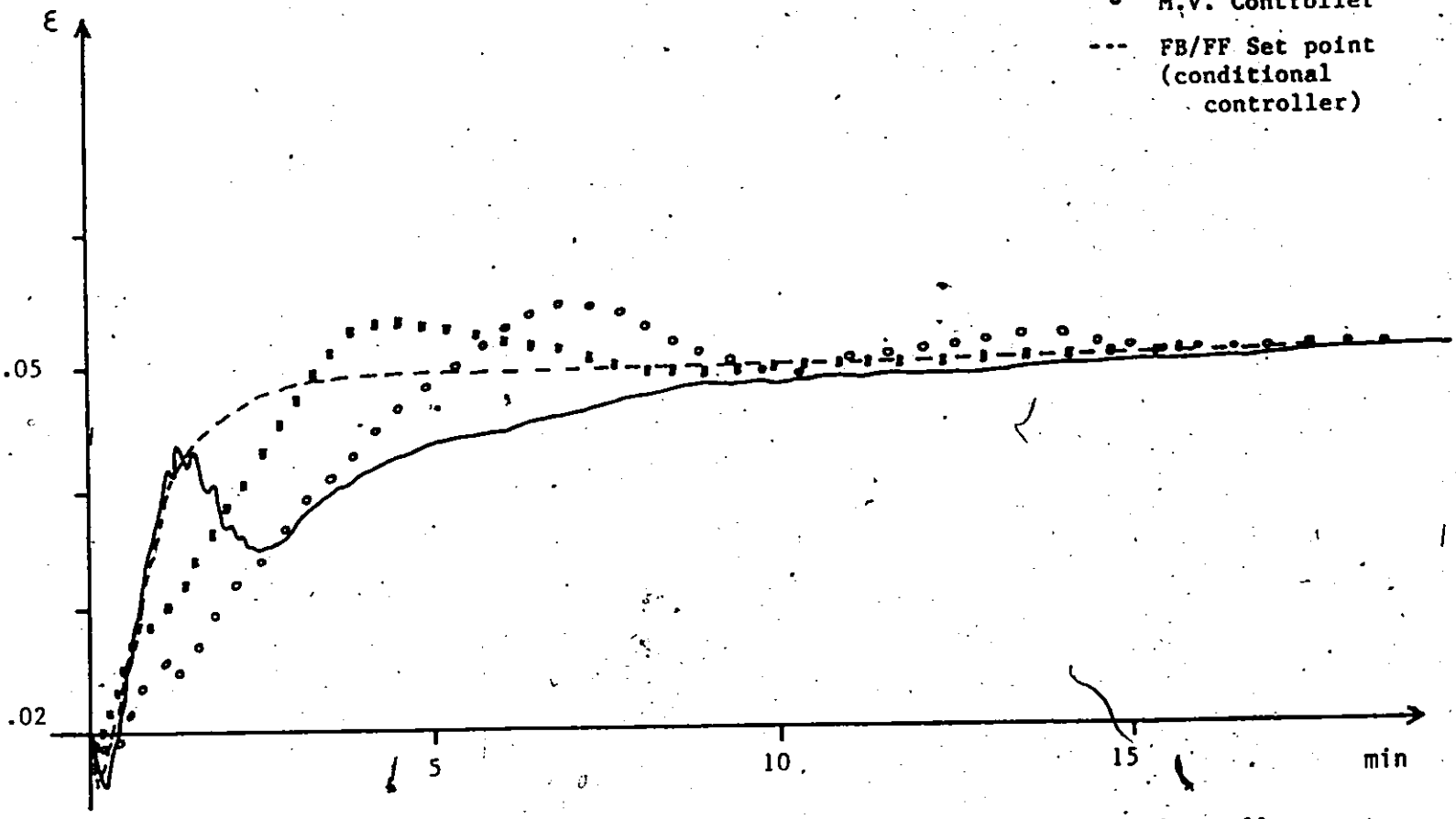

Figure 6.1.1 Comparison of Servo Performance of Various Controllers

minimized the expectation of the error term square. However, the M.V. controller used was the instantaneous minimization of error square instead of expectation of error square (referred to sec. 5.8.1). This simplified minimization could be the reason for M.V. controller having a more oscillatory response than the Dahlin controller for the same rise time. The S.T.R., since it is in nature the M.V. controller (provided the true structure m and ℓ in sec. 5.9.1 are used), behaved like the M.V. controller. But comparing the S.T.R. with other controllers at this point is not very relevant, because the parameters of the S.T.R. had not yet converged. The feedback PI controller has the most sluggish response. This is due to the deadtime of the process in frequency loop. If the PI controller was forced to give a faster response, the response would be rather oscillatory with overshoot and would be unacceptable near the flooding zone.

The performance of each controller in handling the non-linearity of the process was obtained when the controller was tested by changing the operating region and by introducing water flow. The comparison for ϵ change from .05 to .08 (using same controller used to bring ϵ from .02 to .05) is shown in Fig. 6.1.2. It can be seen that no fixed parameter controller's performance is acceptable. In this case, S.T.R. was the only controller that can adapt its parameters and brought ϵ to .08 acceptably. With water flowing, the Dahlin and M.V. controler need to be redesigned using the appropriate transfer function, whereas the feedback PI controller need only be retuned when the dynamics was very different. In handling the change of operating region none of them

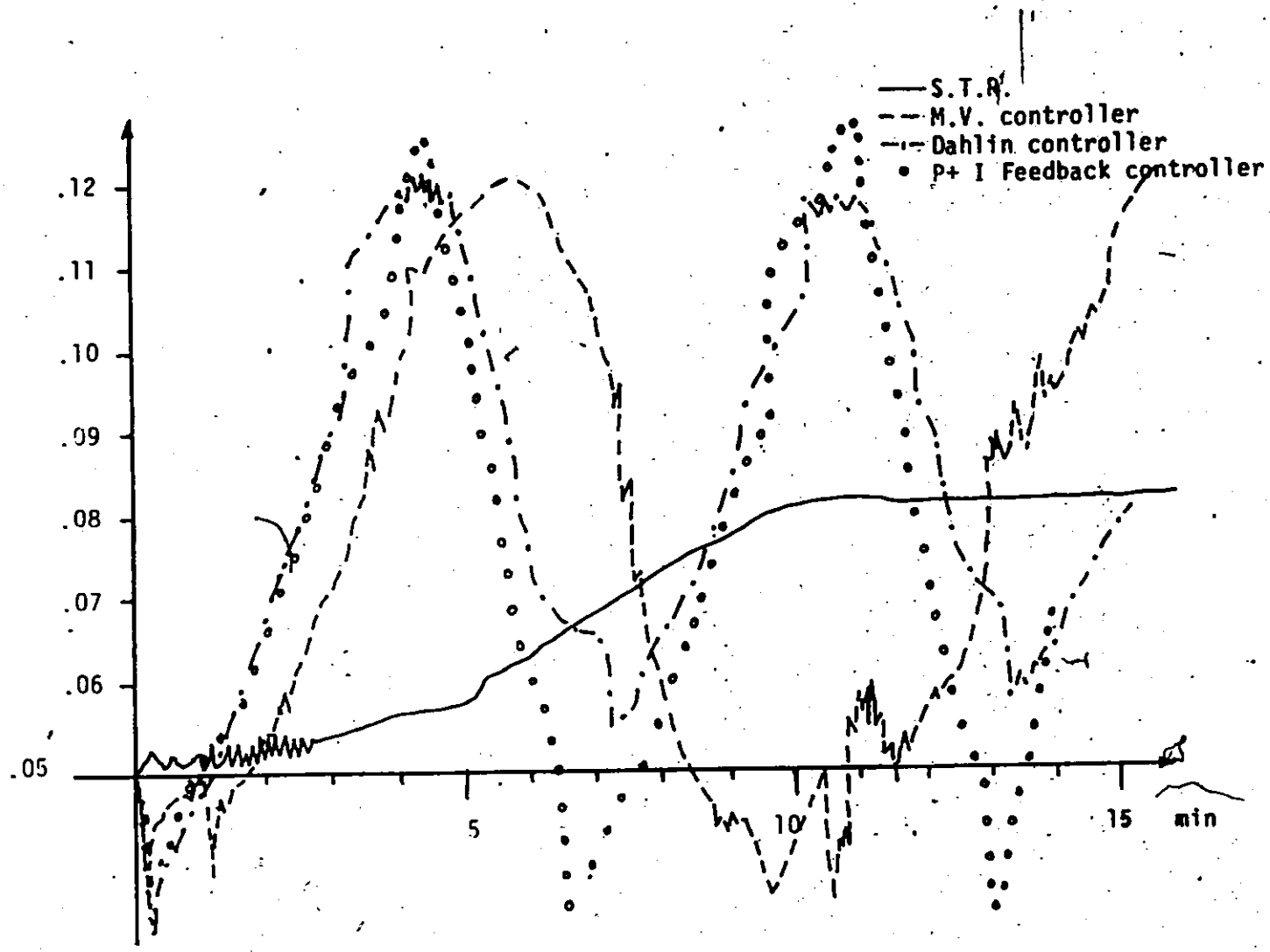

Fig 6.2.1. Comparison of perfomance of various controllers in handling non - linear region.

proved satisfactory, except S.T.R. This can be seen in Fig. 6.1.2., which shows the performance of controllers used in Fig. 6.1.1. when used to overcome ϵ set point change from .05 to .08. The S.T.R. has shown that it is the more suitable controller in the sense that it would readjust the parameters at any operating region, and it could be tuned not to give too much overshoot near the flooding point (at high ϵ). However, some restriction still needs to be imposed on the manipulated variable, the frequency. It should always be less than flooding frequency. This means that to have a practical control scheme, estimation of flooding frequency need to be done. Furthermore, due to the non-minimum phase nature of the process, the feedback only S.T.R. has a rather slow rise time. This is due to the restriction imposed on the variance of (VU_t) (see eqn. 5.9.14) in order to maintain stability. Therefore, a feedback/feedforward S.T.R. with a scheme similar to that presented on sec. 5.5. should be able to give a faster rise time. This point has been confirmed by the discussion on the performances of the controllers under fixed operating region (also see Fig. 6.1.1). The theory on the above feedback/feedforward S.T.R. scheme is available in ref [38].

6.2 COMPARISON OF VARIOUS CONTROLLERS PERFORMANCE ON REGULATOR PROBLEM

As in servo performance, the regulator performance of each controller discussed in chapter 5 is compared with those of others at U_d change of δU_d = 1.35 mm/s, i.e. U_d = 1.35 mm/s to 2.7 mm/s. The responses of the controllers in this case are superimposed on the graph

in Fig. 6.2.1. It can be seen that feedback/feedforward on disturbance has the most desirable feature, i.e. has the least integral of error ($\int_0^\infty |e|dt$) and the shortest settling time. M.V. controller, Dahlin and S.T.R. have similar responses, in that the system was brought back to the initial value without oscillation, but there was a rather large deviation. This is a typical characteristic of a feedback controller, in which correction is made only when the system deviates from its target. The deviation will also depend on the sampling time chosen and the instant the disturbance enter the ysstem. However, despite the drawback discussed above, the performances of Dahlin and M.V. controllers and S.T.R. in the regulator problem are acceptable even though they were designed for set point tracking. In contrast the feedback PI controller needed retuning, otherwise its response is unacceptable.

Since the dynamics of ε set point and U_d change are both nonlinear, a control scheme of S.T.R. with feedback/feedforward on set point and feedforward on U_d change will be the most ideal.

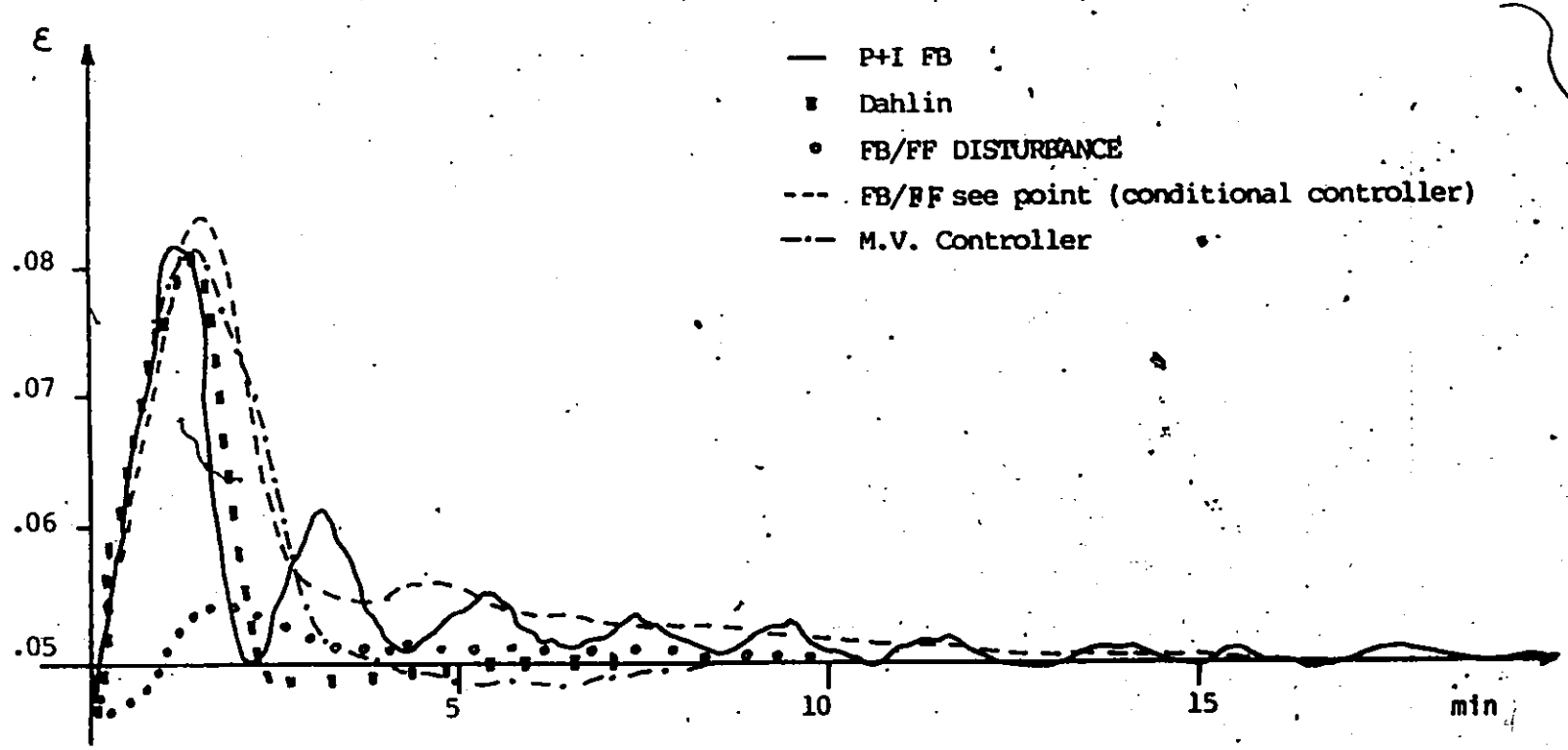

Fig. 6.2.1. Comparison of Load Handling Performance of Various Controllers

CHAPTER 7

7. CONCLUSION AND RECOMMENDATION

The best controller scheme for combined servo/regulatory problem in a fixed operating region has been found to be the feedback/feedforward on set point scheme. It gives a fast rise time for the set point tracking problem and the feedback loop can be tuned for the regulatory problem.

The Dahlin and Minimum variance controllers have been demonstrated to handle the deadtime process better than the PI controller, because they both have deadtime compensator. Therefore, they can be tuned for a faster rise time without too much overshoot. Also they can handle the regulatory problem acceptably, even though they are designed for set point tracking. The self-tuning-regulator behaves like a minimum variance controller if one uses the right structure.

The feedback only PI controller scheme as expected has either sluggish or oscillatory responses for set point changes. When the dynamics of regulatory problems is different than that of servo problem as demonstrated by this process, the PI controller needs to be retuned for regulatory problem.

However, all fixed parameter controllers (the feedback/feedforward on set point controller, Dahlin, Minimum variance and "feedback only" PI controllers) have failed to handle the non-linear dynamics of the Karr column. In the present study, the superiority of the self-

tuning-regulator in handling the non-linear dynamics of Karr column has been clearly demonstrated, in that the holdup can be moved to any desirable level without any problems. Furthermore, similarly to the Minimum variance controller, the self-tuning-regulator can be tuned not to give too much overshoot for faster rise time than PI feedback controller. This is critical when operating near the flooding region (high holdup), since overshoot will flood the column.

RECOMMENDATION

Certain improvements on this work can be suggested. Due to the nature of the non-minimum phase and flooding constraint of the column, the feedback only sefl-tuning-regulator gives rather sluggish responses. Because excessive control action will cause instability and high overshoot which will flood the column. To have a faster rise time, a feedback/feedforward self-tuning-regulator on set point is recommended.

The problem of variation of interface level, which has been ignored in this work, can be tackled by introducing an interface level controller.

The use of a metering pump for the water outlet can make the runs (with water flowing) more accurate and convenient. It should be pointed out that this pump would have to be hooked into the interface controller device.

Since the on-line measurement of holdup via differential pressure transducer is restricted to systems with constant density difference, it could only be used in dilute systems when mass transfer occurs.

Therefore, development of other less restricted on-line measurement techniques for holdup can be useful.

It will be interesting to include the mass transfer aspect of the operation in the future work. In this case a cascade control scheme which uses the concentration outer loop to monitor the inner holdup loop can be implemented.

REFERENCES

1. Treybal, R.E., "Liquid Extraction", McGraw Hill, 1951.

2. Bailes et al, Chemical Engineering, Jan. 19th. 1976.

3. Rushton, J.H., Symposium on relationship between pilot-scale and commercial Chem. Eng. Equipment, Am. Inst. Chem. Eng. White Sulfur Springs (March, 1951).

4. Wiegandt, H.F. and R.C. Von Berg, Chem. Eng., 61 (July, 1954).

5. Thornton, J.D., Chem. Eng. Progr., Symp. Ser. No. 13, 50, (1954).

6. Woodfield, F.W. and G. Sege, Chem. Eng. Progr. Symp. Ser. No. 13, 50, 14 (1954).

7. Wellek R.M., Ozsoy, M.V., Carr J.J., Thompson D. and Konkle T.V., Ind. Engng Chem. Proc. Des. Dev. 1969, 8 515.

8. Karr, A.E., A.I.Ch.E. Journal 5, p. 446, (1956).

9. Lo, T.C. and Karr, A.E., Ind. Eng. Chem. process Des. Dev. 11, 495, (1972).

10. Karr, A.E., Separation Science and Technology, 15(14) p. 877 (1980).

11. Baird, M.H.I., McGinnis, G.C. and Tan, G.C., Proc. Intl. Solvent Extn. conference, Society of Chem. Industry, The Hague, April 1971, p.251.

12. Baird, M.H.I. and Lane, S.J., Chem. Eng. Sci. 28, 947 (1973).

13. Karr, A.E. and Lo, T.C., Proc. Int. Sovent Extraction Conf., The Hague, 1971, p.299 (Soc. Chem. Ind., London, 1971).

14. Karr, A.E. and Lo, T.C., paper presented at AIChE 82nd. National metting, Atlantic City, N.J., Aug. 29 - Sept. 1, 1976, Chem. Eng. Progr. 72 (11), 68 (1976).

15. Hafez, M.M., Baird, M.H.I. and Nirdosh, J., Can. J. Chem. Eng. 57, 150 (1979).

16. Thornton, J.D., Chem. Eng. Sci. 5, 201 (1956).

17. Jiricny, V., Prochazka, J., Chemical Eng. Science 35, p.2237, (1980).

18. Pollock, G.G. and Johnson, A.I., "Ion Exchange and Solvent extraction", A series of advances, vol. 6, Chapter 2 (1974).

19. Wilkinson W.l., and Ingham, J. Chapter submitted for Solvent Extraction Handbook, (Wiley-Interscience to be published, 1982).

20. McDonald, C.R., Wilkinson, W.L., Proc. Intl. Solv. Extr. Conf. (ISEC'74) 3, 2608 (1974).

21. Hafez, M.M. and Baird, M.H.I., Trans. IchemE, Vol. 56, p.229 1978.

22. "Programming in MACBASIC: Introduction to MACBASIC and ADVANCED MACBASIC", Analog Devicer, Inc., Measurement and control product Div. (1979).

23. Berlin, Howard M., "The Design of Active Filters with Experiments.

24. Smith, "Digital Computer Process Control", Index Educational publishers.

25. Tao, "Digital and Sampled - Data control systems",

26. Box, G.E.P. and Jenkins, G.M. "Time series Analysis: Forcasting and Control", Holdenday, 1976.

27. Astrom, K.J., "Introduction to stochastic control theory", Academic press, 1970.

28. Astrom, K.J. and Wittenmark, B., Automatica 9, p.185-199, (1973).

29. Astrom, K.J. and Wittenmark, B., IFAC Symposium on Stochastic control, p.165-173, (1974).

30. Astrom, K.J., Borrison, U, Ljung, L. and Wittenmark, B., Automatica 13, p.457-476, (1976).

31. Clark, D.W. and Hasting-James, R. (1971), proc. IEE 118 p.1503-1506.

32. Clark, D.W. and Gawthrop, B.A., Proc. IEE 122, p.929-934, (1973).

33. MacGregor, J.F. and Tidwell, P., Proc. IEE 124, p.732-734 (1977).

34. Sodestrom, Gustorsson and Ljung, IEEE Trans. AC-19, p.836 (1974).

35. Sodestrom, Gustorsson and Ljung, IEEE Trans. AC-22, p.837, (1976).

36. Sodestrom, Gustorsson and Ljung, Int. J. Control 21, P.243 (1975).

37. Box, G.E.P. and MacGregor, J.F., Technometrics 16, p.391, (1974).

38. Box, G.E.P. and MacGregor, J.F., Technometrics 18, p.371 (1976).

39. Wellstead, P.E. and Zanker, P., Int. J. Control, vol. 30, No.1, 27-36 (1979).

40. Baird, M.H.I., private communication, Feb. 1981.

APPENDIX A

A filter to filter the lowest frequency of 1.3 Hz and to retain the signal having frequency of about .04Hz ($\tau = \frac{1}{5} * 100$ sec, 100 sec for the system to read steady state) is needed.

A fourth order Butterworth, low pass filter with cut off frequency equal to .25 Hz was designed for this purpose. The circuit for 4th order filter is presented as follows:

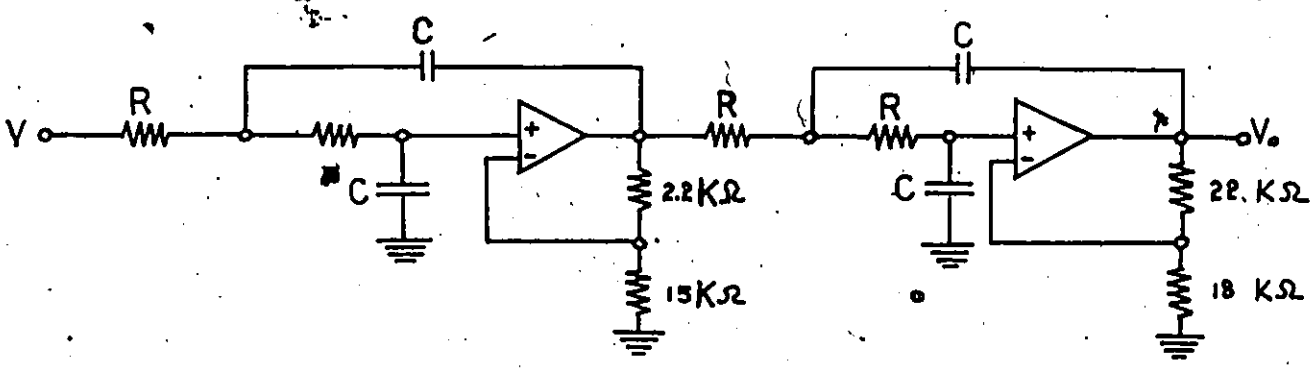

$$\text{The Amplitude ratio} = \text{A.R.} = \frac{1}{\sqrt{(1 + (\frac{\omega}{\omega c})^{2N}}}$$

where N = 4 in this case

$$\omega c = \frac{1}{RC} \text{ or } fc = \frac{1}{2\pi RC}$$

The overall gain is a function of the damping coefficients. For a fourth order filter = 2.57.

$$fc = \frac{1}{2\pi RC}$$

using C = 1 μF

$$R = \frac{10^6}{2\pi \cdot fc} = 636619.77\ \Omega$$

680 KΩ is the nearest preferred; hence

$$fc = \frac{1}{2\pi\ (10^{-6})(680*10^3)} = 0.234\ \text{Hz}$$

To check numerically if the designed filter is acceptable, using fc = .234 Hz, c = 1 μF and R = 680 KΩ, the input frequency of 1.5 Hz and .04 Hz were used to calculate the A.R. It shows that:

Input frequency	A.R.
1.5 Hz	.00059
.04 Hz	.9999996

Thus this fourth order Butterworth filter is considered adequate for the purpose.

APPENDIX B

Consider a Karr column arrangement as Fig. (3.1). We are interested in frictional effects on Δp as distinct from hydrostatic effects.

The theoretical predictions on frictional Δp are developed for the 3 possible cases of interest[40]:

Case 1: Plate oscillation in the absence of flow.

For one phase (water) filling the systems, with zero net flow, we would expect that the time-averaged pressure drop $\bar{\Delta p}$ would be zero with a symmetrical wave-form; the motion is equally up and down.

However, the pressure at point 1 will be less than $(P_2 - \rho gh)$ because the liquid in the column is in motion (dynamic pressure).

Let liquid velocity = u(t), plate velocity = U. From Bernouilli's theorem, dynamic pressure:

$$\Delta P_d = \frac{1}{2} \rho u^2 \qquad (B.1)$$

The indicated pressure at point 1 will be reduced by this amount. The liquid velocity is calculated by displacement through the plates given the fractional open area σ. Since there is zero net flow,

$$U(1 - \sigma) + u \sigma * C_o = 0$$

$$u = - U\left(\frac{1 - \sigma}{C_o \sigma}\right) \qquad (B.2)$$

Substitute eqn (B.2) into (B.1), gives:

$$\Delta P_d = \frac{1}{2} \rho U^2 \left(\frac{1 - \sigma}{c_o \sigma}\right)^2$$

Now, $U = A\omega \sin \omega t$

Thus, $\overline{\Delta P}_d = \frac{1}{2} \rho A^2 \omega^2 \left(\frac{1 - \sigma}{c_o \sigma}\right)^2 \overline{\sin^2 \omega t}$

It can be shown that $\overline{\sin^2 \omega t} = \frac{1}{2}$

Therefore, $\overline{\Delta P}_d = \frac{1}{4} \rho A^2 \omega^2 \left(\frac{1 - \sigma}{c_o \sigma}\right)^2$

Case 2: Continuous phase flow, with plate oscillation

Let the superficial velocity of the water be U_c and let the actual velocity of water through the holes be U_h. The pressure drop per plate can be calculated assuming complete loss of kinetic energy:

$$\frac{-\Delta P}{n} = \frac{1}{2} \rho_c (U_h^2 - U_c^2) \qquad (B.3)$$

By the continuity equation,

$$U_c = \sigma U_c \qquad (B.4)$$

Hence, eqn (C.3) becomes:

$$\frac{-\Delta P}{n} = \frac{1}{2} \rho \left(\left(\frac{U_c}{\sigma}\right)^2 - U_c^2\right)$$

$$\frac{-\Delta P}{n} = \frac{1}{2} \rho_c U_c^2 \left(\frac{1 - \sigma^2}{\sigma^2}\right) \qquad (B.5)$$

In practice, orifice flows usually involve a contraction with increases the pressure drop, and we rewrite eqn (B.5) as:

$$-\Delta P = \frac{\frac{1}{2} n \rho_c U_c^2}{C_o^2} \frac{1 - \sigma}{\sigma^2} \qquad (B.6)$$

Case 3 Continuous phase flow, with plate oscillation

Let the plate displacement be: $y = a \sin \omega t$ where a = amplitude; w = angular frequency = $2\pi f$. The plate velocity is therefore

$$\dot{y} = a \omega \cos \omega t \qquad (B.7)$$

Consider the continuity of flow of water between the open column and a section adjacent to a plate:

$$\dot{y} (1 - \sigma) + \sigma U_h = U_c \qquad (B.8)$$

The instantaneous pressure drop will consist of a frictional component plus an inertial component due to the acceleration of the flow.

The flow accelerates alternately in opposite directions, so the time-averaged inertial pressure is neglected, but we are interested in the time-averaged frictional pressure.

Equation (B.6) can not be applied in the same form to the oscillating plate situation, because the sign of the Δp will depend on the sign of the velocity U_h. Therefore we must write:

$$\frac{-\Delta P}{n} = \frac{1}{2} \rho_c (U_h |U_h| - U_c^2) \qquad (B.9)$$

From eqn (B.7) and (B.8), one gets

$$U_h = (U_c - y(1 - \sigma)/\sigma$$

$$= (U_c - A w \cos \omega t (1 - \sigma)/\sigma$$

$$U_h = U_c (1 - V \cos \omega t)/\sigma \qquad (B.10)$$

where $V = A \omega (1 - \sigma)/U_c$

Substituting eqn. (C.10) into (C.9), gets:

$$\frac{-\Delta P}{n} = \frac{1}{2} \rho_c U_c^2 \left\{ \frac{(1 - V \cos \omega t)\,|1 - V \cos \omega t|}{\sigma^2} - 1 \right\} \qquad (B.11)$$

The time-averaged frictional pressure drop is thus:

$$\overline{-\Delta P} = \frac{\frac{1}{2} n \rho_c U_c^2}{c_o^2} \left\{ \frac{\overline{(1 - V \cos \omega t)\,|1 - V \cos \omega t|}}{\sigma^2} - 1 \right\} \qquad (B.12)$$

Special case of small oscillations

Consider $V < 1$, in this case, U_h is always positive and the modulus expression (eqn B.9) is not needed. Then eqn (B.9) can simply be written as:

$$\frac{\overline{-\Delta P}}{n} = \frac{1}{2} \rho_c \overline{\{U_h^2 - U_c^2\}}$$

$$= \frac{1}{2} \rho_c U_c^2 \left\{ \frac{\overline{(1 - V \cos \omega t)^2}}{\sigma^2} - 1 \right\} \qquad (B.13)$$

The time-averaged value of $(1 - V \cos \omega t)^2$ is:

$$\overline{1 - 2 V \cos \omega t + V^2 \cos^2 \omega t} = 1 + V^2/2 \qquad (B.14)$$

Hence, from (B.13), again inserting the orifice factor and rearranging

$$\overline{-\Delta P}_f = \frac{\frac{1}{2} n \rho_c U_c^2}{c_o^2} \left\{ \frac{1 - \sigma^2}{\sigma^2} + \frac{V^2}{2\sigma^2} \right\} \qquad (B.15)$$

APPENDIX C
OPEN LOOP RESPONSES

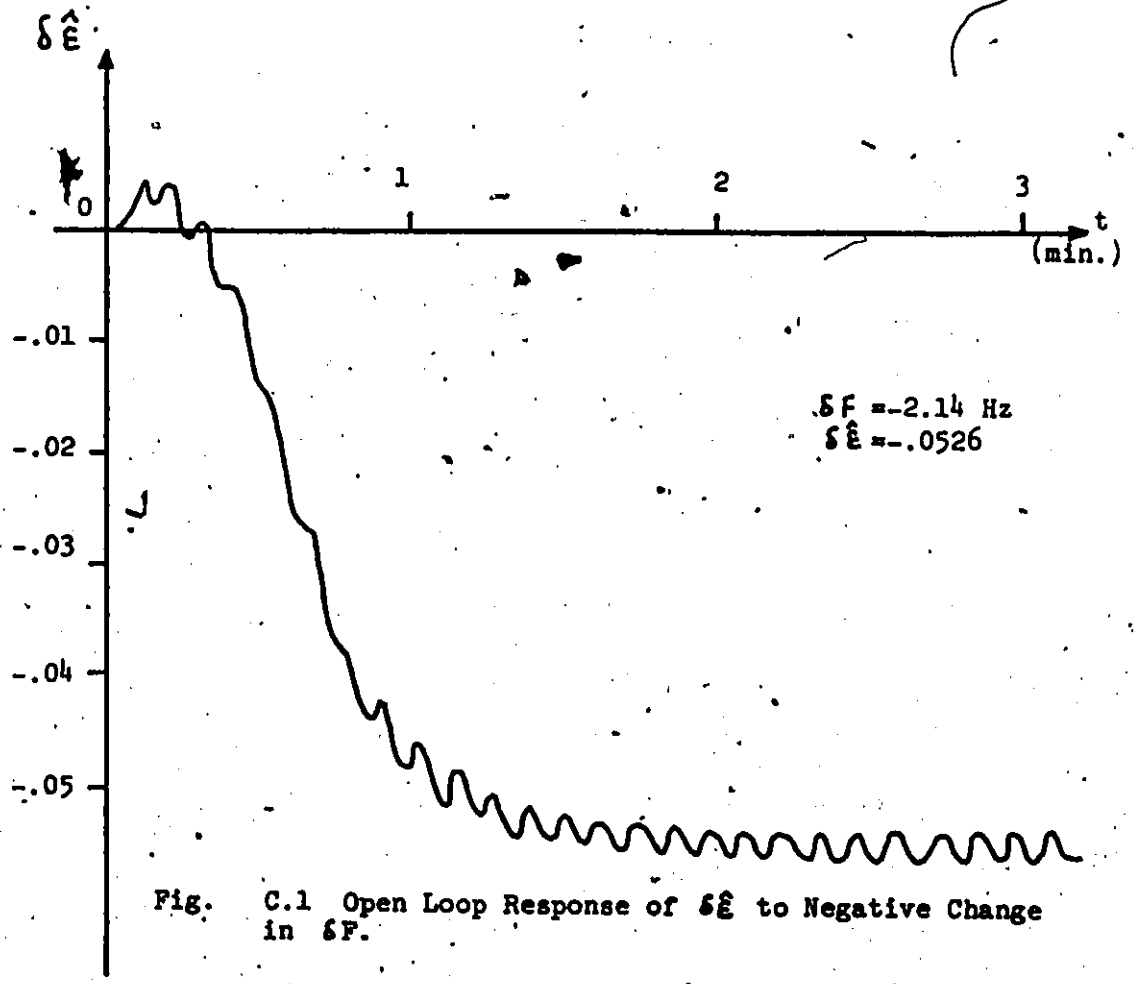

Fig. C.1 Open Loop Response of $\delta\hat{E}$ to Negative Change in δF.

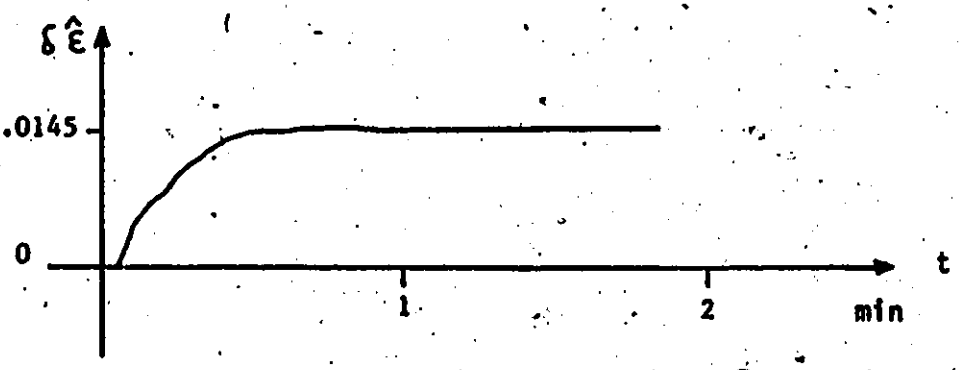

Fig. C.2 Open Loop Response of δUd to Positive Change in δF

APPENDIX D
COMPUTER PROGRAM

APPENDIX D.1

Program For Implementing P & I Controller

```
 10 OPENW :5 "$QTO:0"
 20 DIM F(300)
 30 REM U1=UO,FLOW,H1=HOLDUP SET POINT,T=PROCESS TIME CONSTANT
 40 REM T1=SAMPLING TIME,N1=WHOLE PERIOD OF DELAY
 50 REM L7=TUNING CONSTANT OF DAHLIN CONTROLLER
 60 INPUT "U1="U1
 70 INPUT "H1="H1
 80 INPUT "T="T
 90 INPUT "T1="T1
100 INPUT "N1,TIME DELAY="N1
110 INPUT "LAMDA="L7
120 TASK 2,200
130 ACTIVATE 2
140 WAIT (55.)
150 BREAK
160 TASK 1,370
170 ACTIVATE 1
180 END
190 REM INITIALIZATION OH THE TRANSDUCER'S SIGNAL
200 N=0
210 FOR I=1 TO 10
220   N=AIN(14,0)+N
240 NEXT I
250 S=N/10.
260 PRINT "S=",S;"H="
270 END
280 REM CONTROL PROGRAM BEGINS
290 REM INITIALIZE THE FREQUENCY MEASUREMENT
300 F9=0
310 FOR I=1 TO 10
320   F9=AIN(14,7)+F9
330 NEXT I
340 F9=F9/10
350 C=.72*F9
370 A2=.01275
380 U2=0.
390 K=.014
400 REM SET UP DELAY
410 N=N1+1
420 FOR I=1 TO N
430   F(I)=C
440 NEXT I
450 P=EXP(-T1/L7)
460 A=EXP(-T1/T)
470 B=1./(K*(1.-A))
```

```
480 M=N+1
490 F2=C
500 I=M
510 X=AIN(14,0)
520 X1=X-S
530 A1=A2*F(I)
540 V=1./.000861*X1
550 REM CALCULATE HOLDUP FROM DP SIGNAL
560 H=.00023*V+2.289*U1-2.*U2-.016*A1+.00476
570 IF I>M THEN  GOTO 590
580 E0=H1-H
590 E1=H1-H
600 REM CONTROLLER
610 F(I)=(1.-P)*B*(E1-A*E0)+P*F(I-1)+(1.-P)*F(I-N)
620 REM LIMITS ONMAX AND MIN FREQUENCY
630 IF F(I)>4.75 THEN  F(I)=4.75
640 IF F(I)<1.33 THEN  F(I)=1.33
650 IF M6<0 THEN  Y=0
720 IF M6>0 THEN  Y=1
740 X5=111 *M5
750 X5'=X5
770 FOR J=1 TO X5'
780   DOT(15,0,9)=1
790   DOT(15,8,9)=1+Y*2
800   IF AIN(14,6)>2.5 GOTO 800
810   DOT(15,0,9)=0
820 NEXT J
830 REM GET THE FREQUENCY MEASUREMENT
840 F9=0
850 FOR J=1 TO 10
860   F9=AIN(14,7)+F9
870 NEXT J
880 F9=F9/10
890 F8=.72*F9
910 E0=E1
920 F2=F(I)
930 I=I+1
940 WAIT (T1)
950 GOTO 510
```

APPENDIX D.2

Program for Implementing FB/FF Controller on Set Point Change in ϵ

```
 10 OPENW :5 "$QTO:0"
 20 PNT :5 27
 30 WAIT (1.)
 40 PNT :5 17
 50 WAIT (.5)
 60 DIM H1(200),R(200)
 65 REM K=PROPORTIONAL GAIN,K1=PROCESS GAIN
 66 REM T1=SAMPLING TIME,T2=RESET TIME,H3=HOLDUP SET POINT
 70 INPUT "K="K
 80 INPUT "K1="K1
 90 INPUT "T1="T1
100 INPUT "T2="T2
110 INPUT "H3="H3
120 TASK 2,180
130 ACTIVATE 2
140 BREAK
150 TASK 1,260
160 ACTIVATE 1
170 END
175 REM INITIALIZATION OF THE TRANSDUCER'S SIGNAL
180 N=0.
190 FOR I=1 TO 10
200   N=AIN(14,0)+N
210   PRINT "N=",N
220 NEXT I
230 S=N/10.
240 PRINT "S=",S;"TASK 2 TERMINATED"
250 END
255 REM CONTROL PROGRAM START
260 A=.01275
270 U1=.00135
280 U2=0.
285 REM GET INITIAL FREQUENCY
290 F9=0
300 FOR I=1 TO 10
310   F9=AIN(14,7)+F9
320 NEXT I
330 F9=F9/10
340 C=.72*F9
350 F=C
360 PRINT :5 "F INIT =",C
370 B=-1./33*T1
380 P=EXP(B)
390 M=1.-15./T1
400 M1=-1./33*T1*M
```

```
410 Q=EXP(M1)
420 L6=1.-Q
430 L7=Q-P
435 REM INITIALIZATION OF SET POINT H1
440 FOR I=3 TO 200
450   H1(I)=H3
460 NEXT I
470 J=3.
480 L=1-P
490 I=0.
500 X=AIN(14,0)
510 X1=X-S
520 V=1./.000861*X1
530 A1=A*F
535 REM CALCULATE HOLDUP FROM DP SIGNAL
540 H=.00023*V+2.289*U1-2.*U2-.016*A1+.00476
550 IF J>3 THEN  GOTO 590
560 R(2)=H
570 H1(2)=H
580 H1(1)=H
585 REM SET POINT MODIFICATION
590 R(J)=L6*H1(J-1)+L7*H1(J-2)+P*R(J-1)
600 E=R(J)-H
610 I=I+E*T1/T2
615 REM CALCULATE THE FEED-BACK ACTION F1
620 F1=K*(E+I)+C
630 IF J>3. THEN  GOTO 650
635 REM CALCULATE FEED-FORWARD COMPENSATOR FOR SET POINT F2
640 F2=1./K1*(H3-H)
650 F3=F1+F2
660 J=J+1
665 REM LIMITS ON MAX AND MIN OF FREQUENCY
670 IF F3>4.75 THEN  F3=4.75
680 IF F3<1.25 THEN  F3=1.25
690 PRINT :5 "F=",F3;"H=",H;"F1=",F1;"F2=",F2
700 PRINT "F3=",F3;"X1=",X1;"H=",H;"F1=",F1;"F2=",F2
705 REM PLOT CONTROLLER'S OUTPUT ON CHART RECORDER
710 AOT(13,0)=F3
715 REM OUTPUT TO STEPPING MOTOR
720 M5=F3-F
730 IF M5>0 THEN  Y=1
740 IF M5<0 THEN  Y=0
750 F4=ABS(M5)
760 X5=111*F4
770 X5'=X5
780 FOR I1=1 TO X5'
790   DOT(15,0,9)=1
800   DOT(15,8,9)=1+Y*2
```

```
810   IF AIN(14,6)>2.5 GOTO 810
820   DOT(15,0,9)=0
830 NEXT I1
835 REM GET THE MEASUREMENT OF FREQUENCY
840 F9=0
850 FOR I1=1 TO 10
860   F9=F9+AIN(14,7)
870 NEXT I1
880 F9=F9/10
890 F8=.72*F9
900 PRINT :5 "ACT F=",F8
910 F=F3
920 WAIT (T1)
930 GOTO 500
```

APPENDIX D.3

Program for Implementing FB/FF controller on Disturbance

```
 10 OPENW :5 "$QTO:0"
 20 PNT :5 27
 30 WAIT (1.0)
 40 PNT :5 17
 50 WAIT (.5)
 52 REM T1=SAMPLING TIME,U0=UD OLD,U9=UD NEW
 53 REM KC=PROPORTIONAL GAIN,T2=RESET TIME
 54 REM T3,T4=PROCESS OLD ,AND NEW TIME CONSTANTS
 55 REM K3,K4=PROCESS OLD AND NEW GAINS
 60 INPUT "T1="T1
 70 INPUT "U0="U0
 80 INPUT "U9="U9
 90 INPUT "KC="K
100 INPUT "T2="T2
110 INPUT "T3="T3
120 INPUT "T4="T4
130 INPUT "K3="K3
140 INPUT "K4="K4
150 TASK 2,210
160 ACTIVATE 2
170 BREAK
180 TASK 1,300
190 ACTIVATE 1
200 END
205 REM INITIALIZATION OF TRANSDUCER'S SIGNAL
210 N=0
220 FOR I=1 TO 10
230   N=AIN(14,0)+N
240   WAIT (.1)
250   PRINT "N=",N
260 NEXT I
270 S=N/10
280 PRINT "S=",S
290 END
295 REM CONTROL PROGRAM BEGINS
300 A1=.01275
310 PRINT : 5 "KC=",K; "TS=",T1;"TI=",T2
320 U7=U0
330 U8=0
340 A=-T1/T3
350 O=EXP(A)
360 B=-T1/T4
370 P=EXP(B)
380 M=1-O
390 N=1-P
```

```
400 L=O*P
410 DOT(15,0,9)=0
415 REM GET THE INITIAL FREQUENCY MEASUREMENT
420 F9=0
430 FOR J=1 TO 10
440   F9=F9+AIN(14,7)
450 NEXT J
460 F8=F9/10
470 C=.72*F8
480 PRINT "F INIT=",C
490 F2=C
500 K1=-K4/K3
510 X=AIN(14,0)
520 X1=X-S
530 V=1/.000861*X1
540 A6=A1*F2
545 REM GET HOLDUP FROM DP MEASUREMENT
550 H1=.00023*V+2.289*U7-2*U8-.016*A6+.00476
560 U2=U9-U0
570 U1=U0-U8
580 L6=N*U2
590 I=0
600 L7=(L-O)*U1
605 REM CALCULATE FEED-FORWARD COMPENSATOR F1
610 F1=K1/M*(L6+L7)
620 K2=(L-P)/(1-O)
630 F1=F1-K2*(F2-C)+C
640 X=AIN(14,0)
650 X1=X-S
660 V=1/.000861*X1
670 A6=A1*F2
680 H=.00023*V+2.289*U7-2. *U8-.016*A6+.00476
690 PRINT "H1=",H1;"H=",H
700 PRINT :5 "F INIT=",C;"H1=",H1;"H=",H
710 E=H1-H
720 I=I+E*T1/T2
725 REM CALCULATE FEED-BACK CONTROLLER'S ACTION F3
730 F3=K*(E+I)
740 F4=F1+F3
745 REM LIMITS ON MAX AND MIN FREQUENCY
750 IF F4>4.75 THEN  F4=4.75
760 IF F4<1.25 THEN  F4=1.25
770 PRINT "F4=",F4
775 REM PLOT CONTROLLER'S OUTPUT ON CHART RECORDER
780 AOT(13,0)=F4
785 REM OUTPUT TO STEPPING MOTOR
790 M5=F4-F2
800 IF M5>0 THEN  Y=1
810 IF M5<0 THEN  Y=0
820 F3=ABS(M5)
830 X5=111*F3
```

```
840 X5'=X5
850 PRINT "X5=",X5'
860 FOR J=1 TO X5'
870   DOT(15,0,9)=1
880   DOT(15,8,9)=1+Y*2.5
890   IF AIN(14,6)>2.5 THEN  GOTO 890
900   DOT(15,0,9)=0
910 NEXT J
915 REM GET FREQ MEASUREMENT
920 F9=0
930 FOR J=1 TO 10
940   F9=F9+AIN(14,7)
950 NEXT J
960 F9=F9/10
970 F5=.72*F9
980 PRINT "AVT F=",F5
990 PRINT :5 "F=",F4;"F ACT =",F5
1000 PRINT "-----------------------------------"
1010 PRINT :5 "-----------------------------------"
1020 F2=F4
1030 U1=U2
1040 WAIT (T1)
1050 GOTO 600
```

APPENDIX D.4

Program for Implementing Dahlin Controller

```
 10 OPENW :5 "$QTO:0"
 20 DIM F(300)
 30 REM U1=UD FLOW,H1=HOLDUP SET POINT,T=PROCESS TIME CONSTANT
 40 REM T1=SAMPLING TIME,N1=WHOLE PERIOD OF DELAY
 50 REM L7=TUNING CONSTANT OF DAHLIN CONTROLLER
 60 INPUT "U1="U1
 70 INPUT "H1="H1
 80 INPUT "T="T
 90 INPUT "T1="T1
100 INPUT "N1,TIME DELAY="N1
110 INPUT "LAMDA="L7
120 TASK 2,200
130 ACTIVATE 2
140 WAIT (55.)
150 BREAK
160 TASK 1,370
170 ACTIVATE 1
180 END
190 REM INITIALIZATION OH THE TRANSDUCER'S SIGNAL
200 N=0
210 FOR I=1 TO 10
220   N=AIN(14,0)+N
230   PRINT "N=",N
240 NEXT I
250 S=N/10.
260 PRINT "S=",S;"TASK 2 TERMINATED"
270 END
280 REM CONTROL PROGRAM BEGINS
290 REM INITIALIZE THE FREQUENCY MEASUREMENT
300 F9=0
310 FOR I=1 TO 10
320   F9=AIN(14,7)+F9
330 NEXT I
340 F9=F9/10
350 C=.72*F9
360 PRINT "F INIT=",C
370 A2=.01275
380 U2=0.
390 K=.014
400 REM SET UP DELAY
410 N=N1+1
420 FOR I=1 TO N
430   F(I)=C
440 NEXT I
450 P=EXP(-T1/L7)
```

```
460 A=EXP(-T1/T)
470 B=1./(K*(1.-A))
480 M=N+1
490 F2=C
500 I=M
510 X=AIN(14,0)
520 X1=X-S
530 A1=A2*F(I)
540 V=1./.000861*X1
550 REM CALCULATE HOLDUP FROM DP SIGNAL
560 H=.00023*V+2.289*U1-2.*U2-.016*A1+.00476
570 IF I>M THEN  GOTO 590
580 E0=H1-H
590 E1=H1-H
600 REM CONTROLLER
610 F(I)=(1.-P)*B*(E1-A*E0)+P*F(I-1)+(1.-P)*F(I-N)
620 REM LIMITS ONMAX AND MIN FREQUENCY
630 IF F(I)>4.75 THEN  F(I)=4.75
640 IF F(I)<1.33 THEN  F(I)=1.33
650 PRINT "H=",H;"E0=",E0;"E1=",E1;"F=",F(I)
660 M6=F(I)-F2
670 REM PLOT CONTROLLER'S OUTPUT ON CHART RECORDER
680 AOT(13,0)=F(I)
690 REM OUTPUT TO THE STEPPING MOTOR
700 M5=ABS(M6)
710 IF M6<0 THEN  Y=0
720 IF M6>0 THEN  Y=1
730 PRINT "Y=",Y
740 X5=111 *M5
750 X5'=X5
760 PRINT "X5=",X5'
770 FOR J=1 TO X5'
780   DOT(15,0,9)=1.
790   DOT(15,8,9)=1+Y*2
800   IF AIN(14,6)>2.5 GOTO 800
810   DOT(15,0,9)=0
820 NEXT J
830 REM GET THE FREQUENCY MEASUREMENT
840 F9=0
850 FOR J=1 TO 10
860   F9=AIN(14,7)+F9
870 NEXT J
880 F9=F9/10
890 F8=.72*F9
900 PRINT "F=",F8
910 E0=E1
920 F2=F(I)
930 I=I+1
940 WAIT (T1)
950 GOTO 510
```

APPENDIX D.5

Program for Implementing Minimum Variance Controller

```
 10 OPENW :5 "$QTO:0"
 20 PNT :5 27
 30 WAIT (1.)
 40 PNT :5 17
 50 WAIT (.5)
 53 REM L7=TUNING CONSTANT (CONSTRAINT),H1=HOLDUP SET POINT
 55 REM K=PROCESS GAIN,T=PROCESS TIME CONSTANT,TS=SAMPLING TIME
 60 INPUT "L7="L7
 70 INPUT "H1="H1
 80 INPUT "K="K
 90 INPUT "T="T
100 INPUT "TS="T1
110 INPUT "C="C
120 TASK 2,180
130 ACTIVATE 2
140 BREAK
150 TASK 1,270
160 ACTIVATE 1
170 END
175 REM INITIALIZE THE TRANSDUCER'S SIGNAL
180 N=0
190 FOR I=1 TO 10
200   N=N+AIN(14,1)
210   WAIT (.2)
220   PRINT "N=",N
230 NEXT I
240 S=N/10
250 PRINT "S=",S
260 END
265 REM CONTROL PROGRAAM START
270 A=.01275
280 B=-T1/T
290 D=EXP(B)
300 C1=5./T1
310 L=1.-C1
320 W0=K*(1.-(D^L))
330 W1=K*(D-(D^L))
335 REM GET INITIAL FREQUENCY
340 B1=0
350 FOR I= 1 TO 10
360   B1=B1+AIN(14,7)
370 NEXT I
380 B3=B1/10
390 F8=.72*B3
400 PRINT "F8=",F8
```

```
410 PRINT :5 "INITIAL F=",F8
420 U1=.00135
430 U2=.0035
440 F=F8
450 D2=0
455 REM,CONTROLLER IS ON
460 FOR J=2 TO 300
470   A1=A*F
480   X=AIN(14,1)
490   PRINT "X=",X
500   X1=X-S
510   V=1./.000861*X1
515   REM CALCULATE HOLDUP FROM DP MEASUREMENT
520   H=.00023*V+2.289*U1-2.*U2-.016*A1+.00476
530   IF J>2 THEN  GOTO 550
540   Y1=0
550   Y2=H-H1
560   S1=W1+L7*D
570   D2=1./(W0+L7)*(-Y2+D*Y1+S1*D2)
580   F=E+D2
585   REM LIMITS ON MAX AND MIN OF FREQUENCY
590   IF F>4.75 THEN  F=4.75
600   IF F<1.25 THEN  F=1.25
605   REM PLOT CONTROLLER'S OUTPUT ON CHART RECORDER
610   AOT(10,0)=F
615   REM OUTPUT TO STEPPING MOTOR
620   M5=F-F8
630   IF M5>0 THEN  Y=1
640   IF M5<0 THEN  Y=0
650   F3=ABS(M5)
660   X5=111*F3
670   X5'=X5
680   PRINT "X5=",X5'
690   FOR I=1 TO X5'
700     DOT(15,0,9)=1
710     DOT(15,8,9)=1+Y*2
720     IF AIN(14,6)>2.5 GOTO 720
730     DOT(15,0,9)=0
740   NEXT I
760   PRINT "H=",H;"F=",F;"DU=",D2
770   PRINT :5 "H=",H;"F=",F;"DU=",D2
774   REM GET FREQUENCY MEASUREMENT
775   F9=0
780   FOR I=1 TO 10
790     F9=F9+AIN(14,7)
800   NEXT I
810   F9=F9/10
820   F8=.72*F9
830   PRINT "F8=",F8
840   PRINT :5 "F ACTUAL=",F8
850   PRINT :5 "-----------------------------------"
860   WAIT (T1)
870   Y1=Y2
880 NEXT J
```

APPENDIX D.6

Program for Implementing S,T.R.

```
 10 OPENW :5 "$QTO:0"
 20 PNT :5 27
 30 WAIT (1.)
 40 PNT :5 17
 50 WAIT (.5)
 60 DIM K(150),A0(150),A1(150)
 70 DIM A2(150),B0(150),B1(150)
 80 DIM P1(5),T1(5)
 90 DIM P(5,5),Y1(150),U(150)
100 DIM S5(10),K(10)
110 REM DATA INPUT
120 REM L7=CONSTRAINT PARAMETER
130 REM R=FLAG TO TURN ON THE PARAMETERS UPDATE
140 REM R=1 UPDATE,R=0 NO UPDATE
150 REM T9=SAMPLING TIME,H7=HOLDUP SET POINT
160 REM L9=FORGETTING FACTOR, G=DIAG. ELEMENTS OF P MATRIX
170 REM L,M=ORDER OF CONTROLLER,U1=UD,U2=UC
180 REM Z1 TO Z4=INITIAL CONTROLLER'S PARAMETERS
190 REM D=DELAY TIME,A6=FLOODING FREQUENCY
200 INPUT "L7="L7
210 INPUT "R="R
220 INPUT "T SAMPLING="T9
230 INPUT "H SET POINT=",H7
240 INPUT "FL=L9="L9
250 INPUT "G=P DIAG.="G
260 INPUT "L="L
270 INPUT "M="M
280 INPUT "U1="U1
290 INPUT "NUMBER OF CONTROL STEPS="N2
300 INPUT "U2="U2
310 INPUT "Z1=" Z1
320 INPUT "Z2=" Z2
330 INPUT "Z3=" Z3
340 INPUT "Z4=" Z4
350 INPUT "D,DELAY TIME="D
360 INPUT "F FLOODING=" A6
370 TASK 2,450
380 ACTIVATE 2
390 WAIT (5.)
400 BREAK
410 TASK 1,530
420 ACTIVATE 1
430 END
440 REM INITIALIZATION OF TRANSDUCER'S SIGNAL
```

```
450 N=0
460 FOR I=1 TO 10
470   N=N+AIN(14,1)
480   PRINT "N=",N
490 NEXT I
500 S=N/10
510 PRINT "S=",S;"TASK 2 TERMINATED"
520 END
530 REM CONTROL PROGRAM START
540 REM INITIALIZE THE T1 VVECTOR
550 T1(1)=Z1
560 T1(2)=Z2
570 T1(3)=Z3
580 T1(4)=Z4
590 REM GET INITIAL FREQUENCY MEASUREMENT
600 F9=0
610 FOR I=1 TO 10
620   F9=AIN(14,7)+F9
630 NEXT I
640 H1=H7
650 F9=F9/10
660 F8=.72*F9
670 PRINT "F INITIAL=",F8
680 PRINT :5 "F INIT=",F8
690 REM INDEX FOR SHIFTING
700 D1=D+1
710 M1=M+1
720 M2=M+2
730 E1=M+D+1
740 E2=M+D+2
750 E3=M+D+3
760 L1=L+1
770 O=L+D
780 O1=L+D+1
790 O2=L+D+2
800 O3=L+D+3
810 N1=M+L+2
820 REM INITIALIZATION OF P MATRIX
830 FOR I= 1 TO N1
840   P(I,I)=G
850 NEXT I
860 P(3,3)=0.
870 REM INITIALIZATION OF AND H
880 FOR I=1 TO 6
890   GOSUB 2020(F8,H1)
900 NEXT I
910 REM INITIALIZATION OF U AND Y1 FOR P1
920 FOR I=1 TO O1
930   U(I)=0.
940 NEXT I
950 FOR J=1 TO E1
```

```
 960   GOSUB 2020(F8,H1)
 970   Y1(E3-J)=Y
 980 NEXT J
 990 REM CONTROLLER ON FROM T TO NTIMES
1000 FOR T=E2 TO N2
1010   REM UPDATE VECTOR P1 WITH NEW VALUE OF Y1 AND U
1020   REM MODIFY Y1 FOR SET POINT CHANGES
1030   IF (H1-H7)=0 THEN  GOTO 1120
1040   H1=H7
1050   GOSUB 2020(F8,H1)
1060   FOR I=1 TO M1
1070     P1(I)=H-H7
1080   NEXT I
1090   Y1(1)=H-H7
1100   Y1(2)=H-H7
1110   GOTO 1180
1120   H1=H7
1130   GOSUB 2020(F8,H1)
1140   Y1(1)=Y
1150   FOR I=1 TO M1
1160     P1(I)=Y1(D1+I)
1170   NEXT I
1180   FOR I=1 TO L1
1190     P1(M1+I)=U(D+I)
1200   NEXT I
1210   IF R=0 GOTO 1310
1220   FOR I=1 TO N1
1230     PRINT "P1(I)=",P1(I)
1240     PRINT :5 "P1(I)=",P1(I)
1250   NEXT I
1260   Y=Y+L7*U(1+D)
1270   PRINT "Y=",Y
1280   PRINT :5 "Y=",Y;"H=",H
1290   REM CALL RLS TO UPDATE P1(I)
1300   GOSUB 2120(P1,T1,P,S5,K)
1310   A0(T)=T1(1)
1320   A1(T)=T1(2)
1330   B0(T)=T1(3)
1340   B1(T)=T1(4)
1350   FOR I=1 TO N1
1360     PRINT "THETA(I)=",T1(I)
1370     PRINT :5 "THETA(I)=",T1(I)
1380   NEXT I
1390   REM COMPUTER CONTROL ACTION
1400   S1=0
1410   S2=0
1420   FOR I=1 TO M1
1430     S1=S1+T1(I)*Y1(I)
1440   NEXT I
1450   FOR J=1 TO L
1460     S2=S2+T1(M2+J)*U(J)
```

```
1470   NEXT J
1480   FOR I=1 TO 0
1490     U(O2-I)=U(O1-I)
1500   NEXT I
1510   U(1)=-(S1+S2)/B0(T)
1520   F=U(1)+F8
1530   REM LIMITS ON MAX AND MIN OF FREQUENCY
1540   IF F>A6 THEN  F=A6
1550   IF F<1.25 THEN  F=1.25
1560   PRINT "F=",F
1570   REM PLOT CONTROLLER'S OUTPUT ON CHART RECORDER
1580   AOT(13,0)=F
1590   U(1)=F-F8
1600   FOR I=1 TO 2
1610     PRINT "U(I)=",U(I)
1620   NEXT I
1630   PRINT "U=",U(1);"Y=",Y1(1)
1640   PRINT :5 "U=",U(1);"Y=",Y1(1)
1650   REM OUTPUT TO THE STEPPING MOTOR
1660   M5=F-F8
1670   IF M5>0 THEN  Y5=1
1680   IF M5<0 THEN  Y5=0
1690   F3=ABS(M5)
1700   X5=111*F3
1710   X5'=X5
1720   PRINT "X5=",X5'
1730   FOR I=1 TO X5'
1740     DOT(15,0,9)=1
1750     DOT(15,8,9)=1+Y5*2
1760     IF AIN(14,6) >2.5 GOTO 1760
1770     DOT(15,0,9)=0
1780   NEXT I
1790   REM GET FREQUENCY MEASUREMENT
1800   F9=0
1810   FOR I=1 TO 10
1820     F9=F9+AIN(14,7)
1830   NEXT I
1840   F9=F9/10
1850   F8=.72*F9
1860   PRINT "F8=",F8
1870   PRINT :5 "F ACT =",F8
1880   F8=F
1890   REM UPDATE VECTOR Y1' BY SHIFTING
1900   FOR I=1 TO E1
1910     Y1(E3-I)=Y1(E2-I)
1920   NEXT I
1930   FOR I=1 TO 4
1940     PRINT "I=",I;"P(I,I)=",P(I,I)
1950     PRINT :5 "I=",I;"P(I,I)=",P(I,I)
1960   NEXT I
1970   PRINT :5 "----------------------------------------"
```

```
1980   WAIT (T9)
1990 NEXT T
2000 REM SUBROUTINE OUTPUT
2010 REM THIS SUBROUTINE GET THE CURRENT HOLDUP VALUE
2020 DECLARE (F8,H1)
2030 A=.01275
2040 X1=AIN(14,1)
2050 X2=X1-S
2060 V=1./.000861*X2
2070 A9=A*F8
2080 H=.00023*V+2.289*U1-2.*U2-.016*A9+.00476
2090 Y=H-H1
2100 RETURN
2110 REM SUBROUTINE RLS
2120 DECLARE (P1,T1,P,S5,K)
2130 S1=0.
2140 FOR I=1 TO N1
2150   FOR J=1 TO N1
2160     S1=S1+P1(I)*P1(J)*P(I,J)
2170   NEXT J
2180 NEXT I
2190 D6=S1+L9
2200 E=0.
2210 FOR I=1 TO N1
2220   S1=0
2230   FOR J=1 TO N1
2240     S1=S1+P(I,J)*P1(J)
2250   NEXT J
2260   S5(I)=S1
2270   K(I)=S1/D6
2280   E=E+P1(I)*T1(I)
2290 NEXT I
2300 E=Y-E
2310 FOR I=1 TO N1
2320   FOR J=1 TO N1
2330     P(I,J)=(P(I,J)-S5(I)*S5(J)/D6)/L9
2340   NEXT J
2350   T1(I)=T1(I)+K(I)*E
2360 NEXT I
2370 RETURN
```